

ABSTRACT

Title of Dissertation: PROTEIN AND PEPTIDE ENGINEERING FOR IMPROVING THERAPIES FOR APPLICATIONS IN HUMAN HEALTH

Parisa Moghaddam-Taaheri, Doctor of Philosophy, 2018

Dissertation directed by: Professor Amy J. Karlsson, Department of Chemical and Biomolecular Engineering, Fischell Department of Bioengineering

The work in this dissertation focuses on protein and peptides engineering for improving therapies for applications in human health. First, we describe a directed evolution approach to engineer antibody fragments to bind to intracellular targets. An antibody fragment library was displayed using the twin arginine translocation inner-membrane display pathway, in order to allow only antibodies that are well-folded in the reducing cytoplasmic environment to be screened for binding. Displayed libraries were screened for binding to the apoptosis inhibitor survivin, and scFv cytoplasmic solubility and specificity was characterized. Though the antibodies isolated through this method displayed strong intracellular folding and high binding to survivin, they exhibited non-specific binding as well. We improved the screening approach by using whole-plasmid

PCR to recover sequences of isolated antibodies. Additional improvements to the screening process to increase stringency will allow better isolation of antibodies with high affinity and specificity for their target.

In a rational design approach, we designed an antimicrobial peptide-based approach for the treatment of candidiasis. *Candida albicans* is a commensal organism that resides asymptotically in the body. This opportunistic pathogen can overgrow and cause potentially fatal bloodstream infections. *C. albicans* biofilms that colonize implanted devices exhibit increased resistance to antimicrobial treatments and current antifungal treatments contribute to the rise of resistant strains of *C. albicans* or may cause toxicity. Thus, there is a clinical need for new or improved antifungal therapeutics to treat *C. albicans* infections. Histatin-5 (Hst-5) is an antimicrobial peptide secreted by the salivary glands that exhibits antifungal activity against *C. albicans*. Hst-5 can, however, be degraded by secreted aspartic proteases (Saps) produced by *C. albicans* cells, reducing its antifungal activity. Amino acid substitutions made to Hst-5 reduced the likelihood of proteolytic degradation to better maintain antifungal activity. Of these modifications, the K11R-K17R and E16R peptides showed enhanced antifungal activity in preventing *C. albicans* biofilm formation and eradicating preformed biofilms as compared to parent Hst-5. The improvements to methods and experimental findings in this research contribute to the improvement of therapies to treat human disease.

PROTEIN AND PEPTIDE ENGINEERING FOR IMPROVING THERAPIES FOR
APPLICATIONS IN HUMAN HEALTH

by

Parisa Moghaddam-Taaheri

Dissertation submitted to the Faculty of the Graduate School of the
University of Maryland, College Park, in partial fulfillment
of the requirements for the degree of
Doctor of Philosophy
2018

Advisory Committee:
Professor Amy J. Karlsson, Chair
Professor William E. Bentley
Professor Steven Jay
Professor Kimberly Stroka
Professor John Orban

© Copyright by
Parisa Moghaddam-Taaheri
2018

Dedication

I dedicate my PhD dissertation to my parents for their continued love and support.

Acknowledgments

I would like to first express my deepest gratitude to my advisor, Dr. Amy Karlsson. Thank you for supporting me, encouraging me, and challenging me throughout my studies. I am most grateful for your profound empathy and genuine belief in my success. I will forever consider you a great mentor and friend in my life.

Thank you to my committee members Dr. William Bentley, Dr. Steven Jay, Dr. Kimberly Stroka, and Dr. John Orban for your support throughout my studies and professional development.

I would also like to thank my fellow members of the Karlsson lab. I have enjoyed my time working with you and have learned so much from you all over the past few years. I want to thank Dr. Svetlana Ikonomova and Dr. Zifan Gong for their mentorship and guidance from the moment I joined the lab. I know I can always count on them to provide great advice regarding both lab work and life. I'd like to thank Sayanee Adhikari, my current partner in crime, for being a great friend and working with me to solve problems; I sincerely appreciate all the laughs we have had together over silly things. I'd also like to thank my undergraduate mentees, Janna Wisniewski and Tomer Zohar, for all the hours they put into the experiments that contributed valuable data to our projects. Thank you to Dr. Angela Jones for being a great mentor and for helping to develop my teaching skills. Special thanks to Dr. Christopher Jewell, Dr. Qin Zeng, and Haleigh Eppler for their guidance in carrying out the peptide-loaded polyelectrolyte multilayer film experiments, Mary Doolin and Dr. Kimberly Stroka for their help in performing mammalian cell

cytotoxicity experiments, and Kenneth Class and Dr. Xiangbin Zeng for their guidance in performing flow cytometry experiments.

Most importantly, I want to thank my friends and family. To my mother Parvin and father Ebraahim, thank you for showering me with love, encouragement, and pride for the past twenty-seven years; without you I would not have achieved any of my successes. To my sister Sara, thank you for being my role model from day one. Thank you to my fiancé Joe for supporting me and believing in my dreams and reminding me to always put faith in myself. Finally, thank you to my friends Erika Moore, Nardos Makonnen, Hilena Addis, Mana Jabbour, Atma Khalsa, Tariq Noaman, Mahlet Makonnen, Juliana Cano-Mejia, and Lauren Resutek for your friendship and constant support.

This work was supported by the National Science Foundation Award Number CBET 1511718 and a University of Maryland Tier 1 award.

Table of Contents

Dedication	ii
Acknowledgments.....	iii
Table of Contents	v
List of Tables	ix
List of Figures	x
List of abbreviations	xii
Chapter 1: Introduction to protein engineering.....	1
1.1 Engineering proteins and peptides for enhancement of therapeutic potential ...	1
1.2 Directed evolution approach.....	2
1.3 Rational design approach.....	3
1.4 Overview of thesis work	4
Part I: Directed evolution for engineering intracellular antibodies	6
Chapter 2: Directed evolution of a single chain variable fragment library for binding survivin	7
2.1 Introduction.....	7
2.1.1 Selection of target protein, survivin.....	7
2.1.2 Structure and properties of single chain variable fragments (scFvs).....	11
2.1.3 Tat inner-membrane display and screening of antibody libraries.....	12
2.2 Materials and methods	17
2.2.1 Selection of parent scFv for library generation.....	18
2.2.2 Library construction.....	20
2.2.2.1 Error-prone PCR	20
2.2.2.2 Plasmid construction.....	20
2.2.2.3 Transformation of library into <i>E. coli</i>	21
2.2.3 Panning of library to enrich for survivin-binding members	23
2.2.3.1 Biotinylation of survivin and other proteins	23
2.2.3.2 Immobilizing biotinylated survivin on streptavidin-coated magnetic beads	24
2.2.3.3 Spheroplasts with periplasmic-anchored scFvs	24
2.2.3.5 Positive panning, PCR amplification, and library construction.....	26
2.2.4 Library secondary screening	28
2.2.5 Library tertiary screening	29
2.2.6 Expression and binding characterization of isolated clones	30
2.3 Results and discussion	33
2.3.1 scFvs isolated through inner-membrane display and screening are soluble	33
2.3.2 Isolated scFvs are non-specific and do not exhibit saturable binding	34
2.4 Conclusion	38

Chapter 3: Improving antibody library construction and screening assays	39
3.1 Introduction.....	39
3.2 Methods of improvement.....	39
3.2.1 Whole plasmid PCR.....	39
3.2.1.1 Determination of feasibility of whole plasmid PCR.....	39
3.2.1.2 Whole plasmid PCR on spheroplasts.....	42
3.2.2 Recovery of plasmids from spheroplast.....	43
3.2.2.1 Determining minimum spheroplast concentration for direct transformation of <i>E.coli</i> cells.....	43
3.2.2.2 PCR amplification of spheroplasts.....	43
3.2.3 Increasing stringency	44
3.2.3.1 Inclusion of a non-specific target, competitive inhibitor, additional blocking reagents in panning reactions.....	44
3.2.3.2 Additional negative panning steps to improve elimination of non-specific library members.....	46
3.2.4 Specificity ELISA.....	46
3.3 Results and discussion	48
3.3.1 Whole plasmid PCR recovers plasmid from purified plasmid and spheroplast lysate	48
3.3.2 <i>E. coli</i> are transformed with spheroplast lysate to recover plasmid	50
3.3.3 Increasing assay stringency modulates scFv binding behavior does not result in improved specificity.....	52
3.3.4 Specificity of screening assay may be dependent on library quality and parent antibody.....	56
3.4 Conclusion	58
Chapter 4: Directed evolution of a single domain antibody library for binding survivin	60
4.1 Introduction.....	60
4.1.1 Structure and properties of single domain antibodies.....	61
4.1.2 High-throughput screening	63
4.2 Materials and methods	66
4.2.1 Selection of library basis.....	66
4.2.2 Optimization for library screening.....	66
4.2.2.1 Cloning scFv13 and scFv13-R4 into yeast surface display vector ...	67
4.2.2.2 Transformation of <i>S. cerevisiae</i>	67
4.2.2.3 Flow cytometry optimization.....	68
4.2.3 Library construction.....	69
4.2.3.1 VHH library construction for yeast surface display	69
4.2.3.2 scFv library construction for yeast surface display.....	70
4.3 Results and discussion	70

4.3.1	Flow cytometry needs further optimization	70
4.3.2	Generation and cloning of VHH library into yeast surface display vector requires optimization	71
4.3.3	Generation and cloning of VHH library into yeast surface display vector requires optimization	71
4.4	Conclusion	72
Part II:	Rational Design of antimicrobial peptides	74
Chapter 5:	Antifungal peptides for treatment of <i>C. albicans</i>	75
5.1	Introduction.....	75
5.1.1	Selection of <i>C. albicans</i> as a therapeutic target	75
5.1.2	Histatin-5 as an antifungal agent.....	76
5.1.3	Secreted aspartic proteases	79
5.1.4	Proteolytic susceptibility of Hst-5 to Saps.....	79
5.2	Previous experiments	80
5.2.1	Rational design of Hst-5 peptides	80
5.2.2	Peptides and enzymes	81
5.2.3	Proteolytic degradation of Hst-5 and variants by Saps	82
5.2.4	Antifungal activity assay.....	84
5.2.4.1	Antifungal activity assay performed with intact peptides.....	84
5.2.4.2	Antifungal activity assay performed with degraded peptides.....	86
5.2.6	Peptide degradation by <i>C. albicans</i>	90
5.2.7	Mass spectrometry analysis	91
5.2.8	Additional modification of Hst-5 peptides and results	93
5.3	Materials and Methods.....	98
5.3.1	Peptide degradation by <i>C. albicans</i> culture supernatant.....	98
5.4	Results.....	99
5.4.1	Saps found in <i>C. albicans</i> culture supernatant degrade Hst-5 and variants	99
5.5	Conclusion	100
Chapter 6:	Antifungal peptides for treatment of <i>C. albicans</i> biofilms	102
6.1	Introduction.....	102
6.1.1	Properties of <i>C. albicans</i> biofilms	102
6.1.2	Selection of antifungal peptides for the treatment of <i>C. albicans</i> biofilms	105
6.2	Materials and methods	106
6.2.1	Planktonic candidacidal assay.....	106
6.2.2	Biofilm formation assay.....	108
6.2.3	Biofilm susceptibility assay	109
6.2.4	Cytotoxicity analysis of peptides	110
6.2.5	Incorporation of peptides into polyelectrolyte multilayer films	111
6.3	Results.....	112
6.3.1	Modified peptides exhibit enhanced antifungal activity	112

6.3.2 Histatin-5 and modified peptides inhibit biofilm formation	114
6.3.3 Histatin-5 and modified peptides show antifungal activity against preformed biofilms.....	115
6.3.4 Peptides are not cytotoxic to mammalian cells.....	117
6.3.5 Peptides can be incorporated into PEMs	118
6.4 Conclusion	120
Part III: Summary and recommendations for future work.....	122
Chapter 7 : Summary and recommendations for future work.....	123
7.1 Summary	123
7.2 Improving library screening for the isolation of intrabodies	125
7.2.1 Improving library quality	125
7.2.1.1 Use of an immunized library.....	125
7.2.1.2 Use of a commercial anti-survivin antibody.....	125
7.2.1.3 Modifications to the antibody fragment frameworks to improve solubility	126
7.2.2 Increasing assay stringency.....	127
7.2.3 Modifications to survivin target.....	127
7.3 Understanding histatin-5 cell entry mechanisms and potential as a candidacidal therapy	128
7.3.1 Oriented CD.....	128
7.3.2 Formation of peptide-loaded PEMs to coat implantable surfaces	129
7.3.3 Assessment of Hst-5 and modified peptides ability to prevent hyphal formation.....	130
Appendix.....	131
Publications and Presentations.....	133
References.....	134

List of Tables

Chapter 2

Table 2.1. PCR reaction preparation for amplification of scFv library from bead bound spheroplasts

Table 2.2. Thermal cycler protocol for PCR amplification of scFv library from bead bound spheroplasts

Chapter 3

Table 3.1. Whole plasmid PCR primer sets

Table 3.2. PCR reaction preparation for PCR amplification of whole plasmids

Table 3.3. Thermal cycler protocol for PCR amplification of whole plasmids

Table 3.4. Preparation of a ligation reaction to recircularize linear whole plasmid PCR product

Table 3.5. Correlation of spheroplast sample cell density to transformed *E. coli* CFU/mL

Chapter 5

Table 5.1. Hst-5 and variants with single leucine or arginine substitutions

Table 5.2. Hst-5 and variants with one or two residue substitutions

Chapter 6

Table 6.1. Cytotoxicity analysis of Hst-5 and variants

List of Figures

Chapter 1

Figure 1.1. Directed evolution

Chapter 2

Figure 2.1. Dimeric structure of survivin

Figure 2.2. IgG and scFv structure

Figure 2.3. *E. coli* twin-arginine translocation pathway and periplasmic display

Figure 2.4. Properties of scFv variants isolated using inner-membrane display

Figure 2.5. Binding of scFv-F4 to survivin

Figure 2.6. pIMD plasmid map

Figure 2.7. *E. coli* cells and spheroplasts

Figure 2.8. Subtractive and positive panning

Figure 2.9. ELISA-based secondary screening

Figure 2.10. Soluble fraction of cytoplasmically expressed scFvs

Figure 2.11. Binding of scFv variants

Chapter 3

Figure 3.1. Whole plasmid PCR

Figure 3.2. Whole plasmid PCR using purified plasmid template

Figure 3.3. Whole plasmid PCR using lysed spheroplasts as template

Figure 3.4. Effect of supplementary soluble β -gal on saturable binding

Figure 3.5. Effect of lysate diluent on binding profile

Figure 3.6. Effect of supplementary soluble β -gal on specificity

Figure 3.7. Tat inner-membrane display and screening for selection of specific antibodies

Chapter 4

Figure 4.1. Camelid antibody structures

Figure 4.2. Yeast surface display

Figure 4.3. pCTcon2 plasmid map

Chapter 5

Figure 5.1. Hst-5 sequence and antimicrobial fragments

Figure 5.2. Degradation of Hst-5 and modified peptides by purified Sap9 and Sap2

Figure 5.3. Antifungal activity of Hst-5 and modified peptides

Figure 5.4. Degradation of Hst-5 and modified peptides by high concentrations of purified Sap9 and Sap2

Figure 5.5. Antifungal activity of Hst-5 and modified peptides following incubation with Sap9 and Sap2

Figure 5.6. Degradation of Hst-5 and Hst-5 variants by *C. albicans*

Figure 5.7. Extent of proteolysis of parent Hst-5 and Hst-5 variants by purified Sap9 and Sap2, Extent of degradation for Hst-5 and its variants after exposure to *C. albicans*

Figure 5.8. Antifungal activity of Hst-5 and modified peptides

Figure 5.9. Extent of proteolysis of parent Hst-5 and Hst-5 variants by higher concentrations of purified Sap9 and Sap2, Antifungal activity of the peptides after incubation with or without Sap9 or Sap2

Figure 5.10. Degradation of Hst-5 and modified peptides by *C. albicans* culture supernatant

Chapter 6

Figure 6.1. Microscopy of treated and untreated *C. albicans* biofilms

Figure 6.2. Candidacidal assay

Figure 6.3. Planktonic candidacidal assay

Figure 6.4. Biofilm formation assay

Figure 6.5. Biofilm susceptibility assay

Figure 6.6. Thickness of fabricated PGA/Hst-5/PLL polyelectrolyte multilayer films

Appendix

Figure A1. Mass spectrometry of Hst-5 and single substitution variants

Figure A2. Mass spectrometry of Hst-5 and modified peptides

List of abbreviations

6XHis	hexahistidine
AF488	Alexa-Fluor 488
β-gal	β-galactosidase
bp	base pairs
BSA	bovine serum albumin
CDR	complementarity determining regions
Cm	chloramphenicol
ELISA	enzyme-linked immunosorbent assay
FACS	fluorescence-activated cell sorting
FBS	fetal bovine serum
HRP	horse-radish peroxidase
Hst-5	histatin-5
IEX	ion exchange chromatography
IgG	immunoglobulin G
IMAC	immobilized metal affinity chromatography
IPTG	isopropyl β-D-1-thiogalactopyranoside

kb	kilobase pairs
kDa	kilodaltons
LB	lysogeny broth
MW	molecular weight
MWCO	molecular weight cut off
NaPB	sodium phosphate buffer
OD₄₉₂	optical density at 492 nm
OD₆₀₀	optical density at 600 nm
PBS	phosphate buffered saline
PBS + 0.1% BSA	phosphate buffered saline supplemented with 0.1% w/v BSA
PBST	phosphate buffered saline supplemented with Tween 20
PCR	polymerase chain reaction
PI	propidium iodide
PVDF	polyvinylidene difluoride
RPMI-1640	Roswell Park Memorial Institute 1640
Sap	secreted aspartic protease
SDS-PAGE	sodium dodecyl sulfate polyacrylamide gel electrophoresis

scFv	single-chain variable fragment
SEC	size exclusion chromatography
SEM	standard error of the mean
Tat	twin-arginine translocation
VH	variable heavy chain
VHH	camelid single-domain antibody fragment
VL	variable light chain
XTT	2,3-Bis-(2-methoxy-4-nitro-5-sulfophenyl)-2 <i>H</i> -tetrazolium-5-carboxanilide
YPD	yeast peptone dextrose media

Chapter 1: Introduction to protein engineering

1.1 Engineering proteins and peptides for enhancement of therapeutic potential

Protein engineering is the design of proteins to improve the properties of an existing protein or to develop novel proteins to serve a desired function [1]. Engineered proteins have relevance in a variety of sectors including but not limited to pharmaceuticals, biofuels, food and agriculture, and manufacturing [2,3]. Of particular interest in the biomedical field is the use of proteins and peptides as therapeutic agents to treat disease. New and emerging methods allow for improved engineering of existing therapeutic proteins. For example, newer insulin analogs have enhanced properties over first-generation recombinant insulin as protein engineering and characterization methods have improved [4].

The fastest-growing class of protein therapeutics is antibody-based drugs, which have been approved for use in treatment of cancer, rheumatoid arthritis, asthma, transplant rejections, and Crohn's disease among other applications [4–8] and monoclonal antibodies are among these biopharmaceuticals. Since cell signaling pathways contributing to cancer progression are complex [9,10] there are many potential targets for antibody-mediated therapy. The approval for use of antibodies as cancer therapeutics in healthcare establishes their potential as therapeutic agents.

Another emerging class of protein therapeutics is that of antimicrobial peptides, which are naturally found in a variety of organisms and serve as a defense against microbial pathogens [11,12]. These peptides are of particular interest due to recent increases in antibiotic-resistant bacteria and fungi, resulting in increased mortality rates and healthcare

spending [13,14]. There is a need for the development of new therapeutics for the treatment of bacterial and fungal disease. In this work, we focused on two methods of protein and peptide engineering for developing an antibody fragment to target cancer pathways and antifungal peptides for the treatment of fungal infections.

1.2 Directed evolution approach

Directed evolution is a widely-used protein-engineering method that mimics natural selection to generate and isolate proteins with desired properties [15,16], such as antibodies with high affinity to a particular target. To begin, a diversified library is generated or obtained. For example, the gene for a protein of interest can be amplified in a low-fidelity manner that produces a library of protein genes each with varying nucleic acid mutations. The protein library is then expressed and screened for desired properties. In an iterative process, well-performing library members are then subjected to subsequent rounds of diversification and screening to enrich for proteins with the best properties (Figure 1.1). This process relies on the generation of an adequate library size to increase the probability of isolating a protein with improved fitness. The quality of the library, which is largely determined by the parent protein sequence and method of mutagenesis, is also of importance [16].

The most commonly used methods for screening protein libraries are phage display and yeast surface display [17,18] though in a comparison of these methods, it has been found that yeast surface display provides better sampling of the library repertoire and is less labor-intensive than phage display [19,20]. These methods have been used to isolate high-affinity antibodies for a variety of targets[21–24]and allow for fine affinity

discrimination, particularly with use of yeast surface display and flow cytometry [25]. For example, yeast surface display has been used to engineer antibodies to target antigens such as T cell receptors, botulinum neurotoxin, and the proapoptotic protein Bax, among other targets [21,26]. Yeast surface display, phage display, and traditional bacterial surface rely on secretory protein expression pathways [27,28] in which unfolded proteins are translocated to an oxidizing environment for folding [27,28]. Thus, these display methods are limited in the engineering of proteins that need to be well-folded in the reducing cytoplasmic environment. In Chapter 2, we describe the use of the twin-arginine translocation (Tat) pathway, which has an intrinsic intracellular protein folding quality control mechanism, which allows for display of proteins that are properly folded intracellularly [29].

1.3 Rational design approach

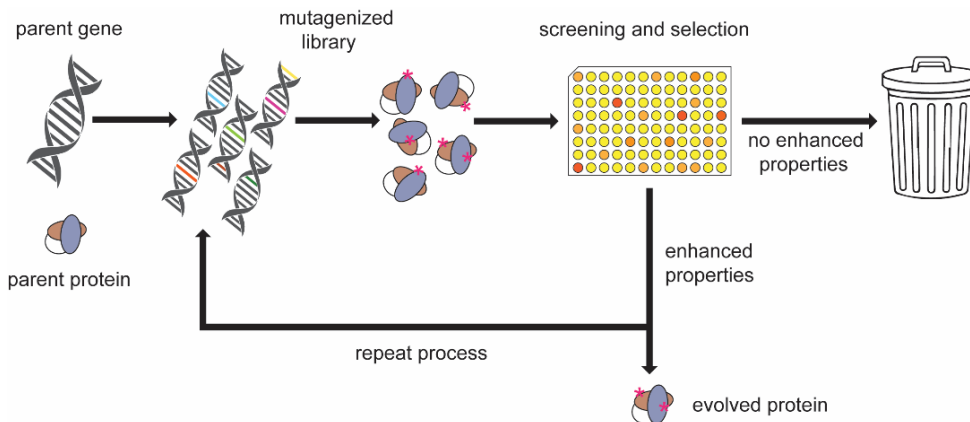


Figure 1.1 Directed evolution. An iterative process mimicking natural selection whereby a gene is mutated to generate a diverse library of genes that is screened for a desired property.

Rational design of proteins is the manipulation of protein sequence or composition in a hypothesis-driven manner for the purpose of enhancing desired properties [30]. This

requires an educated prediction based on previous findings about which modifications will impart the desired effect on the engineered protein structure or function. The study of these small, deliberate changes and their impact on protein structure, function, and kinetics can provide valuable insight for the engineering of additional proteins. Previous work demonstrates the ability to rationally modify proteins to alter physiochemical properties, pharmacokinetics, affinity, and immunogenicity [30–33].

It is important to note that in recent years, both rational design and directed evolution have benefited from advances in computer simulations of molecular interactions that can aid in design of functional proteins. For example, the Rosetta Antibody server can predict the structure of antibody variable regions based on optimization of dihedral angles and free energy of conformations [34]. Additionally, the Rosetta Snug dock application can be used to assess antibody-antigen docking taking into account the conformational degrees of freedom of the antibody portions relevant to binding [35].

1.4 Overview of thesis work

In Chapter 2, we describe the use of directed evolution to generate and screen an antibody fragment library for binding the intracellular target survivin, an inhibitor of apoptosis protein, using a bacterial inner-membrane display method. In Chapter 3, we focus on improvement of this method to simplify the process and increase the likelihood of isolating antibodies that specifically bind the target antigen. Methods presented in Chapter 4 serve as an alternative display and screening method for the isolation of antibodies that bind survivin. In chapters 5 and 6, we describe a rational design approach to modify the antimicrobial peptide histatin-5 for the treatment of *Candida albicans* biofilms. Finally, in

Chapter 7, we discuss future studies to continue the improvement of protein and peptide engineering methods for therapeutic applications.

**PART I: DIRECTED EVOLUTION FOR
ENGINEERING INTRACELLULAR
ANTIBODIES**

Chapter 2: Directed evolution of a single chain variable fragment library for binding survivin

2.1 Introduction

Directed evolution is commonly used to engineering antibodies. Intracellular antibodies (intrabodies) are particularly challenging to engineer as they must be correctly folded in the reducing cytoplasmic environment to ensure proper function and binding. They cannot contain the disulfide bonds that typically contribute to correct antibody folding and structure, and thus, must be engineered for solubility and folding. In this chapter, we focused on a novel bacterial protein display technique to engineer antibody fragments that are well-folded in the cytoplasmic environment and bind an intracellular target that plays a crucial role in anti-apoptotic cancer pathways.

2.1.1 Selection of target protein, survivin

The United States Centers for Disease Control reports over 1 million new cases of invasive cancer and more than 582,000 cancer-related deaths per year, making cancer one of the deadliest pathologies [36]. While the phenotypic manifestation of different cancers varies, one hallmark spanning all cancer types is the increased viability of cancerous cells. In addition to a loss of mitotic cell cycle checkpoints and increased proliferation, malignant cells lack a fully functional apoptotic program. In normal cells, there is a delicate balance between pro-apoptotic proteins and inhibitor of apoptosis proteins (IAPs) whereby cell-physiological stimuli lead to a shift in this balance that can allow the cell to undergo apoptosis if need be. However, in cancer cells, this balance is disrupted and a loss of pro-

apoptotic protein function or an increase in anti-apoptotic protein expression or function allows cells to evade apoptosis [37].

Survivin is an IAP that is overexpressed in many cancer cell types including but not limited to breast, lung, colon, prostate and bladder cancers [38–42]. Overexpression of survivin leads to decreased patient survival rates in several cancer types [43,44] and to a particularly aggressive prognosis and increased metastasis in colorectal carcinoma [44,45]. Survivin is an ideal intracellular cancer target since, unlike other IAPs, it is only overexpressed in neoplastic tissues, but not in differentiated normal tissue [43,46]. This research addresses the need to understand survivin's role in cancer pathology and aims to develop a therapy to directly target survivin.

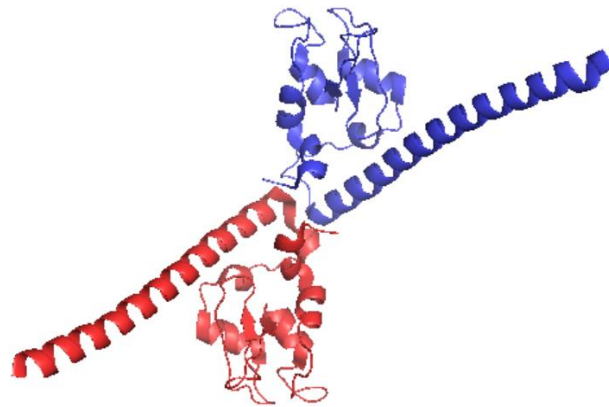


Figure 2.1 Dimeric bowtie structure of survivin. Each C-terminal helical domain interfaces with the BIR domain of partnering monomer via hydrogen bonding. (PDB ID : 1E31)

Survivin has a pro-mitotic function [43,47] which is in part illustrated by its ubiquitous expression in embryonic and fetal developmental stages [46,48], during which

high cell division rates are expected. In contrast, survivin has a very low level of expression in normal adult cells [49]. Survivin plays a key role cytokinesis as part of the chromosomal passenger complex among other mitotic phenomena and is a critical regulator of mitosis [50–52] with increased expression during the G2-M transition phase of the cell cycle [50] of proliferating cells. Many cancers are marked by increased cell proliferation which agrees with the presence of survivin and its ability to increase proliferation. Survivin also plays an anti-apoptotic role, as explained below, and although many studies have been conducted to elucidate its role, gaps remain in the understanding of survivin's inhibition of apoptotic moieties. Thus, there is a need to target survivin to inhibit its pro-mitotic and anti-apoptotic functions.

Survivin's structure provides some insight as to which domains are relevant to its pro-mitotic functions. Similar to other IAPs, survivin possesses a baculovirus inhibitor of apoptosis protein repeat (BIR) domain. It also has a 65Å long C-terminal helix domain that is essentially locked in position with respect to the BIR domain via hydrogen bonding and hydrophobic contacts [53](Figure 2.1). The crystal structure of bacterially expressed recombinant full-length human survivin indicates a 35 kDa dimeric structure, which is maintained in solution. It is suggested that the two dimerization interfaces contribute to localization to the spindle centrosome as well as recruitment of other BIR domain containing proteins for the purpose of forming larger functional units. Furthermore, it is postulated that the dimeric structure with extended helical arms may play a role in bridging proteins involved with microtubule organizing centers (MTOC) [53], to which survivin spatially and temporally localizes to during mitosis [54].

While it has been speculated that survivin's anti-apoptotic activity involves its inhibition of caspases, this has not been confirmed by structural studies [53]. Survivin's caspase-inhibiting behavior may be due to its conserved BIR domain, which has been shown to be vital in targeting caspases in other IAPs [47,55]. Debate exists over whether or not survivin can directly bind to caspases, but evidence shows that it indirectly prevents caspase activation. Survivin binds to the X-linked inhibitor of apoptosis protein (XIAP) to prevent XIAP from forming a complex with the second mitochondrial activator of caspases (Smac) [43]. Smac's role is to bind IAPs like XIAP to disrupt their interaction with caspases so that apoptosis may proceed. Survivin disrupts the formation of the Smac-XIAP complex such that XIAP instead binds to survivin. This survivin-XIAP complex inhibits the activation of caspase-9, whose activation is a crucial step in the apoptotic pathway [47,56,57]. A potential therapeutic strategy could be to prevent survivin from binding to XIAP.

Regardless of whether or not survivin can directly inhibit caspases or if it needs to bind to another IAP to prevent caspase activation, it is clear that preventing protein-protein interactions between survivin and other apoptosis associated proteins can inhibit survivin's function. A potential challenge in designing a molecule to block these interactions is that survivin has acetylation and phosphorylation-diversified functions inside the cell [43]. In fact, while survivin inhibits apoptosis cytoplasmically, nuclear survivin can inhibit cell survival and repress transcription of oncogenes [58]. It is clear that the functional role of survivin is very complex and not fully understood. Thus, in this research, we sought to engineer a molecule to inhibit survivin's protein-protein interactions to help elucidate survivin's specific binding domains and its role in the apoptotic pathway. This approach

would allow direct binding and inhibition of survivin, which is an advantage to more indirect methods such as survivin expression knockdown which may impart undesired effects. While parts of survivin's structure-function relationship have been determined, we aim to target the survivin dimer as a whole rather than targeting specific domains. This will allow isolation of a more diverse group of survivin-binding molecules which may exhibit different modes of survivin binding and inhibition.

2.1.2 Structure and properties of single chain variable fragments (scFvs)

scFvs comprise a variable light chain (VL) and a variable heavy chain (VH) of a full-length IgG connected by a flexible peptide linker (Figure 2.2). Each VL and VH contains four framework regions and three complementarity determining regions (CDRs). The CDRs are highly variable, loop-structured regions that are responsible for antigen specificity and binding [59]. All scFv regions can contribute to antigen specificity, however, in order of importance to antigen binding these regions are CDR3H, CDR2H, CDR3L, CDR1H, CDR1L, CDR2L, and framework residues [59]. Thus, mutations can be made to the entire scFv sequence or focused solely on CDRs of higher importance to antigen specificity. scFvs maintain all antigen specificity of a full-length IgG antibody but are smaller and easier to produce [60].

scFvs rely on domain association to maintain full antigen binding capabilities. One critical VH-VL domain interaction is an intradomain disulfide bond between two highly conserved cysteine residues. While most scFvs require this intradomain bond to fold to the native conformation and intradomain association, the correct native structure can in some cases be reached with the absence of disulfide bonds [61]. scFvs engineered for intracellular function can be well-folded and functional even in the reducing cytoplasmic environment and have been shown to demonstrate cytoplasmic solubility [29]. scFvs are strong candidates for use as intrabodies as scFv libraries can be generated with high CDR diversity which gives a higher chance of success in finding scFvs that bind survivin. In these studies we enrich and screen a naïve scFv library for binding to survivin and discuss methods to improve specificity with our choice of display and screening method.

2.1.3 Tat inner-membrane display and screening of antibody libraries

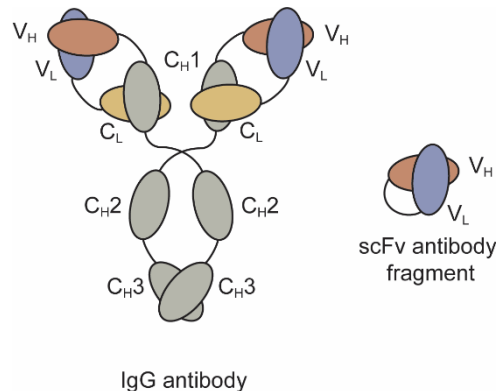


Figure 2.2 IgG and scFv structure. An scFv antibody fragment comprises the heavy and light chains of a full-length IgG antibody, connected via a flexible peptide linker.

It is inherently difficult to engineer antibodies for intracellular function as the cellular cytoplasm is highly reducing [62] and prevents the formation of disulfide bonds

necessary for correct protein structure and function. Commonly used methods of yeast surface display and phage display rely on secretory pathway to display libraries for screening [19,27,28], and thus do not have a quality control mechanism that prevents the display of improperly folded proteins. This contributes to the isolation of intrabodies that show promising binding affinity but that lack the cytoplasmic solubility needed to be function intracellularly [63]. To develop scFvs that are functional in the cytoplasmic milieu, we engineered antibodies using the *Escherichia coli* twin-arginine translocation (Tat) pathway. The Tat pathway contains an intrinsic intracellular protein folding quality control mechanism that only allows soluble, correctly folded proteins to be transported from the *E. coli* cytoplasm, across the inner membrane, and into the periplasm [64,65]. Overexpressed Tat substrates (*i.e.* proteins targeted to the Tat pathway with an N-terminal fusion to the Tat signal peptide ssTorA) that are well folded in the cytoplasm form a long-lived translocation intermediate with the N-terminus in the cytoplasm and the C-terminus in the periplasm [29]. This allows display of correctly folded Tat substrates, including antibody fragments, on the periplasmic face of the *E. coli* inner membrane. After removing the outer membrane by enzymatic digestion to generate spheroplasts, antibodies are exposed to the extracellular space (Figure 2.3). This allows Tat substrates displayed on the inner membrane to be screened for binding to a specific target. Importantly, harnessing the Tat pathway for cell-surface display ensures that only the antibodies in the library that are well folded in the cytoplasm will be interrogated for binding, allowing simultaneous engineering of binding affinity and intracellular folding.

The intracellular protein folding quality control mechanism of the Tat pathway in *E. coli* limits transport across the inner cell membrane to proteins that are well folded in

the reducing cytoplasmic environment. By overexpressing a fusion of an scFv to the ssTorA signal sequence (the signal sequence from the TorA protein, which is naturally transported by the Tat pathway) [64], translocation is stalled, resulting in display of scFvs on the inner membrane [29]. After enzymatic disruption of the outer membrane, the displayed antibodies are made available for screening for antigen-binding activity. The ability to take advantage of the Tat pathway for display was shown by Karlsson et al. [29] (Figure 2.4). The scFv antibodies scFv13 and scFv13.R4 were fused to either the native ssTorA sequence or a modified ssTorA that lacks the arginine-arginine residue pair recognized by the Tat pathway. scFv13.R4 was engineered by Martineau et al. from scFv13 through four rounds of directed evolution and is known to fold well in the cytoplasm [66]. This scFv was displayed on the inner membrane, but only when expressed as a fusion to the native ssTorA signal sequence. Contrarily, scFv13 is not well folded cytoplasmically [66], so it is not displayed well on the inner membrane, regardless of the signal sequence to which it is fused. Additionally, if the scFvs were expressed in cells that lacked the TatC protein, a vital component of the Tat machinery [64,67], display was not observed, showing the important link between inner-membrane display and the Tat pathway (Figure 2.4C).

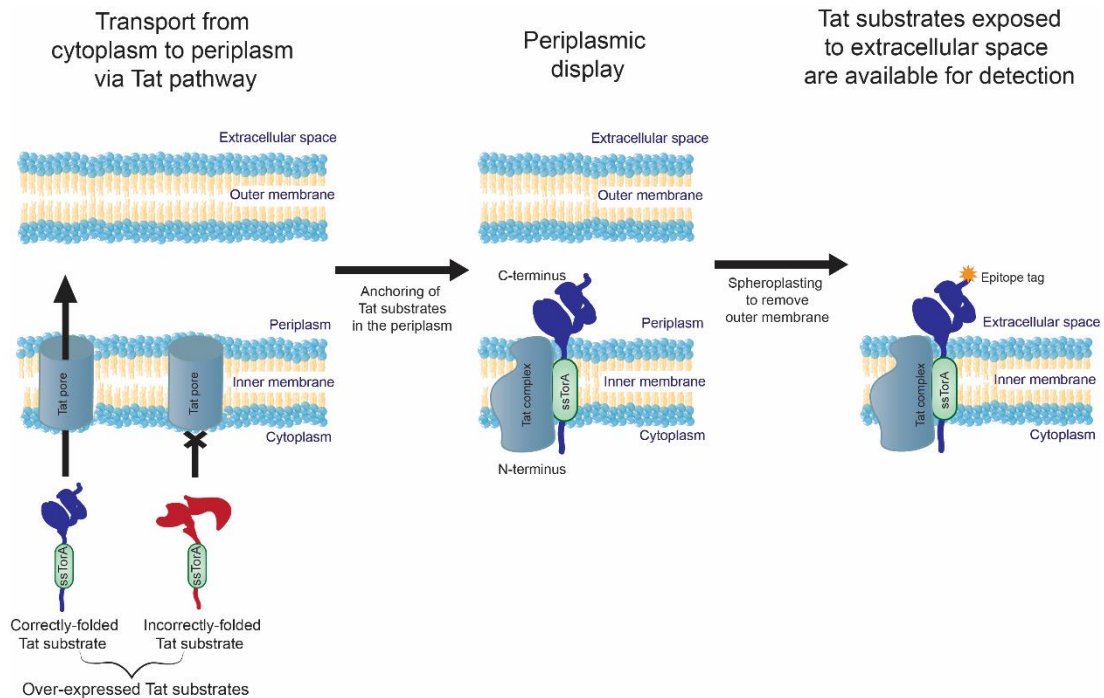


Figure 2.3‡ *E. coli* twin-arginine translocation pathway and periplasmic display. Proteins expressed as fusions to the Tat pathway signal sequence ssTorA are transported for inner membrane anchoring only if they are correctly folded in the cytoplasm. The outer membrane is then enzymatically digested, thus placing the membrane-anchored protein in the extracellular space, available for detection in expression and antigen binding assays.

‡Figure originally published in *J. Vis. Exp.* (2016)

Inner-membrane display can successfully isolate scFv antibodies with high levels of affinity for a target protein and high levels of cytoplasmic solubility. Additionally, subsequent rounds of directed evolution using inner-membrane display improve antibody characteristics¹. To demonstrate this, an error-prone PCR library based on scFv13, which has a low level of binding affinity for β -galactosidase (β -gal), was panned against the target antigen β -gal. scFv 1-4 was isolated after one round of mutagenesis and panning and exhibited higher binding affinity to β -gal than scFv13 (Figure 2.4A) and a higher level of cytoplasmic solubility (Figure 2.4B).

A new library, based on scFv 1-4, was made using error-prone PCR, and panning of this second-generation library against β -gal was done in the presence of purified, soluble scFv 1-4 as a competitor. After this second round of mutagenesis and panning, scFv 2-1 and scFv 2-3 were isolated using the enzyme-linked immunosorbent assay (ELISA)-based secondary screening. These scFvs not only exhibited higher binding affinity for β -gal than scFv13, but also exhibited better binding than the first-round clone scFv 1-4. scFv 2-1 exhibited β -gal binding comparable to that of scFv13.R4 (Figure 2.4A). scFv 2-3 also shows a further increase in cytoplasmic solubility compared to scFv 1-4, highlighting the simultaneous engineering of solubility and antigen-binding. Since affinity and soluble expression of the scFvs are screened for simultaneously, it is possible that a selected scFv has moderate solubility but high binding or vice versa. For example, scFv 2-1 has lower soluble expression than scFv 2-3, but it exhibits higher binding affinity to β -gal.

The Tat display and screening method can be used on its own or in combination with yeast surface display to enrich for well folded library members. Here, we use the Tat display method to screen a library of scFvs for binding to survivin. The display and screening of a naïve library using this method highlighted challenges in engineering for antigen binding specificity and reinforce the use of inner-membrane displayed libraries for the enrichment of cytoplasmically soluble isolates.

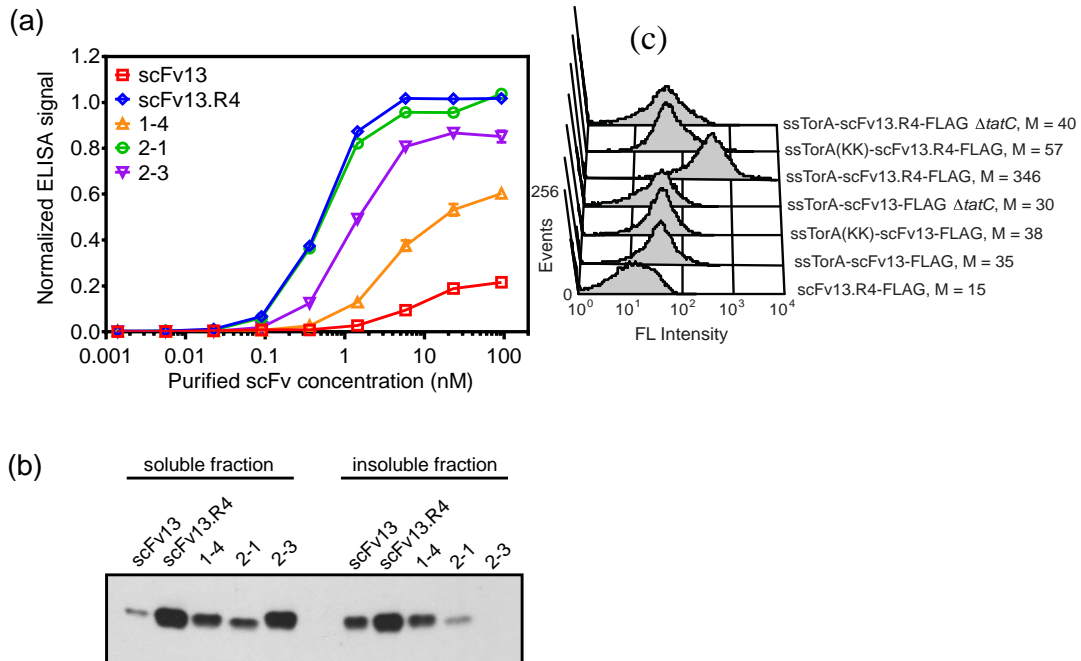


Figure 2.4‡ Properties of scFv variants isolated using inner-membrane display. (a) Target binding. scFvs were expressed in the cytoplasm of *E. coli* cells (i.e. not using Tat display) with a 6X-His tag and purified using nickel-nitrilotriacetic acid spin-columns. Binding of the purified scFvs to β -galactosidase was measured via ELISA. Purified scFvs were loaded onto β -galactosidase-coated ELISA plates, and the bound scFvs were detected with an anti-6X-His antibody. **(b) Cytoplasmic expression.** Soluble and insoluble fractions of the cell lysates from cells expressing the scFvs cytoplasmically were analyzed via Western blot probed with an anti-6x-His antibody. Total protein concentration was used to normalize sample loading. **(c) Detection of displayed scFvs on the inner membrane.** Flow cytometry analysis was performed to detect the display of poorly folded scFv13 and well-folded scFv13.R4 on the inner membrane. scFvs were fused to native ssTorA or ssTorA(KK), where the Arg-Arg pair in the ssTorA sequence was modified to Lys-Lys. The C-terminal FLAG epitope tags on the scFvs were detected with a fluorescein isothiocyanate (FITC)-conjugated anti-FLAG antibody. Cells without the TatC protein (*AtatC*) and ssTorA-scFv13 without the FLAG tag were tested as controls. M indicates the median fluorescence value.

‡Figure and caption originally published in *J. Vis. Exp.* (2016)

2.2 Materials and methods

2.2.1 Selection of parent scFv for library generation

As previously discussed, intrabodies must be engineered for cytoplasmic solubility and intracellular folding. As such, a parent scFv with high cytoplasmic solubility is an ideal starting point for the generation of a diversified library. One such scFv is scFv13-R4, which exhibits high solubility and has been shown to bind β -gal with high affinity, implying that it is well folded. Cytoplasmic solubility is a desired property as it improves the chance that the scFv is correctly folded and functional in the highly reducing cytoplasmic environment. Since survivin is an intracellular target, this is of extreme importance. Thus, an scFv13-R4 based library was selected as the parent scFv on which the library would be based.

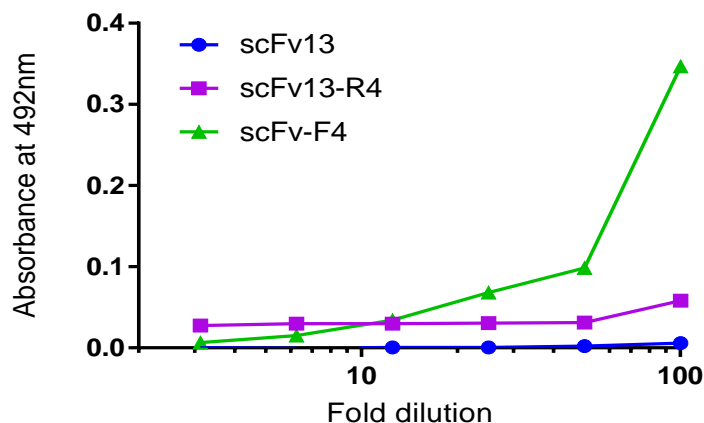


Figure 2.5 Binding of scFv-F4 to survivin. A concentration-dependent ELISA was performed to observe binding of scFv13, scFv13-R4, and scFv-F4 to survivin. scFvs bound to survivin were detected with an anti-FLAG epitope antibody. (Dr. Amy Karlsson, unpublished data).

The initial selection of the scFv13-R4 library, screening, and isolation of a new parent scFv, scFv-F4, were previously performed as follows (Dr. Amy Karlsson, unpublished data). A naïve scFv13-R4 library was obtained from the Martineau lab (IRCM, Montpellier, France). This library was constructed by introducing variation to the CDR3 regions of scFv13-R4, by performing PCR with degenerate NNK oligonucleotides such that resulting scFv library constituents had varying CDR3 length [66]. This library was displayed using the *E. coli* Tat display method and subtractive panning and positive panning (detailed below in Sections 2.2.2 – 2.2.3) were performed to eliminate non-specifically binding library constituents and to enrich for scFvs that bind to survivin (Figure 2.8). The resulting sublibrary was screened using an ELISA for binding to survivin (detailed below in Section 2.2.4). From the screening, one potential scFv variant of interest, scFv-F4, was isolated and showed higher concentration-dependent binding to survivin than other potentially interesting variants. In Figure 2.5, it can be seen that scFv-F4 exhibits higher binding signal to survivin than its parent scFv, scFv13-R4, or scFv13 from which scFv13-R4 was derived. For this reason, scFv-F4 was used as the basis for a new library.

2.2.2 Library construction

scFv-F4 was further mutagenized to create a second-generation library as described below.

2.2.2.1 Error-prone PCR

The Tat inner-membrane display plasmid containing the gene for scFv-F4, pIMD inner-membrane display plasmid (lab stock) (Figure 2.6), was used as the template in PCR using the Mutazyme II low-fidelity polymerase as part of the Genemorph II Random Mutagenesis kit (Agilent), which introduces random nucleotide errors during amplification. Initial template concentration was optimized to give a theoretical error rate of 1 to 4 amino acid mutations per amplicon.

The primers used amplify the scFv genes were the forward primer, with sequence 5'-GCGATGTCTAGAGCCGAGGTGCAGCT-3', and the reverse primer, with sequence 5'-ATGTAGTTCGAATTAACCTTTATCGTCATCGTCTTTGTAGTCTGCGGCCGCA CCTAGGAC-3'. These amplify the scFv genes, including FLAG tag, with inclusion of a 5' XbaI and a 3' BstBI site, to enable cloning into the pIMD vector. The ssTorA signal sequence is excluded from error-prone amplification to allow fair periplasmic display and representation of the library amplicons, which would not be possible if ssTorA regions contained mutations and were thus unable to confer periplasmic display.

2.2.2.2 Plasmid construction

The error-prone PCR amplification product was cleaned and digested with XbaI and BstBI and ligated into the pIMD vector at the XbaI and BstBI restriction enzyme sites.

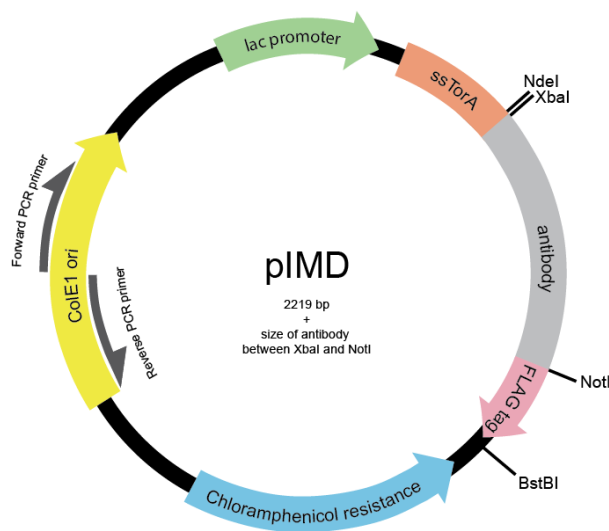


Figure 2.6‡ pIMD plasmid map. This plasmid fuses the inserted antibody gene to a 5' ssTorA signal sequence and a 3' FLAG epitope tag, with all three in the same reading frame. Restriction enzyme sites are indicated.

‡Figure originally published in *J. Vis. Exp.* (2016)

2.2.2.3 Transformation of library into *E. coli*

Test ligations and transformations were performed in order to determine the insert:vector ratio that resulted in the largest number of transformants in comparison to the vector only control. The ligation reaction was scaled up to give an estimated library size of at least 1×10^6 transformants. Following ligation, electrocompetent DH5 α *E. coli* cells were transformed via electroporation as follows. Ligation reaction product was heated at 65 °C for 15 minutes to heat-inactivate DNA T4 ligase, followed by desalting on a microdialysis membrane (Millipore). On ice, per 30 μ L of ligation reaction, 300 μ L of electrocompetent DH5 α was added and each 350 μ L solution of cells and ligation product was added to a 2 mm electroporation cuvette. Cuvettes were pulsed in an electroporator

(Bio-Rad) using manufacturer recommend settings designated for bacteria and cuvette size (2500 V, 25 μ F, 200 Ω .) To recover transformed cells, a flask was filled with 25 mL SOC for every 1 mL cells used, and each cuvette was rinsed with a total of 3 mL SOC, all of which was added to the flask. Cells were recovered for 1 hour at 37 °C. A 300 μ L aliquot was removed from the recovery flask to prepare dilutions and plate onto LB agar + Cm plates, which will be used to determine library size. The absorbance at 600 nm was read from a 1 mL aliquot as another measure to determine library size based on cell density. The remainder of the recovery cell suspension was added to 250 mL LB + Cm + 0.2% glucose and grown at 37 °C for 3 hours. From this, 100 mL was removed and added to 400 mL LB + Cm + glucose and grown overnight to expand the library. The remaining volume was used to prepare lab stocks of the library in a solution of LB + Cm + 0.2% glucose with a final concentration of 50% glycerol which were then stored at -80 °C. The overnight culture was used in a midiprep DNA extraction and library size was estimated from the number of colonies on the plates and volumes used in transformations as follows:

$$\text{Library size} = \frac{\text{Number of CFUs}}{\text{volume plated}} \times \text{dilution factor} \times$$

(total volume of recovery culture)

The purified plasmid obtained from the midiprep of the DH5 α library overnight was used to transform electrocompetent MC4100 strain *E. coli* in the same manner. Transfer into this strain is necessary as DH5 α is a cloning strain, and MC4100 is optimized for better protein expression.

2.2.3 Panning of library to enrich for survivin-binding members

To deplete the library for non-specifically binding members and to enrich for those that bind survivin, a panning of the scFv library was performed against non-specific targets followed by a panning against survivin (Figure 2.9).

2.2.3.1 Biotinylation of survivin and other proteins

Survivin (1 mg/mL stock concentration; MW = 33.490 kDa including calmodulin tag), β -gal (10 mg/ml stock concentration; MW = 465 kDa), and lysozyme (100 mg/mL stock concentration; MW = 14.4 kDa) were biotinylated. Immediately before biotinylation, a 10 mM solution of EZ-link-Sulfo-NHS-LC-biotin (Thermo Fisher) was prepared by adding 360 μ L ultrapure water to 2.0 mg of reagent. This solution was added to each reaction in a 20-fold molar excess, which was calculated from the following equations:

$$1.) \text{ mL protein} \times \frac{\text{mg protein}}{\text{mL protein}} \times \frac{\text{mmol protein}}{\text{mg protein}} \times \frac{20 \text{ mmol Biotin}}{\text{mmol protein}} =$$

mmol biotin required

$$2.) \text{ mmol biotin required} \times \frac{1,000,000 \mu\text{L}}{\text{L}} \times \frac{\text{L}}{10 \text{ mmol}} =$$

μ L biotin reagent required

The calculated amount of 10 mM EZ-link-Sulfo-NHS-LC-biotin solution was added, followed by the addition of PBS to a total volume of 50 μ L. Solutions were incubated at room temperature for 30 minutes.

2.2.3.2 Immobilizing biotinylated survivin on streptavidin-coated magnetic beads

This protocol for directly immobilizing a biotinylated protein-of-interest from cell lysate onto streptavidin-coated magnetic beads is based on the Dynabeads manufacturer protocol (Invitrogen) and on procedures in Tayapiwatana et al. [68]. Dynabeads biotin binder streptavidin-coated magnetic beads (Invitrogen) were prepared by resuspension and washing with PBS + 0.1% BSA. Supernatant was removed by incubated tubes containing beads on a magnet and carefully pipetting. Survivin, β -gal, and lysozyme were immobilized onto separate aliquots of washed beads by adding 100 μ L of biotinylated protein (from step 2.2.3.1) to 45 μ L washed beads and PBS up to a total volume of 500 μ L and incubated at room temperature for 30 minutes while rotating. Beads were collected and washed 4 times with PBS + 0.1% BSA and were then resuspended in 1 mL PBS + 0.1% BSA.

2.2.3.3 Spheroplasts with periplasmic-anchored scFvs

Spheroplasting of *E. coli* expressing library scFvs is necessary to make periplasmically anchored scFvs available for binding interactions as it permeabilizes the outer membrane (Figure 2.7). One freezer aliquot of the MC4100 scFv-F4 library was thawed and grown in 250 mL LB + Cm at 37°C for 3 hours. The cultures were transferred to 20°C and grown for 18 hours, allowing the scFvs to be expressed. Following overnight expression 1×10^{10} cells were harvested and centrifuged. The pellet was rinsed with ice-cold fractionation buffer (3.0 mL 1M Tris-HCl (pH = 8.0) + 20.0 g sucrose + 200 μ L 0.5 M Na₂EDTA + sterile water to final volume of 100 mL) and then resuspended in fractionation buffer supplemented with lysozyme. While slowly vortexing, 1 mM EDTA was added in a dropwise manner and the solution was incubated at room temperature for 20 min. Ice cold 0.5 M MgCl₂ was added and incubated on ice for 10 minutes. The sample

was centrifuged and the supernatant, which contains the dilute periplasmic fraction, was carefully removed. The remaining spheroplast pellet was then resuspended in 1 mL ice-cold PBS.

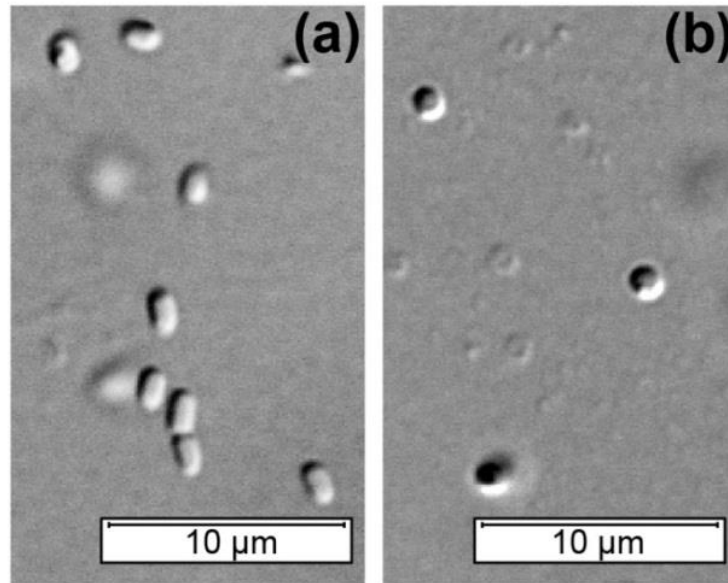


Figure 2.7 ‡ *E. coli* cells and spheroplasts. (a) Untreated *E. coli* cells are cylindrical in shape. (b) Spheroplasting *E. coli* using EDTA and lysozyme causes rupturing of the outer membrane and the spheroplasts are spherical in shape. Differential interference contrast microscopy images were obtained using a 100X objective on an inverted microscope.

‡Figure originally published in *J. Vis. Exp.* (2016)

2.2.3.4 Negative panning

The spheroplast-displayed library against magnetic beads coated in a nonspecific protein was implemented in order to deplete the library of non-specific binders. A sample of 4×10^9 spheroplasts was added to 8×10^8 lysozyme-coated beads and the volume was adjusted to 4 mL by adding PBS + 0.1% BSA. The reaction was split into 4 aliquots and

gently rotated at 4 °C for 4 hours. Following incubation, the tubes were placed on a magnet and the supernatant containing the unbound spheroplast population was collected and used in a new negative panning preparation with fresh lysozyme-coated beads and the panning was repeated. Negative panning was repeated a third and fourth time with β -gal coated beads.

2.2.3.5 Positive panning, PCR amplification, and library construction

Immediately following negative panning, the collected supernatant, which contains any remaining unbound spheroplasts, was used to prepare panning reactions with survivin-coated beads. Reactions were incubated at 4 °C while gently rotating for 5 hours. Polymerase chain reaction (PCR) to amplify the scFv genes of plasmids contained in the bead-bound spheroplasts was performed. Bead-bound spheroplasts were prepared for PCR by washing with PBS + 0.1% BSA followed by resuspension in 25 μ L water. Multiple identical PCR reactions were prepared as seen in Table 2.1 and boiled at 98 °C for 15 minutes prior to adding polymerase. High fidelity Phusion polymerase (New England Biolabs) was used to ensure errors that could change the scFv sequence could not occur. The PCR was completed using the thermal cycler program in Table 2.2. PCR products were pooled, cleaned using a PCR cleanup kit, and scFv genes were cloned into the pIMD vector as described in step 2.2.2.2 and transformed into *E. coli* as described in step 2.2.2.3.

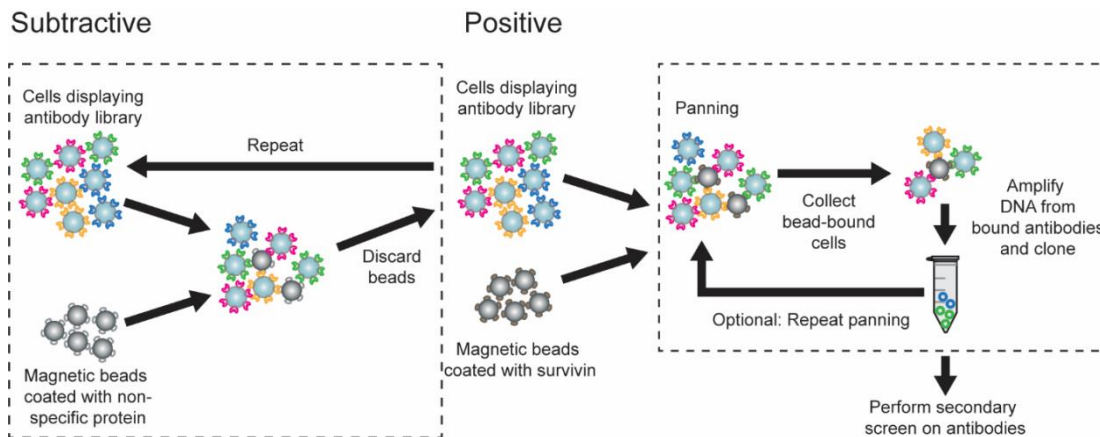


Figure 2.8 Subtractive and positive panning. Spheroplasts expressing antibody library variants are incubated with magnetic beads coated with non-desired target to deplete the library of antibodies that bind non-specifically. Spheroplasts remaining in solution are incubated with survivin-coated magnetic beads. Antibody genes from bead-bound spheroplasts are amplified for generation of an enriched sublibrary.

Table 2.1 PCR reaction preparation for amplification of scFv library from bead bound spheroplasts

Reagent	Volume (μL)
Washed beads with bound spheroplasts	5.0
40 mM (10 mM each) dNTP mix	0.4
Forward primer "MD 6283" (33 μM)	0.75
Reverse primer "MD 6284" (33 μM)	0.75
5X Phusion HF buffer	10.0
Water	32.6
Phusion polymerase (added after boiling step)	0.5
Total	50.0

Table 2.2 Thermal cycler protocol for PCR amplification of scFv library from bead bound spheroplasts

Step	Temperature (°C)	Duration
1	98	30 seconds
2	98	30 seconds
3	62	30 seconds
4	72	25 seconds
5	<i>Repeat steps 2 – 4 30 times</i>	
6	72	8 minutes
7	12	∞

2.2.4 Library secondary screening

An initial screening on the binding activity of library variants was performed in order to isolate potentially interesting clones to further characterize. The MC4100 panned scFv-F4 library was plated onto 20 µg/mL Cm LB agar plates and grown at 37 °C. Sterile flat-bottom 96-well culture plates were filled with 200 µL per well with 20 µg/mL Cm LB media. Individual colonies from the library plate were picked using a pipette tip and used to inoculate individual wells of the culture plate. Controls included were wells with cells harboring scFv-13, scFv-R4, and scFv-F4 containing plasmids, as well as a negative control well with no inoculation. Plates were incubated at 37 °C for 4-6 hours at 350 rpm on a microplate shaker until OD₆₀₀ = 0.6. Cell suspension from wells was spotted as an array onto a 15 cm LB + Cm agar plate, which was incubated at 37 °C. This enables recovery of specific clones after the screening assay is completed. Plates were further incubated at 37 °C shaking overnight to promote growth and induction of scFv expression. A high-binding polystyrene ELISA plate was coated with 50 µL of a 1 µg/mL survivin solution and incubated at 4 °C overnight. The ELISA plate was emptied and blocked with 2% milk in PBS for 2 hours. Cells in the growth plate were lysed by the addition of 20 µL PopCulture reagent (EMD Millipore) per well and incubated at room temperature while shaking for 15 minutes. The ELISA plate was washed 4 times with 0.05 % PBST followed

by a transfer of 50 μL from each well of the cell lysis plate to the ELISA plate. Plates were incubated at room temperature for 2 hours then washed as before. The conjugated primary anti-FLAG (HRP) antibody was prepared at a 1:10000 dilution in 2% milk PBST and 50 μL of the antibody solution was added to each ELISA plate well and incubated at room temperature for 2 hours. Plates were washed as before and 200 μL of SigmaFast OPD (*o*-phenylenediamine dihydrochloride) HRP substrate (Sigma Aldrich) was added to each well and incubated for 1 hour at room temperature in the dark. The reaction was quenched by addition of 50 μL 3 M H_2SO_4 per well and absorbance at 492 nm was measured. Data was analyzed by first subtracting background signal and then comparing absorbance values for each well to that of the average absorbance of the scFv-F4 wells as a higher signal indicates higher binding of expressed scFvs clones to survivin. Interesting clones were selected on this basis to further characterize their survivin-binding properties.

2.2.5 Library tertiary screening

This assay was performed in order to determine the binding properties of interesting clones at different dilutions in order to characterize binding to survivin. Cells were inoculated from the spotted agar plates from step 2.2.4 into 5 μL LB + Cm each and grown overnight at 37 °C. ELISA plates were coated with survivin as described in step 2.2.4. Plates were blocked with PBS + 0.1% BSA for 2 hours at room temperature then washed with PBST. Cell lysates were prepared by centrifuging overnight samples, adding BugBuster MasterMix (EMD Millipore) as directed in the manufacturer protocol, and centrifuging at 16,000 $\times g$ for 20 minutes at 4 °C to separate soluble cell lysate from insoluble cell debris. Two-fold dilutions of cell lysate were performed, using PBS + 0.1% BSA as a diluent such that all wells contained 50 μL of lysate. Samples were incubated for 1.5 hours at room

temperature then washed with PBST as before. A 1:10,000 dilution of Anti-6XHis (HRP conjugated) antibody was prepared in PBS-BSA and 50 μ L was added per well and incubated for 1.5 hours, followed by a PBST wash as before. HRP substrate was prepared as directed in manufacturer instructions and 200 μ L was added to each well on the ELISA plate and incubated for 30-45 minutes in the dark. To quench the reaction, 50 μ L of 3M H₂SO₄ was added to each well and mixed by pipetting. The absorbance at 492 nm was measured.

2.2.6 Expression and binding characterization of isolated clones

A Western blot was performed to determine the level of soluble scFv expression of newly-isolated library members as compared to scFv-R4 and scFv-F4 which have high soluble expression. For this experiment, genes encoding scFvs were expressed using the pET21 expression vector that expresses protein in the cytoplasm. Thus, scFvs will no longer be anchored in the periplasm, and will be partitioned into either the lysis buffer (soluble fraction) or remain in the cell debris (insoluble fraction).

Standard molecular cloning techniques were used to clone the genes encoding for scFv13, scFv13-R4, scFv-F4, and selected isolated scFvs into the pET21 expression plasmid, which expresses proteins with a C-terminal 6XHis tag. BL21-DE3 *E. coli* were transformed with the recombinant plasmids via electroporation as previously described. BL21-DE3 cells with no plasmid were included as a control. Cells were grown at 37 °C overnight, subcultured to OD₆₀₀= 0.5-0.8 and induced with IPTG at 20 °C overnight. Cells were transferred to microcentrifuge tubes and centrifuged at 16,000 \times g for 5 minutes. The supernatant was removed and 5 mL/g cell pellet of BugBuster MasterMix was added to each sample and resuspended. Samples were incubated at room temperature for 20 minutes

while gently rotating then centrifuged at $16,000 \times g$ at $4\text{ }^{\circ}\text{C}$ for 20 minutes to pellet the cell debris. The supernatant containing the soluble fraction of protein was collected and the total protein concentration was measured at A_{280} . Samples were diluted with BugBuster MasterMix to normalize by total protein concentration. SDS loading buffer was added and samples were boiled at $98\text{ }^{\circ}\text{C}$ for 5 minutes, and then loaded onto an Any kD Mini-PROTEAN TGX precast protein gel (Bio-Rad) for gel electrophoresis. Protein was transferred to a polyvinylidene difluoride membrane, which was then stained with a horseradish peroxidase (HRP)-conjugated anti-6XHis antibody and incubated with HRP substrate. Blots were imaged on ChemiDoc gel imaging system (Bio-Rad) using a chemiluminescence protocol.

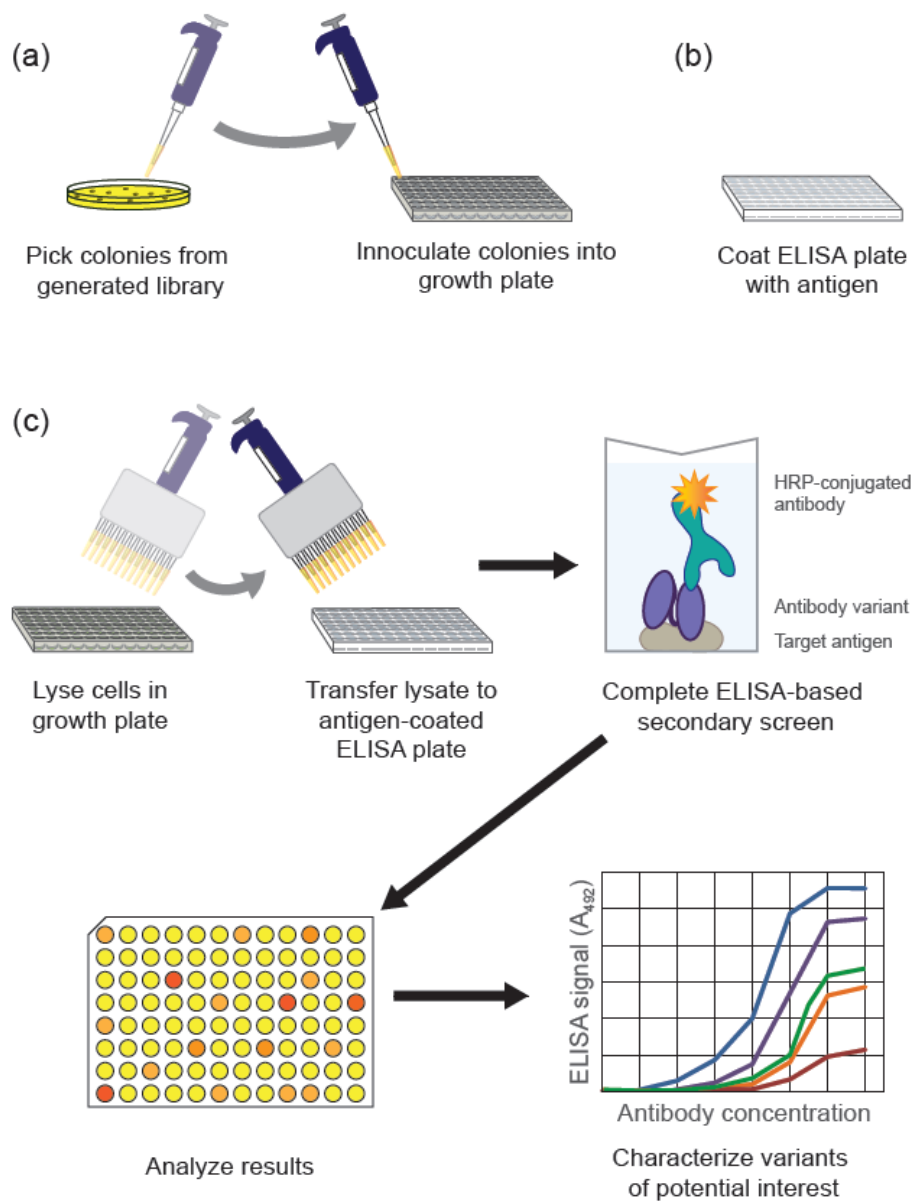


Figure 2.9‡ ELISA-based secondary screen. (a) To grow and express antibodies, wells of a culture plate are inoculated with individual library variants from the sublibrary enriched during panning. (b) An ELISA plate is coated with target antigen. (c) Library variants are screened using the ELISA-based secondary screen described. Upon analysis of data obtained from the secondary screen, variants of interest are selected and characterized further via concentration-dependent ELISA using cell lysates.

‡Figure originally published in *J. Vis. Exp.* (2016)

2.3 Results and discussion

2.3.1 scFvs isolated through inner-membrane display and screening are soluble

In order for intrabodies to function properly, they must be soluble and correctly folded in the cytoplasmic environment. Insolubility of intrabodies results in aggregation that can renders them non-functional [63]. To determine whether or not isolated scFvs are cytoplasmically soluble, the soluble fraction of newly-isolated variants was compared to that of scFv-F4 and scFv13-R4. Similar levels of soluble protein expression are observed, which indicates that the Tat inner-membrane display and screening method is not selecting against this property and that solubility of library variants is maintained because insoluble library members are not displayed for screening (Figure 2.10). As expected, scFv13 exhibits lower soluble expression levels as previously observed by Karlsson et al. [29]. Since scFvs need to be soluble in the cytoplasm, this property is imperative to their function. These results demonstrate the application of the Tat inner membrane display system as a tool to engineer intrabody solubility.

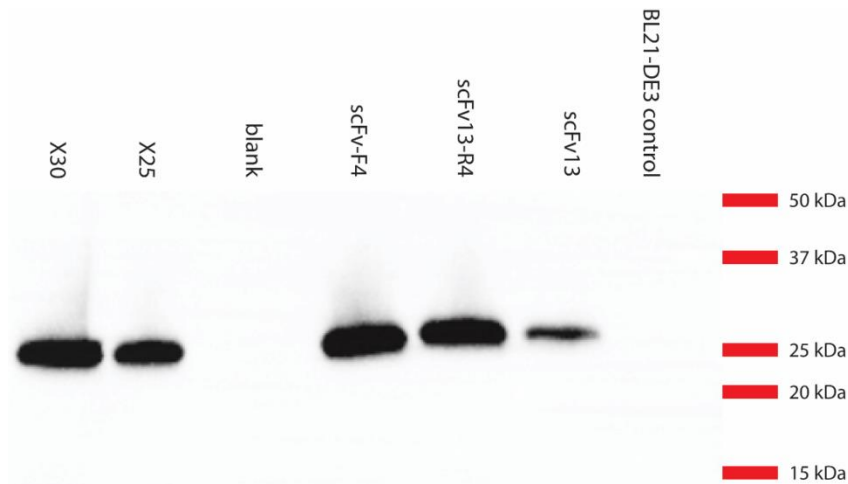


Figure 2.10 Soluble fraction of cytoplasmically expressed scFvs. scFv13, scFv13-R4, and scFv-F4 controls were compared to X25 and X30 scFv library isolates for soluble expression. Genes encoding each scFv were cloned into the pET21 (+) a plasmid and expressed as a fusion to a polyhistidine tag in BL21-DE3 *E. coli*. Samples were normalized by total protein concentration prior to gel loading and detected using an ant-6XHis antibody in a Western blot assay.

2.3.2 Isolated scFvs are non-specific and do not exhibit saturable binding

Library scFv variants of interest were isolated and further characterized for surviving-binding capabilities and showed high ELISA signal that increased with increasing scFv concentration. However, saturable binding was not seen as higher scFv concentrations were used, which may be indicative of nonspecific binding or aggregation of scFvs (Figure 2.11A). While a saturable binding curve is not a requirement, it suggests that the binding signal seen is predominantly from scFvs binding specifically to the antigen. Since there is a finite amount of antigen present, binding that does not show saturation at higher scFv concentrations is indicative of scFvs nonspecifically binding to each other such that the signal is amplified. It could also indicate that an isolated scFv is binding to multiple epitopes on a single antigen, which indicates some level of nonspecificity.

Additionally, when the same scFvs were tested via ELISA for binding to nonspecific targets such as β -gal and lysozyme (method in Section 3.2.4), similar binding patterns and absorbance intensities were seen, indicating that isolated scFvs bind to all targets, including survivin, nonspecifically (Figure 2.11B). This nonspecific binding is an undesirable property as for therapeutic purposes, it is imperative that the antibody binds only survivin, as binding other proteins may disrupt other pathways and cellular properties that may change the properties of the cancerous cells in undesirable ways.

A potential reason for the high binding signal seen in the secondary screen that led the pursuit of the scFvs that bind nonspecific targets with high affinity is binding avidity. The secondary screen relies on the data from just one well with an uncontrolled number of cells, and thus an uncontrolled number of displayed scFvs, to convey information about that particular scFv binding affinity for survivin. It is possible that some wells contain more cells and thus, more scFv copies, which can lead to an inaccurate comparison of two scFvs with equal binding affinity. Additionally, the secondary screening assay involved the use of surface-immobilized antigen, which can also increase avidity due to a high local concentration of available antigen binding sites. As the survivin is not oriented on the surface in any particular way during the bead-coating process, there will also be a higher number of scFvs that can bind as there are more potential antigen epitopes that isolated scFvs may bind.

A strategy was employed to elucidate implications of secondary screen apparent binding signal as it relates to specificity. We hypothesized that those variants showed very high secondary screen signal may be doing so due to scFv crowding or avidity and that scFvs showing mid-range signals may be more accurately representative of scFv binding

strength. Following secondary screening, the variants were grouped into three bins based on the A₄₉₂ signal and scFvs from each bin were compared to those of other bins in a specificity ELISA (data not shown). It was found that the differences in secondary screen signal did not convey differences in specificity among scFv variants as those from different signal bins showed similar non-specific binding behavior.

We hypothesize that the non-specific properties of scFvs isolated from the library may be a result of reduced library quality and choice of parent scFv. While scFv-F4 was selected due to its high binding signal to survivin and the fact that its parent scFv, scFv13-R4, exhibited high cytoplasmic solubility [29], its intrinsic binding affinity for β -gal may be difficult to overcome when targeting other antigens. However, as the scFv also bound to lysozyme, to which scFv13-R4 does not bind, this is likely not the case. The issue may be caused by overall library quality, that is determined by functional library size and not by apparent library size [69]. Preferences for mutation and high percentage of stop codon mutations could result in a poor sampling of possible scFv mutants. We reviewed a sampling of scFv library member sequences throughout these studies and all were unique, in frame with the ssTorA signal sequence, and a low percentage contained stop codons (data not shown.) As high-affinity antibodies have been isolated from non-immunized libraries with some groups indicating specificity of isolated antibodies [70,71], however, it may be of interest to consider obtaining an immunized library.

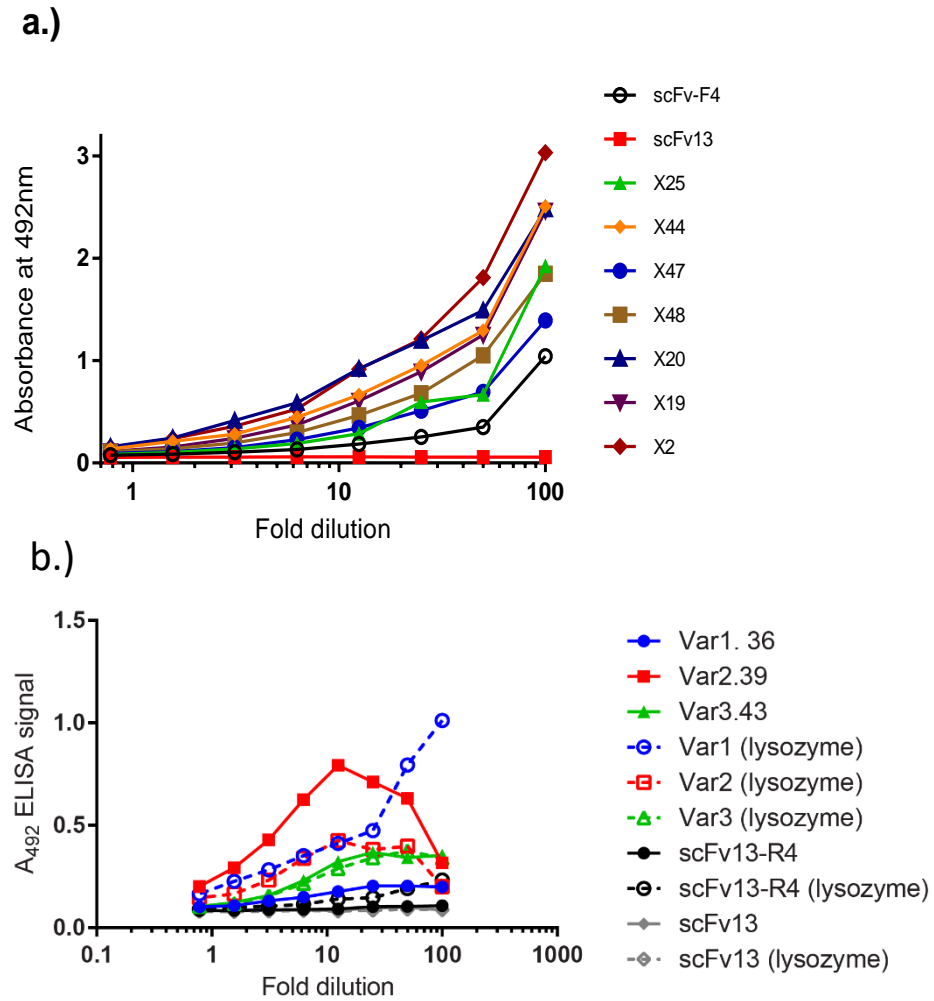


Figure 2.11 Binding of scFv variants. (a) A concentration-dependent ELISA was performed on variants of scFv-F4 to observe binding to survivin. Variant names begin with “X”. (b) To observe specificity, a concentration-dependent ELISA was performed using variants of scFv13-R4 on ELISA plates coated with either survivin or lysozyme. BL21-DE3 cells expressing scFvs were lysed and lysates were serially diluted in an ELISA plate coated with survivin or lysozyme. scFvs were detected with an HRP-conjugated anti-FLAG antibody and incubation with HRP substrate, followed by absorbance measurement at 492 nm. Closed icons indicate samples binding to survivin and open icons indicate samples binding to lysozyme. Variant names begin with “Var”. Samples labeled with (lysozyme) indicate their binding to lysozyme and those with no designation in parentheses indicate binding to survivin.

2.4 Conclusion

Overall, scFvs isolated from the scFv-F4 library using Tat inner-membrane display and screening exhibited high binding to survivin. They also showed high binding to non-specific targets, which is not ideal when aiming for binding to a specific intracellular target. While the underlying cause of this nonspecific behavior has yet to be determined, these results clearly indicate a need to characterize the specificity of antibodies derived from all library display and screening protocols.

Still, isolated scFvs were soluble, indicating that they are likely well folded in the cytoplasmic environment which highlights the capability of the Tat inner membrane display system as a vital tool to engineering intrabody solubility. Additional modifications to the screening protocol will improve the specificity of isolated antibodies. These results highlight that advantages of the Tat inner-membrane display and screening method for the isolation of soluble intrabodies and necessitate the improvement of the methods for the screening of a naïve library to increase intrabody specificity.

Furthermore, these results emphasize the general need to assess specificity when screening a large library, particularly one that is non-immunized. Non-specific binding, both intracellularly and extracellularly, could result in detrimental off-target effects and greatly reduce the ability to use such antibodies as therapeutics. Specificity is often overlooked when engineering for antigen binding affinity; however, our results demonstrate the need for antigen specificity characterization.

Chapter 3: Improving antibody library construction and screening assays

3.1 Introduction

Specificity of binding is an issue, particularly in dense cytoplasmic milieu. Nonspecific binding of intrabodies can lead to undesired off-target effects. In our studies, we found that it was difficult to isolate scFvs that specifically bound to survivin and not to other proteins. Additionally, the screening method of Tat-displayed libraries is a low-throughput method, and thus any techniques that can shorten the timescale of screening would be beneficial. For this reason, we sought to implement techniques to increase the stringency and streamline the screening process to remove time-consuming steps.

3.2 Methods of improvement

3.2.1 Whole plasmid PCR

3.2.1.1 Determination of feasibility of whole plasmid PCR

In the interest of simplifying the protocol and saving time, we sought to eliminate a cloning step by utilizing whole plasmid PCR. Previously, scFv genes were amplified via PCR, digested with restriction enzymes and ligated back into the vector plasmid.

To ensure whole plasmid PCR can be performed, purified pIMD-scFv13 plasmid was used to set up a PCR reaction with various sets of primers that are in conserved regions of the vector, for example, the origin of replication. Five sets of primers (Table 3.1) were tested to see which gave the best results in addition to variance of the type of polymerase, Phusion

or Q5 (New England Biolabs), used for primer sets that benefited from adjustment in annealing temperature. In each set of primers, the forward and reverse primers were designed to anneal to the template end-to-end, on complementary strands, such that when amplified, the entire plasmid will be accounted for (Figure 3.1). Primers were phosphorylated at the 5' end with T4 Polynucleotide Kinase (PNK) (New England Biolabs) to ensure re-circularization can occur. The template DNA used to test amplification was pIMD-scFv13 and each reaction was set up as shown in Table 3.2 and using the thermal cycler program in Table 3.3. Following PCR, 5 μ L of each PCR product was run on an agarose gel alongside uncut plasmid template controls to determine size. The remainder of each product was cleaned using a PCR cleanup kit (Promega) and ligation was performed at 16 $^{\circ}$ C overnight at a low template concentration of 1 ng/ μ L to re-circularize the DNA (Table 3.4).

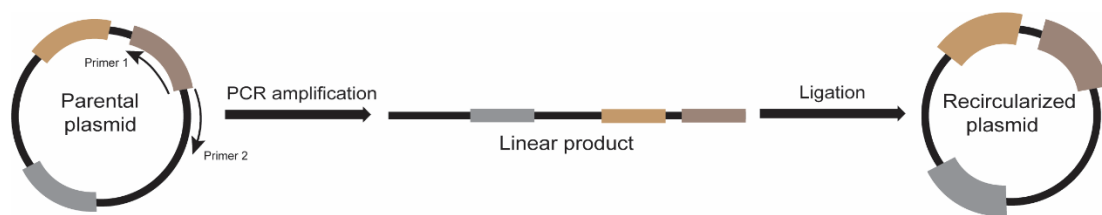


Figure 3.1 Whole plasmid PCR. End-to-end primers that anneal to a common plasmid feature are used to amplify the entire plasmid. The linear product is ligated resulting in the recircularized plasmid.

Table 3.1 Whole plasmid PCR primer sets

Set	Primer Name	Sequence	Annealing region on plasmid
1	Forward P-125	5'- CCAACTCTTTTTCCGA AGGTAAGT-3'	ColE1/pMB1/pBR322/pUC origin of replication
	Reverse P-126	5'- TAGCTCTTGATCCGG CAAACAAA-3'	
2	Forward P-127	5'- TATAGTCCTGTCGGG TTTCGCCAC-3'	ColE1/pMB1/pBR322/pUC origin of replication
	Reverse P-128	5'- AAGATACCAGGCGTT TCCCCCT-3'	
3	Forward P-129	5'- GCGGGCAAGAATGTG AATAAAG-3'	chloramphenicol acetyltransferase
	Reverse P-130	5'- CTGATGAATGCTCAT CCGGAA TT-3'	
4	Forward P-131	5'- TTTCAGTTTGCTCATG GAAAACG-3'	chloramphenicol acetyltransferase
	Reverse P-132	5'- CGTTTTTCATCGCTCTG GAGTGAATA-3'	
5	Forward P-133	5'- CTTATTTTCATTATGGT GAAAGTTGGAACCTC TT-3'	promoter of the <i>E. coli</i> cat gene encoding chloramphenicol acetyltransferase
	Reverse P-134	5'- ATCACTACCGGGCGT ATTTTTTGAGTTGTC- 3'	

Table 3.2 PCR reaction preparation for PCR amplification of whole plasmids

Reagent	Volume (μ L)
Plasmid template (0.5 ng)	0.9
Phosphorylated forward primer (10 μ M)	2.5
Phosphorylated reverse primer (10 μ M)	2.5
5X polymerase-appropriate reaction buffer	10
40 mM dNTP mix	1
Sterile water	32.6
Polymerase	0.5
Total	50

Table 3.3 Thermal cycler protocol for PCR amplification of whole plasmids

Step	Temperature (°C)	Duration
1	98	30 seconds
2	98	10 seconds
3	T _a	30 seconds
4	72	1 minute, 30 seconds
<i>Repeat steps (2 – 4) 35 times</i>		
5	72	6 minutes
6	12	∞

Table 3.4 Preparation of a ligation reaction to recircularize linear whole plasmid PCR product

Reagent	Volume (μL)
Linearized PCR product (200 ng)	Dependent on concentration
10X T4 DNA ligase buffer	20
T4 DNA ligase	1
Sterile water	To a total of 200 μL

3.2.1.2 Whole plasmid PCR on spheroplasts

We then sought to show that whole plasmid PCR can be performed on recovered spheroplasts. Following a panning of library spheroplasts against survivin-coated beads, beads were collected and used to set up PCR reactions. Each PCR reaction was prepared as in Table 3.2 but instead of purified plasmid template, 5 μL of beads collected from panning were used and the volume of sterile water was adjusted. Only the primer set 2 (P-127 + P-128) was tested. PCR product was run on an agarose gel alongside PCR product from amplification of solely the scFv gene region to compare size.

3.2.2 Recovery of plasmids from spheroplast

3.2.2.1 Determining minimum spheroplast concentration for direct transformation of *E.coli* cells

FACS sort cell suspensions of different cell densities were simulated by spheroplasting *E. coli* and resuspending them in PBS (Table 3.5). Samples were centrifuged at $16,000 \times g$ at $4\text{ }^{\circ}\text{C}$ for 10 minutes and $900\text{ }\mu\text{L}$ of the supernatant was carefully removed by pipetting. To each sample, $500\text{ }\mu\text{L}$ of sterile water was added to lyse the spheroplasts. Each sample was then sterile filtered through a $0.2\text{ }\mu\text{M}$ filter to remove any residual cells and de-salted on a microdialysis membrane (EMD Millipore). MC4100 cells were transformed by addition of $20\text{ }\mu\text{L}$ of filtered, de-salted lysates to $50\text{ }\mu\text{L}$ *E. coli* and transformation via electroporation as previously described. Each reaction of transformed cells was recovered for 1 hour at $37\text{ }^{\circ}\text{C}$ in $400\text{ }\mu\text{L}$ SOC media. For each condition, $380\text{ }\mu\text{L}$ of recovery was plated on 15 cm LB agar + Cm plates and incubated at $37\text{ }^{\circ}\text{C}$ overnight. The number of CFUs per plate was counted. No replicates were performed initially.

3.2.2.2 PCR amplification of spheroplasts

To assess whether or not spheroplasts at low concentrations that are not bound to magnetic beads can be used in PCR amplification reactions, the following experiment was performed. MC4100 *E. coli* containing pIMD-F4-FLAG plasmid were grown and spheroplasts were prepared as previously described. Spheroplasts were diluted to concentrations of 1×10^4 cells/mL, 1×10^6 cells/mL, or 1×10^8 cells/mL in 1 mL PBS each. Samples were centrifuged at $4\text{ }^{\circ}\text{C}$ at $11,000 \times g$ for 20 minutes and $500\text{ }\mu\text{L}$ of supernatant was removed by pipetting. To each sample, 2 mL of sterile water was added to lyse the spheroplasts. Samples were then sterile filtered through a $0.2\text{ }\mu\text{m}$ filter to

eliminate *E. coli* that were not spheroplasted or lysed, which could contaminate results. A small volume from each was collected at this step to use as a comparison to test the necessity of performing a cleanup of the lysed spheroplasts. A PCR cleanup kit was used to concentrate the remaining filtered samples, which were eluted into a volume of 35 μL .

Whole PCR reactions were prepared for each starting spheroplast concentration, with either 75 μL pre-PCR cleanup sample, 5 μL post-PCR cleanup sample, or 20 μL post-PCR cleanup sample using primer set 2 (P-127 and P128). A positive control was prepared using purified plasmid DNA. A negative control was prepared with water instead of DNA or spheroplast. Taq polymerase (New England Biolabs) was used as it showed better amplification of at low DNA template concentrations as compared to Phusion polymerase.

3.2.3 Increasing stringency

scFvs isolated by screening the inner membrane-displayed library did not bind specifically to survivin and showed similar binding to nonspecific targets of β -gal and lysozyme (Section 2.3.2). To improve the likelihood of isolating scFvs that specifically bind survivin, we sought to alter the panning and screening protocol by manipulating conditions through the use of non-specific proteins, additional blocking reagents or competitive inhibitors.

3.2.3.1 Inclusion of a non-specific target, competitive inhibitor, additional blocking reagents in panning reactions

To increase the probability that potentially interesting library members bind to survivin immobilized on beads specifically, a variety of conditions were manipulated

during panning reactions. Panning reactions were prepared as described in Section 2.2.3 with the addition of 40 μg of β -gal per reaction. Simultaneously, the addition of additional BSA, milk, and Tween 20 was varied.

An experiment was performed to determine the effects of supplementation with 0.05 mg/mL soluble β -gal during the lysate incubation step of the secondary screening process. Potentially interesting clones were selected for further characterization. To determine the effect of this modification on saturable binding, ELISAs to observe binding to survivin were performed that included isolated members from the secondary screen with β -gal and members isolated from screening without β -gal supplementation. Three variants that exhibited saturable binding profiles were selected for further characterization to determine their specificity. ELISAs were performed using these variants against survivin and the nonspecific target lysozyme, including scFv13-R4 and scFv-F4 as controls. Additionally, to compare blocking capabilities of different reagents, lysates dilutions were prepared in either PBST + 50 $\mu\text{g}/\text{mL}$ BSA or PBST + 2 % w/v milk.

In a separate experiment, soluble scFv-F4-6XHis was included as a competitive inhibitor in panning reactions. This would serve as a method to allow only scFvs that bind survivin with higher affinity than scFv-F4 to compete scFv-F4 off of survivin and contribute to a binding signal. BL21-DE3 *E. coli* transformed with pET21-scFv-F4-6XHis were grown overnight at 37 °C then subcultured to $\text{OD}_{600} = 0.5$ and were induced with IPTG and grown at 20 °C overnight. Cells were lysed using a cell disruption system (Avestin) and purification was performed using immobilized metal affinity chromatography (IMAC) on a Next Generation Chromatography system (Bio-Rad). Collected fractions containing soluble scFv-F4-6XHis were sequentially dialyzed into 20

mM Tris supplemented with 100 mM EDTA (pH = 8.5), 20 mM Tris (pH = 8.5), and finally PBS (pH = 7.4). Purity and molecular weight were confirmed by gel electrophoresis and Coomassie staining. Panning reactions were prepared as described in 2.2.3 with the addition varying volumes of soluble scFv-F4-6XHis per reaction.

3.2.3.2 Additional negative panning steps to improve elimination of non-specific library members

Another method modification to improve specificity was the addition of multiple negative panning steps. Originally, there was no inclusion of the negative panning steps detailed in Chapter 2.2.3.4 other than panning the spheroplast library against beads that were not yet coated with anything other than streptavidin. See 2.2.3.4 for sequential negative panning protocol.

3.2.4 Specificity ELISA

Specificity of isolated antibodies is often overlooked but needs to be assessed when engineering intrabodies for therapeutic purposes to prevent any off-target effects that may be unfavorable [72]. To assess the specificity of isolated antibody fragments for binding survivin, those antibodies that showed promising binding activity were assessed. Performing this assay after making modifications to the panning and screening protocols provides a correlation between the inclusion of competitive or blocking factors and the specificity of isolated scFvs.

Survivin and a non-specific target (i.e. β -gal, lysozyme, or BSA) were coated onto high-binding polystyrene 96-well ELISA plates at 4 °C overnight and an ELISA was performed as described in 2.2.5 with dilutions of one replicate of scFv sample lysate added

to wells coated with survivin and the other added to wells coated with non-specific target. Survivin was coated at 1 $\mu\text{g/mL}$, β -gal was coated at 4 $\mu\text{g/mL}$, and lysozyme was coated at 1.2 $\mu\text{g/mL}$. Binding curves were plotted and qualitatively analyzed to compare A_{492} binding signals.

3.3 Results and discussion

3.3.1 Whole plasmid PCR recovers plasmid from purified plasmid and spheroplast lysate

Gel electrophoresis of purified linearized whole plasmid PCR product and

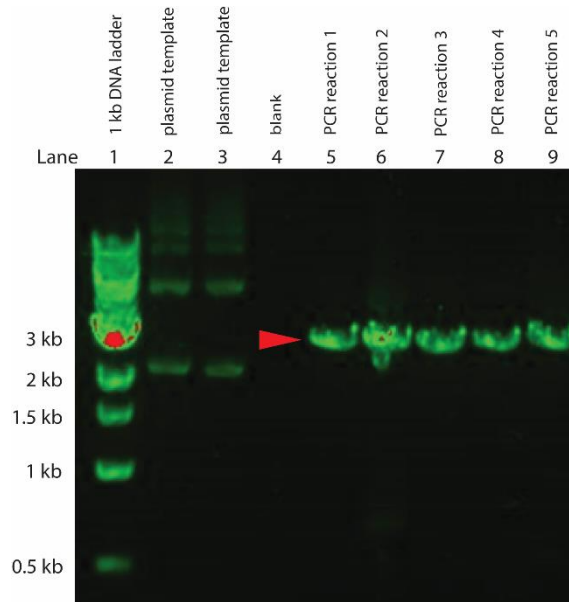


Figure 3.2 Whole plasmid PCR using purified plasmid template. Sizes of linear product obtained from whole plasmid PCR reactions 1 – 5 from Table 3.1 (Lanes 5 – 9) were compared to that of undigested, purified plasmid template (Lanes 2 – 3). Arrow indicates approximate correct size of 2970 bp as determined by the DNA ladder (Lane 1). Red color on DNA band indicates signal saturation.

recircularized whole plasmid PCR product showed bands around the correct size of 2970 bp, with the recircularized plasmid running slightly larger which is expected as supercoiled plasmid tends to run smaller than linearized ladder DNA (Figure 3.2). These results indicate that plasmids can successfully be fully amplified.

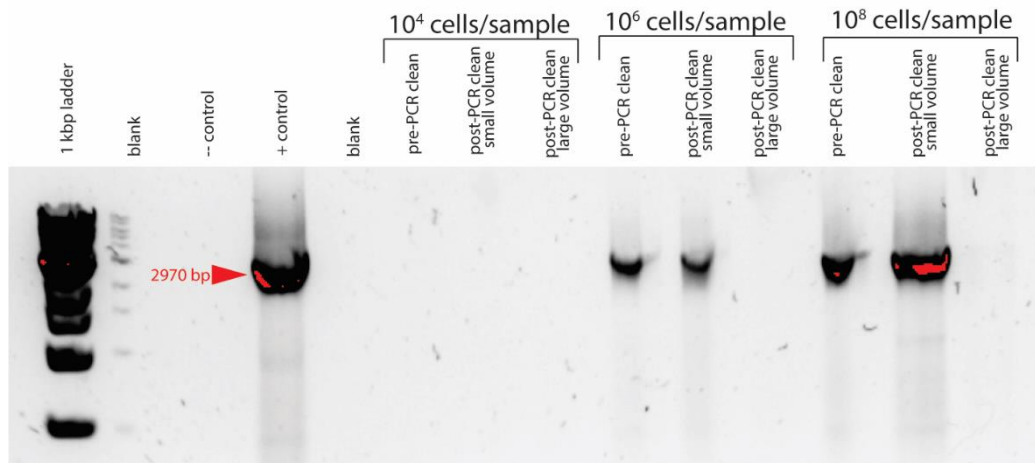


Figure 3.3 Whole plasmid PCR using lysed spheroplasts as template. Spheroplasts containing plasmid of interest were lysed and lysis product was used to prepare whole plasmid PCR reactions as described in 3.2.1.2. Sizes of product were compared to that of a positive control product from whole plasmid PCR of purified plasmid. Red arrow indicated expected full-length plasmid size of 2970 bp. Red color on DNA band indicates signal saturation.

It was also found that whole plasmid PCR can be performed successfully on plasmids taken from spheroplasts. Whole plasmid PCR performed on purified plasmid from spheroplasts was ran on an agarose gel and again bands were present at the correct size of 2970 bp (Figure 3.3). This enables the elimination of cloning step to reinsert recovered scFv genes into the vector plasmid, thus shortening the time needed to screen the library. It should be noted that whole plasmid PCR done on spheroplasts did result in some amplification of smaller products (below 500 bp) and some larger products (above 6 kb) which can be removed by excision of the correct band from the gel followed by cleanup prior to recircularization. The addition of this step would still entail fewer overall steps in the library amplification process.

Both of these methods of whole plasmid PCR save time in the course of library construction as they eliminate the need to produce and purify large amounts of vector plasmid and additional restriction enzyme digestion steps needed to ligate library gene inserts into the vector. Typically, it takes 1 to 2 weeks to perform these steps, which would need to be performed multiple times throughout the directed evolution process as the library is enriched and new libraries are constructed from isolated scFvs. Thus, implementing these changes can eliminate months' worth of plasmid purification, digestion, and cloning procedures. This additional time that the user gains can be allocated to screening additional variants or further characterization.

3.3.2 *E. coli* are transformed with spheroplast lysate to recover plasmid

As an alternative to conducting screening in ELISA plates, there is the potential to use fluorescence activated cell sorting (FACS) to screen and sort individual scFv-displaying spheroplasts for survivin binding. However, this sorting process would return a solution containing a low concentration of spheroplasts, which are very difficult to recover in liquid or agar media. This is because spheroplasts are essentially damaged in that their outer membrane has been removed, which naturally makes it difficult for cell survival and growth and prevents cell division [73]. In order to determine whether or not spheroplasts could be recovered, without the need for an additional PCR and cloning step, we sought to find the minimum sorted spheroplast concentration that could be used to directly transform *E. coli* that could then be recovered and grown. This value can help to determine the quantity of spheroplasts that need to be analyzed and sorted via FACS.

It was determined that at simulated sorting concentration outputs of less than 1×10^6 cells/mL, there was no growth of transformed *E. coli* cells on LB agar plates (Table

3.5). At spheroplast concentrations higher than 1×10^6 cells/mL, transformed *E. coli* cells showed adequate colony growth, though still at amount lower than expected given the theoretical number of cells plated. This recovery is still an improvement in the method as it eliminates multiple steps needed to recover the library gene sequences that show high survivin binding.

From the PCR results, amplification of whole plasmid was seen for initial spheroplast concentrations of 1×10^6 cells/mL and 1×10^8 cells/mL when either pre-PCR cleanup DNA or a small volume of post-PCR cleanup DNA was used to prepare the PCR reaction (Figure 3.3). A higher volume of post-PCR cleanup DNA yielded no product; however, this may be optimized further in the future.

Table 3.5 Correlation of spheroplast sample cell density to transformed *E. coli* CFU/mL

Simulated FACS sort retrieval density (spheroplasts/mL)	Transformed <i>E. coli</i> CFU/mL
Negative control (sterile water)	0
0	0
5×10^3	0
1×10^4	0
5×10^4	0
1×10^5	5
1×10^6	47
1×10^7	159
1×10^8	1537
1×10^9	2947

Again, the implementation of this technique decreases the total time needed to construct a library from a panned sublibrary or new parent scFv. By eliminating the need to perform PCR or ligation, the library construction process is streamlined. This saves approximately 2 weeks total time from each library construction procedure which equates to a few months of time saved in the iterative library screening and construction process.

3.3.3 Increasing assay stringency modulates scFv binding behavior does not result in improved specificity

Method modifications that increased the stringency of the screening assay changed the binding behavior of isolated scFvs but did not improve the likelihood that selected clones specifically bind survivin. The addition of β -gal in the secondary screen improves discrimination of clones with better binding to survivin. When soluble β -gal was supplemented during the lysate incubation step of the secondary screen, the tertiary screen results indicated that fewer isolated variants showed high binding to survivin as compared to those isolated from secondary screens where no soluble β -gal was supplemented (Figure 3.4). Additionally, for those clones from the β -gal supplemented screening that did show high binding to survivin, a concentration-dependent binding profile that was relatively saturable was seen. This is indicative that including β -gal as a competitor limits the number of false positive signals seen when performing a concentration dependent ELISA, which will prevent the pursuit of those clones. Though more studies need to be conducted, observing even one scFv that demonstrates saturable binding gives confidence that utilizing a soluble competitor allows for clones with better binding profiles to bind the target antigen.

Furthermore, comparing binding of these scFvs to survivin under different diluent conditions, using PBST + 50 μ g/mL BSA showed concentration-dependent binding profiles that appeared more saturable than those obtained using PBST + 2 % milk as a diluent (Figure 3.5). This may indicate that milk blocks binding more effectively at lower scFv concentrations until a certain threshold at which high binding signal is seen. Perhaps the reason for this difference in behavior between the two diluents is due to the profile of

proteins present in each. Milk has a heterogeneous distribution of protein sizes whereas BSA is homogeneous in protein size. Thus, milk may block more sites as large proteins binding to sites on the antigen can prevent the binding of scFvs, thus effectively blocking scFv binding. However, use of BSA will likely offer more reproducible results as the molecular weight is consistent and will bind in a more predictable manner.

Ultimately, when isolated scFvs were examined for specificity, binding to both survivin and the nonspecific lysozyme target was still seen, indicating that increased secondary screen stringency does not have a profound effect on the specificity of isolated antibodies (Figure 3.6). This may be a property of this particular library and may not be applicable to other libraries screened using this method.

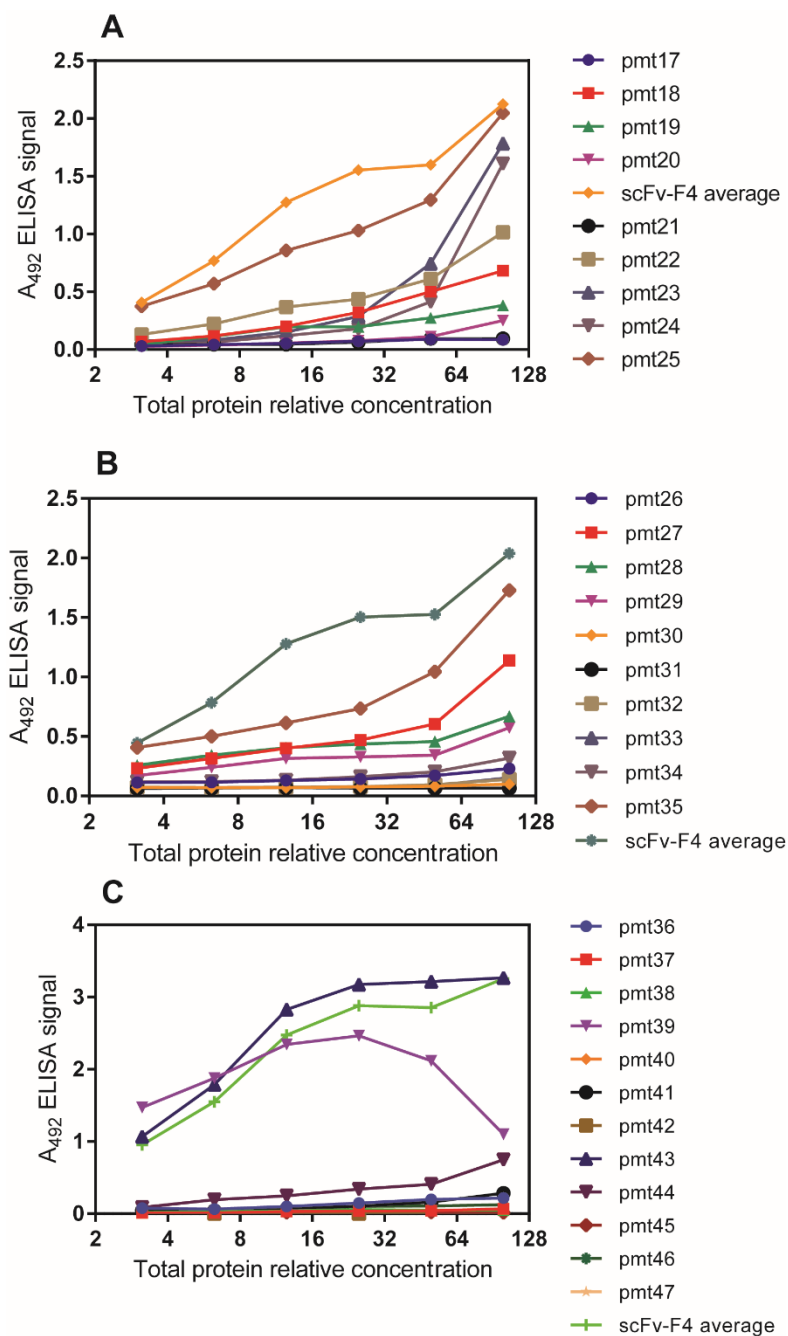


Figure 3.4 Effect of supplementary soluble β -gal on saturable binding. (A), (B) An ELISA to determine binding to survivin was performed on scFv-F4 library variants pmt17 – pmt35 which were isolated from secondary screen in which no soluble β -gal was included. (C) An ELISA to determine binding to survivin was performed on scFv-F4 library variants pmt36 – pmt47 which were isolated from secondary screen in which soluble β -gal was included. scFv-F4 was used as a control for all experiments.

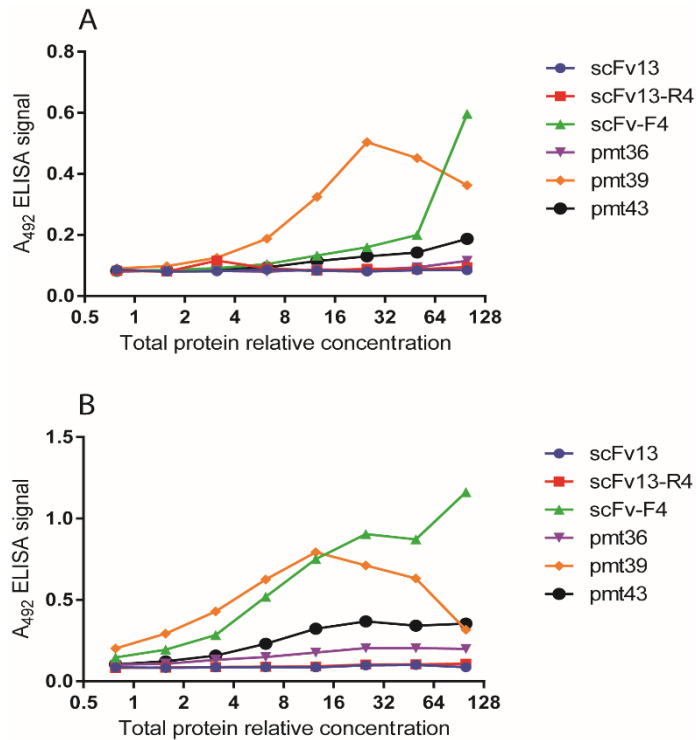


Figure 3.5 Effect of lysate diluent on binding profile. (A) An ELISA for binding survivin was performed using 2 % w/v milk in PBST as a diluent during the lysate incubation step. (B) An ELISA was performed using PBST + 50 µg/mL BSA as a diluent during the lysate incubation step.

Based on these results, we sought to modify the screening protocol to include soluble scFv-F4 as a competitive inhibitor during the panning and secondary screening steps. However, the purification of soluble scFv-F4 was challenging due to aggregation and precipitation. Though purified scFv-F4-6XHis was achieved through IMAC purification, a high level of protein precipitation was observed during buffer exchange procedures and size exclusion chromatography (SEC) revealed a secondary peak indicating presence of aggregates (data not shown.) The optimization of this purification will allow the use of soluble scFv-F4 in future assay modification experiments.

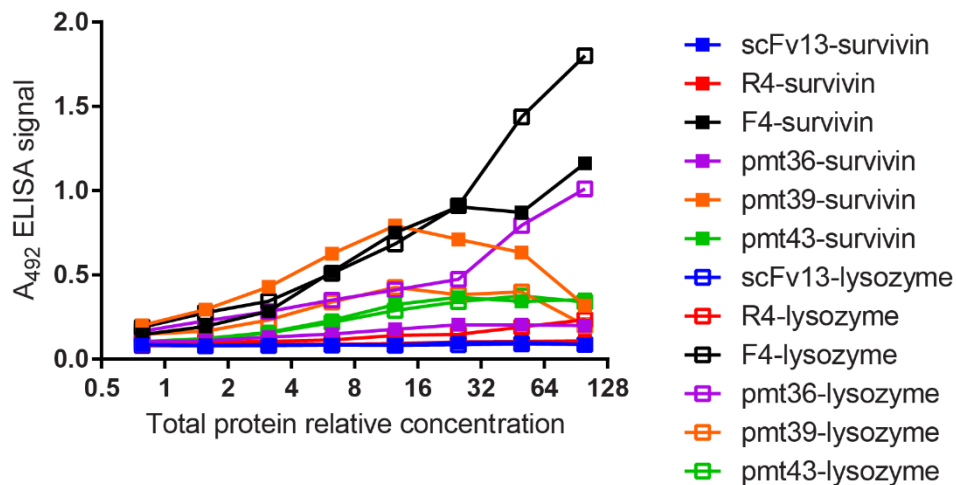


Figure 3.6 Effect of supplementary soluble β -gal on specificity. An ELISA was performed to compare binding of isolated scFvs to survivin to their binding to the nonspecific target lysozyme. BL21-DE3 *E. coli* expressing scFv variants and controls scFv-13, scFv13-R4, and scFv-F4 were lysed and serially diluted in an ELISA plate coated with survivin or lysozyme. scFv binding was detected by incubation with an HRP conjugated anti-FLAG antibody and incubation with HRP substrate and absorbance at 492 nm was measured.

3.3.4 Specificity of screening assay may be dependent on library quality and parent antibody

We speculated that it may not be feasible to achieve high specificity for survivin from a naïve (or β -gal targeted) library using the Tat inner-membrane display method. In previous work done by Karlsson et al. scFv-R4 was found to bind the target antigen β -gal [35]. To check whether or not the isolates from their scFv13-based library were specific, a specificity ELISA was done on isolates 1-4, 2-1, and 2-3, and an scFv13-R4 control to compare their binding to β -gal to their binding to the nonspecific protein target lysozyme. It was found that clones 1-4, 2-1, and 2-3 showed a high level of binding to the target antigen β -gal, and a very low level of binding to lysozyme (Figure 3.7). This indicates that specific antibody fragments can be isolated using Tat inner-membrane display and

screening, but perhaps that it is contingent upon the quality and properties of the initial library. These particular clones were isolated from a library based off of scFv13 which has some low level of binding to β -gal which may contribute to the generation of other library members that have inherent β -gal binding. For our library, we began with an scFv13-R4 based library, which may be the reason behind isolated clones binding β -gal, as scFv13-R4 has inherent binding affinity for β -gal. This does not, however, explain why isolated scFvs also bind other nonspecific targets such as lysozyme. Specific antibodies have been isolated from naïve libraries using other display methods [74–77], so there is a need for further optimization of the Tat inner-membrane display method for the isolation of intrabodies that specifically bind their target antigen.

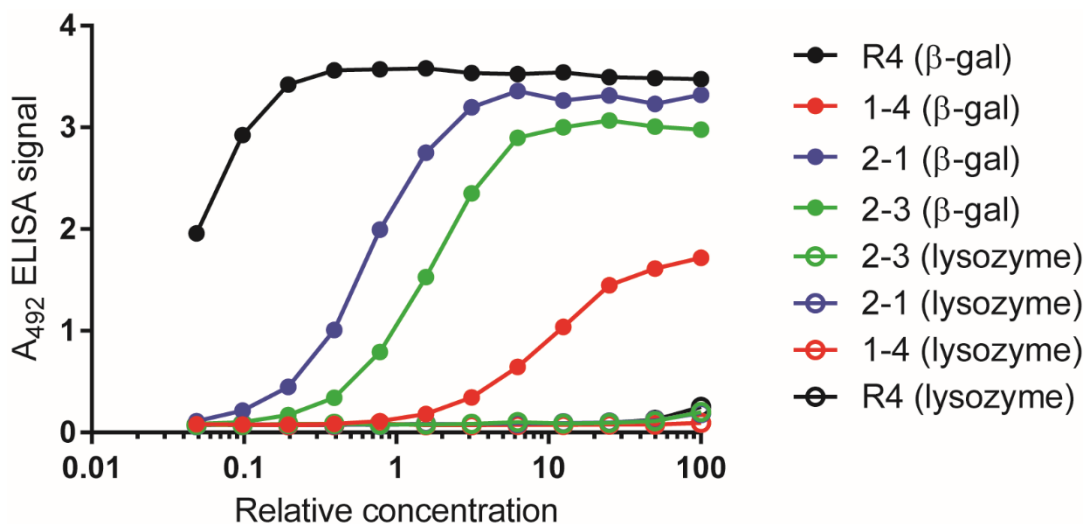


Figure 3.7 Tat inner-membrane display and screening for selection of specific antibodies. scFv clones R4, 1-4, 2-1, and 2-3 isolated by Karlsson et al. [29] were used in a concentration dependent ELISA to compare their binding signals to β -gal and the non-specific target lysozyme.

3.4 Conclusion

Overall, the modifications made will allow for better characterization of isolated clones and save time when performing the screening and library construction protocols. The addition of β -gal to the secondary screen improved the binding profile of isolated clones, which exhibited more saturable binding at higher scFv concentrations. This information will be useful in future experiments to eliminate those clones that would otherwise show a high false positive signal. Since the soluble β -gal behaves as a competitor for antibody binding, it should eliminate those clones that have nonspecific binding properties, particularly those that bind β -gal.

The choice of blocking agent in the lysate incubation step of the tertiary screen ELISA also had an effect on the binding profiles and the use of PBST + BSA allowed for discernable differences in binding amongst isolated scFvs. While this may not aid in improving specificity of clones, once specific clones are isolated, it will assist in discriminating between clones that show very similar levels of binding to the target antigen. This will enable better resolution of antigen binding which will in turn, allow comparison of antibodies with minute differences in binding.

The implementation of whole plasmid PCR and direct transformation of *E. coli* with spheroplast lysate will decrease the overall time it takes to construct a library from a panned sublibrary. With this advancement, libraries can be constructed more quickly which will enable faster and more comprehensive sampling of the library as this allows for more time to be allotted for the screening portion of the procedure.

Despite these improvements, the scFvs isolated from this particular library still displayed nonspecific binding which can be improved upon with additional modifications to increase stringency, choice of library basis, or an alternative display and screening method. In Chapter 4, we discuss an approach to implement changes to the library basis and screening method in order to isolate antibodies specific to survivin.

Chapter 4: Directed evolution of a single domain antibody library for binding survivin

4.1 Introduction

Based on the results in Chapters 2 and 3, in order to proceed with the development of an antibody fragment to target survivin, we developed an alternative engineering approach. We sought to decrease the time spent on the initial library screening process and to improve the likelihood that isolated antibodies are specific to our target. We chose to use yeast surface display and screening using flow cytometry, which is a commonly used antibody engineering method [78–81] and has even been used in the isolation of high-affinity antibodies from naïve libraries [77,82]. Yeast surface display and FACS screening has been used to isolate antibodies that bind a variety of clinically relevant targets [71,74,83,84], which makes it suitable for engineering therapeutic antibodies.

The high-throughput nature of flow cytometry screening and will allow for faster screening of large libraries as compared to the ELISA-based screening method previously described. However, because yeast surface display does not intrinsically screen for intracellular folding, this will serve as an initial screen to isolate antibodies to bind survivin. Isolated antibodies would then be displayed and screened using the Tat inner-membrane display for affinity maturation.

Additionally, we explored a different antibody fragment because of challenges we encountered in the engineering of a naïve scFv library. A library of single domain antibodies derived from camelid species was chosen for screening. The properties of these

antibody fragments that make them ideal candidates for intracellular function are outlined below in Section 4.4.1.

In an interest to improve the antibody engineering and screening method, we decided to also display scFvs using yeast surface display so that results could be compared to those obtained with display of single domain antibodies. The results of this comparison would help to discern which display and screening method yields intrabodies with desired antigen-binding affinity, specificity, and cytoplasmic solubility properties. Insights collected from the results of this comparison could be used to develop a general method of intrabody engineering for applications other than targeting survivin.

4.1.1 Structure and properties of single domain antibodies

Single domain antibodies are small antibodies with a molecular weight of approximately 15 kDa [85], which is significantly smaller than that of scFvs and antigen-binding (Fab) fragments. Single domain antibodies demonstrate high stability and solubility, ease of library cloning and selection, and high expression in yeast [86]. Camelid single domain VHHs are the heavy chain portion of a full length heavy-chain camelid IgG (Figure 4.1) that are derived from camelid species that innately produce functional antibodies lacking light chains. VHHs are highly stable and soluble and possess properties that make them suitable candidates for therapeutic applications [85]. VHH domains are similar to VH domains of scFv fragments in that they comprise four framework regions and three CDRs with high sequence homology between VH and VHH frameworks. One key difference is that four amino acid positions typically conserved in VHs are substituted with more hydrophilic residues in VHHs. At least one of these mutations is important in

stabilizing the single-domain nature of VHs as the hydrophilic nature of these residues, in comparison to hydrophobic residues in these positions in traditional VH domains, contributes to a higher expression level. VHH fragments are easy to produce because they

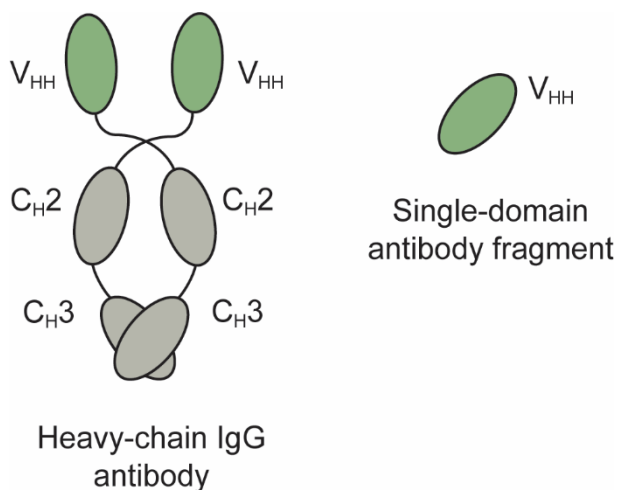


Figure 4.1 Camelid antibody structures. VHs are heavy chain single domain antibody fragments derived from heavy-chain IgG antibodies from camelid species.

are able to fold without a requirement for domain association [85]. VHs have comparable affinity to scFvs, as well as high stability, solubility and expression [21]. Additionally VHs present less intracellular aggregation than other antibody formats [87] and are highly stable [88]. VHs may also be tethered or arranged to give multi-valent effects if necessary [85].

VHs have already been shown to demonstrate therapeutic potential. Gueorguieva *et. al.* have generated camelid VHH intrabodies with specificity to Bax, a proapoptotic protein implicated in oxidative-stress-induced apoptosis extant in several neurodegenerative diseases [21]. The group constructed a naïve llama single domain library from llama blood leukocytes via RNA extraction, polymerase chain reaction (PCR),

and cloning into a phage display vector [89]. This phage library was panned and screened for binding to Bax and six distinct binders were identified and characterized for Bax inhibition in vitro and in vivo in a human neuroblastoma cell line. These anti-Bax VHHs phenotypically transform neuroblastoma cells to become resistant to oxidative-stress-induced apoptosis, thus effectively demonstrating the potential of VHH intrabodies in therapeutic applications [21]. Other previous work has demonstrated the ability to isolate antigen-specific VHHs from immune [90,91], non-immune [71,89,92], and semisynthetic [93] libraries using a variety of display methods [85]. Given their promising characteristics, we chose to engineer VHHs for use as intrabodies.

4.1.2 High-throughput screening

Yeast surface display is a well-developed method in the antibody engineering field [78–81] and has been used in the isolation of high-affinity antibodies from naïve libraries [77,82]. In conjunction with FACS screening, this display method has been used to isolate antibodies that bind the mycotoxin aflatoxin B₁ [74], the toxin ricin [83], haptens [94], and the cancer target chondroitin sulfate proteoglycan 4 [84], among many other targets.

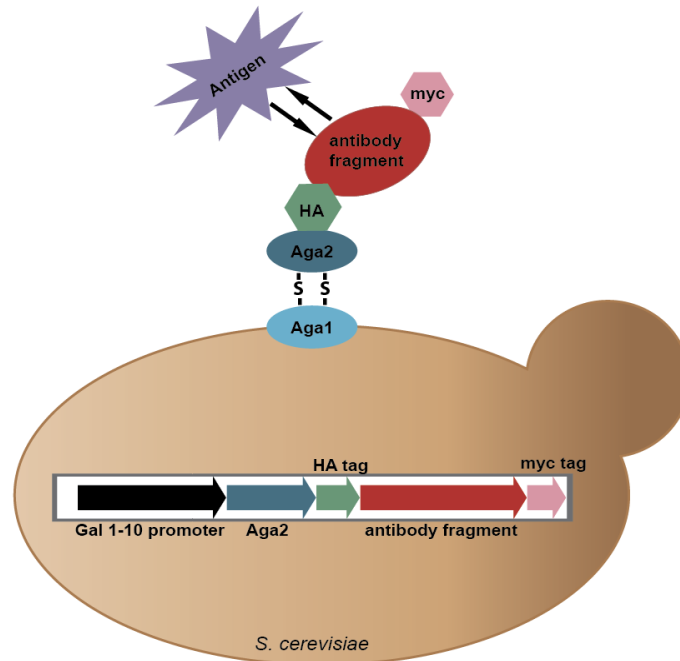


Figure 4.2 Yeast surface display. Antibodies are expressed as fusion scaffold to an N-terminal Aga2 protein and HA tag and C-terminal myc tag. The secreted scaffold binds to cell surface protein Aga1 via disulfide bonding to Aga2. The surface-bound antibody can then be detected in expression and antigen binding assays.

Yeast surface display entails use of a display plasmid that expresses proteins of interest in a fusion scaffold. The fusion scaffold comprises the Aga2 cell wall anchor protein, followed by an HA epitope tag, the protein of interest, and concluded by a C-terminal myc epitope tag [19,80,95] (Figure 4.2). The scaffold is transported out of the cell via a secretory mechanism and the Aga2 protein links to the α -agglutinin Aga1 cell surface protein via two disulfide bridges. Surface display is induced and not constitutive; thus, library bias is eliminated. However, each yeast cell displays approximately 5×10^4 copies of the fusion scaffold, so avidity binding effects must be surveilled [80].

Yeast surface display is advantageous for engineering antibodies for eventual use in human cells as it relies on eukaryotic post translational machinery, which more closely

resembles modifications of mammalian cells than bacterial cells employ [80]. This essentially compensates for the fact that yeast surface display libraries typically have diversity an order of magnitude lower than bacterial or phage display libraries. Additionally, screening of a yeast surface display library using fluorescence-activated cell sorting (FACS) is high throughput, quantitative, and allows for precise discrimination of fluorescence signal allows for screening of a library to two targets simultaneously [20,80].

Yeast surface display has one particular limitation in intrabody engineering applications. Yeast surface display, phage display, and traditional bacterial surface display rely on secretory protein expression pathways [19,27,28]. In the secretory pathway, unfolded proteins are translocated from the cytoplasm to the endoplasmic reticulum in yeast or to the periplasm in bacteria, both of which are oxidizing [96,97]. Folding then ensues in an oxidizing environment such that antibodies are able to form disulfide bonds that would otherwise not form in the cytoplasm [61,98]. Therefore, intrabody libraries screened for antigen binding using these methods would potentially contain many antibodies that do not fold correctly intracellularly as the entire library repertoire, and not just the antibodies that fold correctly intracellularly, is assayed for antigen binding. When using these methods, antigen binding and cytoplasmic solubility must be engineered separately and iteratively. However, this can be mitigated by passing the screened sublibrary through a pathway that does possess a protein folding quality control mechanism, such as the *Escherichia coli* twin-arginine translocation pathway previously described in Chapter 2.

Here we describe the process of preparing VHH and scFv libraries for yeast surface display. While the preparation of these libraries presented some challenges and needs

optimization, the side-by-side comparison of intrabodies isolated from these two methods will allow for improvement of engineering antibodies specifically for intracellular targets.

4.2 Materials and methods

4.2.1 Selection of library basis

The “Nomad #1” semisynthetic hyperdiversified llama VHH library was a gift from the Hayhurst lab at the Texas Biomedical Research institute. It was previously shown by Goldman et al. that high-affinity antibodies can be isolated from this library using phage display techniques [93].

4.2.2 Optimization for library screening

To assess whether or not differences in antibody binding can be determined via flow cytometry techniques, an optimization was performed to compare binding of scFv13 and scFv13-R4 to β -gal.

4.2.2.1 Cloning scFv13 and scFv13-R4 into yeast surface display vector

The genes encoding scFv13 and scFv13-R4 were cloned into the pCTcon2 yeast surface display vector between the *NheI* and *BamHI* restriction enzyme sites using standard molecular cloning techniques. The recombinant ligation products were used to transform DH5 α *E. coli* and a DNA miniprep was used to purify plasmids, which were then sequenced for accuracy.

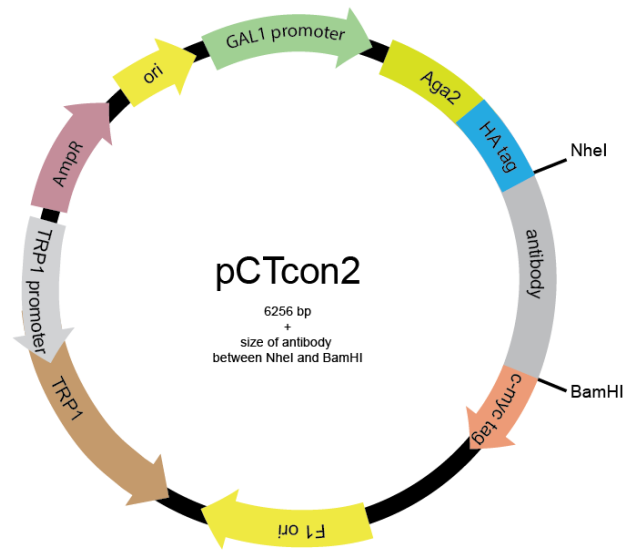


Figure 4.3 pCTcon2 plasmid map. Antibody genes are cloned between *NheI* and *BamHI* restriction enzyme sites such that they are fused to genes encoding the Aga2 protein and HA and c-myc tags. Expression of protein scaffold is mediated by galactose.

4.2.2.2 Transformation of *S. cerevisiae*

The EBY100 strain *Saccharomyces cerevisiae* (ATCC) was transformed with purified pCTcon2-scFv13 and pCTcon2-scFv13-R4 plasmids using the Frozen EZ Yeast Transformation II Kit (Zymo Research). Transformed yeast were grown on SD-CAA minimal media agar plates, to promote selective growth of cells containing the pCTcon2 plasmid, which has a gene to produce tryptophan.

4.2.2.3 Flow cytometry optimization

This optimization was performed to determine quantities of antibodies needed to discern between high-binding and low-binding scFvs via flow cytometry. An individual colony was selected from each plate and used to inoculate SD-CAA media and grown at 30 °C overnight. An EBY100 plasmid –free control was inoculated into YPD media. Subcultures were inoculated at a density of 1×10^7 cells/mL in 15 mL of SD-CAA media and grown for 3.5 hours. Cultures were centrifuged at 4 °C at $3,000 \times g$ for 5 minutes to remove media. Protein expression was induced by resuspending each culture in 15 mL SG-CAA media and growing at 20 °C overnight. The following day, 1×10^7 cells per sample were placed into microcentrifuge tubes and centrifuged at 4 °C at $14,000 \times g$ for 1 minute, then resuspended in 100 μ L of PBS + 0.1% BSA. Cells were prepared for flow cytometry as follows.

To confirm expression of full-length Aga2-HA-scFv-c-myc, 1 μ L of Anti-HA tag [16B12] (mouse) (Abcam) and 1 μ L of Chicken Anti-c-MYC (Gallus Immunotech Inc.) primary antibodies were added to each sample and gently rotated at room temperature for 1 hour. Cells were centrifuged and resuspended as before in PBS + 0.1% BSA, then 1 μ L of Alexa Fluor 488 goat anti-mouse IgG (H+L) and 1 μ L of Alexa Fluor 647 goat anti-chicken IgG (H+L) (Life Technologies) secondary antibodies were added and samples were gently rotated at 4 °C for 30 minutes while protected from light.

To assess binding to β -gal, 5 μ g of biotinylated β -gal was added to a new set of samples in addition 1 μ L Chicken Anti-c-MYC antibody and gently rotated at room temperature for 1 hour. Following centrifugation and resuspension in fresh PBS + 0.1% BSA, 1 μ L of Neutravidin Dylight 488 (Thermo Fisher) and 1 μ L of Alexa Fluor 647 goat

anti-chicken IgG (H+L) were added and samples were gently rotated at 4 °C for 30 minutes while protected from light.

All samples were centrifuged and rinsed once with 1 mL of PBS + 0.1% BSA before being resuspended in 500 µL of PBS + 0.1% BSA and transferred to 5 mL round-bottom tubes. Flow cytometry was performed (BD FACS Canto II) using FITC and APC channels to detect Alexa Fluor 488 and Alexa Fluor 647 fluorescence, respectively, and data was analyzed using FlowJo software.

4.2.3 Library construction

4.2.3.1 VHH library construction for yeast surface display

To transfer the Nomad library, which will hereafter be referred to as the “VHH library,” to an appropriate platform for yeast surface display, the following was performed. The Nomad library format received had the VHH genes situated between 2 discontinuous, non-identical SfiI sites in the pECAN21 plasmid vector. PCR was performed to amplify the VHH genes including the SfiI sites, cleaned, and digested with SfiI. Digested product was then ligated into pCTcon2 and pIMD plasmids which were previously modified to contain SfiI sites. It is important to note that vector plasmids were propagated in the non-methylating INV110 strain of *E. coli* (Thermo Fisher) prior to digestion, as the SfiI enzyme can only digest non-methylated DNA. Ligation product was used to transform DH5α *E. coli* using the previously-described electroporation protocol in 2.2.2.3 and a representative sample of the library was plated on LB agar plates supplemented with ampicillin. Colonies were selected, grown, and midprepped and purified plasmid for each was sent for sequencing to confirm insert sizes and sequence uniqueness.

4.2.3.2 scFv library construction for yeast surface display

The original scFv13-R4 library was also cloned into the pCTcon2 vector. The scFv genes were amplified via PCR with the addition of a 5' NheI and 3' BamHI site, and the PCR product was cleaned and digested with NheI and BamHI restriction enzymes. The digested product was ligated into pCTcon2 vector that had been previously digested with the same two enzymes. Ligation product was used to transform DH5 α *E. coli* using the previously-described electroporation protocol in 2.2.2.3 and a representative sample of the library was plated on LB agar plates supplemented with ampicillin. Colonies were selected, grown, and midprepped and purified plasmid for each was sent for sequencing to confirm insert sizes and sequence uniqueness.

4.3 Results and discussion

4.3.1 Flow cytometry needs further optimization

In order to determine if differences in antigen binding can be observed through flow cytometry screening, scFv13 and scFv13-R4 were expressed using yeast surface display and expression and β -gal binding was analyzed. *S. cerevisiae* expressing scFv13 and those expressing scFv13-R4 showed high fluorescent signal for antibodies binding the HA and c-myc tags, indicating full length expression of the Aga2-HA-scFv-c-myc fusion. When comparing fluorescent signal due to binding of β -gal, slight differences between scFv13 and scFv13-R4 were seen. A larger difference was expected to be seen, indicating the need for optimization of antibody concentrations, washing steps, or cell density.

4.3.2 Generation and cloning of VHH library into yeast surface display vector requires optimization

The cloning of the VHH library into the pCTcon2 yeast surface display vector presented complications. Over 10 sets of primers were designed, including degenerate primers previously used to amplify the library [93]. For primers that only presented one binding site throughout the entire plasmid template sequence, PCR products contained additional bands, indicating non-specific binding of primers. Two sets of adequately specific product were generated, although these results could not be replicated, despite using the exact same conditions, reagents, and thermal cycler protocol. Additionally, when the pCTcon2 vector with added SfiI sites was propagated in non-methylating *E. coli*, SfiI digestion was successful initially, but later attempts to digest the same aliquot of DNA with the same aliquot of SfiI restriction enzyme resulted in a very low level of digestion, even when digested overnight. The minimal amount of PCR product and vector that were used in cloning led to the generation of a library with approximately 10^5 members, which is not an adequately large library size for screening. However, sequencing revealed that VHH inserts are full length (~ 420bp) and have unique sequences. Based on the challenges encountered in amplification and cloning of the VHH library, this needs to be optimized.

4.3.3 Generation and cloning of VHH library into yeast surface display vector requires optimization

The scFv library inserted into the yeast surface display vector was of a more appropriate size of approximately 10^8 variants, as compared to the VHH library. Upon examination of sequencing results, it was observed that truncated scFv genes of varying sizes were being inserted between the NheI and BamHI sites. The PCR amplified scFv

genes were checked for size by gel electrophoresis and were found to be approximately 750 base pairs, which is the correct, full-length size. There are no additional NheI or BamHI restriction enzyme sites within the pCTcon2 vector and it is improbable that every clone that was assessed had an additional BamHI site that could explain the truncated insertion. We hypothesized that the error may lie in some ligation or cellular process that is causing incomplete insertion of full-length scFv genes. Due to the challenges of cloning the scFv13-R4 library into the yeast surface display vector, this needs to be optimized.

4.4 Conclusion

Comparison of different modalities of screening and display of an antibody library can elucidate factors that are important when designing an intrabody engineering strategy. Differences in solubility, stability, specificity, and binding behavior of isolated antibodies are important factors to consider when selecting a display and screening method. Though the preparation of the VHH and scFv libraries presented challenges, we created the plasmid frameworks to prepare these libraries in the future, perhaps with some modifications to ensure proper library amplification and adequate library size for screening purposes.

With an appropriate choice of library format and by utilizing different methods of display and screening, it will be possible to isolate intrabodies with high affinity and specificity for their target antigen. An important factor in managing the feasibility of such a project is ensuring that the transfer of a library from one display plasmid to another is seamless. Some suggestions for improving this method are to introduce the same restriction enzyme sites to flank the intrabody gene in any display plasmids, use enzymes that are active at the same temperature such that double digests can be performed. The use of a tool

such as Primer-BLAST could also be beneficial to prevent any mispriming and nonspecific amplification during PCR. Keeping these modifications in mind will serve to improve the outcomes of library construction moving forward.

**PART II: RATIONAL DESIGN OF
ANTIMICROBIAL PEPTIDES**

Chapter 5: Antifungal peptides for treatment of *C. albicans*

5.1 Introduction

5.1.1 Selection of *C. albicans* as a therapeutic target

The normal human flora comprises a variety of bacterial and fungal organisms [99]. *Candida* species are fungal organisms present on skin and mucosal surfaces in healthy people. However, *Candida* species are commensal organisms and opportunistic pathogens as they can cause infections such as mild rashes, oral thrush, genital yeast infections, and potentially life-threatening systemic infections. Susceptibility to infection is of greater concern in immunocompromised patients, such as those with human immunodeficiency virus (HIV), diabetes, or those undergoing chemotherapy [100]. Given growing concerns over hospital acquired infections amidst increasing numbers of drug-resistant strains, it is imperative to develop novel therapeutics to treat *Candida* infections.

The most common species of *Candida* present in clinical isolates is *C. albicans* [101]. *C. albicans* is a diploid organism and is capable of taking on different forms. It can exist as oval-shaped yeast, budding yeast, pseudo-hyphae, and hyphal forms. *C. albicans* can also form biofilms under certain physiological conditions which can colonize surfaces such as implants, catheters, and dentures [102]. *C. albicans* biofilms comprise yeast, pseudohyphal, and hyphal forms of *C. albicans* embedded in extracellular matrix. Additionally, cells in biofilms have been found to have increased resistance to treatment due to increased virulence and changes in expression of cell membrane components, which are described in more detail below [103–105].

Current treatments for *C. albicans* infections include azoles, amphotericin B, and capsofungin, and while effective, they pose some limitations. Amphotericin B, while robust in its treatment of *C. albicans*, causes kidney toxicity [101,106], which makes it a poor choice for repeated candidiasis. Amphotericin B functions by binding ergosterol [107] and azoles function by preventing the formation of ergosterol, which is an important component of the fungal cell membrane [108]. Topical azole antifungal agents have been paramount in the treatment of mucosal candidiasis in immunocompromised patients [106]. However, increasing usage of antifungal agents has given rise to antifungal-resistant *C. albicans*. In a 2013 report published by the Centers for Disease Control and Prevention, it was noted that fluconazole-resistant *Candida* infections posed a serious threat to human health, with nearly 7% of bloodstream *Candida* isolates exhibiting resistance [14]. Thus, there is a clear need for alternative methods of candidiasis treatment that are both safe and effective.

5.1.2 Histatin-5 as an antifungal agent

C. albicans has a tendency to colonize the oral cavity and infection of the oral cavity is commonly seen in those with compromised immune systems [100]. The human body has defense mechanisms in the form of antifungal salivary peptides and proteins that can prevent overgrowth of *C. albicans*.

Histatins are a family of histidine-rich peptides that are secreted from human salivary glands [109] that possess a variety of functions within the human oral cavity. They play a role in formation of acquired enamel pellicle on teeth, maintenance of mineral-solution dynamics in saliva, and antimicrobial activity against strains of *Streptococcus mutans* among other functions [110].

One of the most interesting properties of histatins is their potency against *C. albicans*. Histatins inhibit *C. albicans* germination and cause *C. albicans* cell death at physiological concentrations [111–113]. Of these, histatin-5 (Hst-5) is of particular interest as it has the strongest antifungal activity against *C. albicans* [109,113]. Hst-5 has been indicated in the maintenance of *C. albicans* at non-virulent levels [114] and kills *C. albicans* in vitro at physiological concentrations of 15 to 30 μM [115]. Hst-5 has an identical sequence to the N-terminal proteolytic fragment of histatin 3 [116,117]. Hst-5 is present at reduced levels in HIV-positive patients [118,119] indicating a connection between reduced Hst-5 and lack of maintenance of *C. albicans* at commensal levels in immunocompromised patients.



Figure 5.1 Histatin-5 sequence and antimicrobial fragment. The minimal antimicrobial fragment comprises residues 4 – 15 as determined by Rothstein et al. [120].

Hst-5 is a 24-amino acid, cationic peptide that has the propensity to form an α -helical structure in non-aqueous solutions and maintains an unstructured form in aqueous solutions [110]. Hst-5 is weakly amphipathic, and this lack of strong amphipathicity prevents spontaneous insertion into microbial membranes. This is consistent with findings that indicate lack of pore formation in the Hst-5 antifungal mechanism [120]. Previous research has focused on making modifications to full-length and truncated versions of Hst-5 in order to determine the effects that charge, hydrophobicity, and amino acid side chain

properties have on the propensity of α -helical structure formation. Substitution of the four charged amino acid types (lysine, arginine, histidine, glutamic acid) with glycine residues resulted in significantly decreased antifungal activity [121–123], suggesting that side chain charge is an important factor in antifungal activity of Hst-5.

Other studies were conducted in which Hst-5 peptides were synthesized and assessed for antifungal activity in order to determine the minimal sequence required for antifungal activity comparable to full-length Hst-5 [121,124,125]. It was determined that the P-113 fragment consisting of residues 4-15 is the minimal sequence required and in fact, has higher antifungal activity than non-truncated Hst-5 [121].

The proposed antifungal mechanism of Hst-5 differs from that of other antimicrobial peptides, which tend to form pores in the cell membrane [118,126,127]. In fact, the α -helical structure important for spontaneous insertion into microbial membranes does not appear to be of importance in Hst-5 antifungal activity, as disruption of helical formation did not result in a loss of activity [122]. Instead, Hst-5 enters the cell and causes an imbalance of ATP, potassium, and magnesium that causes cell volume loss and thus, cell death [115,117,120]. More specifically, Hst-5 binds to *C. albicans* cell wall β -glucans and fungal heat shock proteins Ssa2 and Ssa1 in an energy-independent manner to promote its localization with a transport complex [115,128]. Hst-5 is translocated into the cell via fungal polyamine transporters Dur3 and Dur31 in a nonlytic, energy-dependent manner [115,120]. It is also indicated that Hst-5 uptake can be endocytic in nature as Hst-5 localizes inside vacuoles at low physiological Hst-5 concentrations but is found in the cytoplasm at high concentrations, which requires a high cationic charge on Hst-5. *C. albicans* in which Hst-5 showed vacuolar localization remained viable, while those with cytoplasmic

localization were non-viable [120]. The presence of Hst-5 intracellularly causes depolarization of the cytoplasmic and/or mitochondrial membranes [127,129], that can allow direct transfer of Hst-5 into the cytosol [127]. Thus, Hst-5 uptake in *C. albicans* may be a combination of transporter-mediated uptake, receptor-mediated endocytosis, and direct transfer across the membrane [115].

5.1.3 Secreted aspartic proteases

Secreted aspartic proteases (Saps) are a family of enzymes that are part of the repertoire of hydrolytic enzymes secreted by *C. albicans*. Saps serve to protect *C. albicans* from death and to evade immune response through various protective mechanisms such as inactivation of complement receptors on macrophages, lysosomal permeabilization, and degradation of protective proteins and peptides [130,131]. Of the ten Saps, Sap1 through Sap8 are secreted to the extracellular environment and Sap9 and Sap10 are attached to the cell wall by a glycosylphosphatidylinositol anchor [132,133]. Distribution of Sap expression and function in *C. albicans* is dependent on factors such as pH and morphology of cells [133–136]. Sap7, Sap9, and Sap10 have higher activity in physiologically relevant pH ranges, and of these, Sap9 has been found to be highly expressed in *C. albicans* strains present in patients with vaginal and oral candidiasis [137]. Sap2 is highly expressed by *C. albicans* and its interactions with Hst-5 have been recently studied [114,138].

5.1.4 Proteolytic susceptibility of Hst-5 to Saps

Studies directed at analyzing cleavage site amino acid preferences of Saps reveal that Saps prefer basic or large, hydrophobic residues [134,135,139]. While these studies elucidate some information, they do not take into account the effect that modifications

further from the cut site, that may affect cleavage site accessibility, may have on proteolytic cleavage by Saps. It has been shown that Hst-5 can undergo proteolytic cleavage by Sap2, Sap9, and Sap10 at physiological pH conditions [114] and by the other seven Saps at pH conditions at which each Sap has optimal activity [130]. Degradation of Hst-5 by Saps leads to reduced antifungal activity[114], and thus, improving the proteolytic stability of Hst-5 could improve its half-life and antimicrobial function. Prevalence of Saps and their cleavage site preferences are important factors to consider in the rational design of Hst-5 mutants that can resist proteolytic cleavage by Saps, while maintaining their antifungal properties.

5.2 Previous experiments

The experiments and results discussed in Section 5.2 were performed by Dr. Svetlana Ikonomova and are provided as background and motivation for experiments in Chapters 5 and 6.

5.2.1 Rational design of Hst-5 peptides

In studies conducted by Meiller et. al. and Bochenska et. al. a lysine residue was observed on either side of the Sap cleavage site [114,130], indicating the potential importance of lysine as a recognition or target residue for Saps. This is corroborated by findings that Saps may prefer hydrophobic or basic residues, as lysine is basic [134,135,139]. Due to this apparent importance of the presence of lysine at Sap cleavage sites, modifications were made to substitute lysines at four different locations (K5, K11, K13, and K17) with either an arginine or a leucine. Since charge plays an important role in Hst-5 function, arginine was chosen in order to preserve the positive charge at the modified

residue positions. Leucine was selected as a substitute in order to remove the positive charge incurred by lysine, as this could affect how the modified Hst-5 peptides interact with the aspartic acid residues present in the Sap active sites. Modified peptides are shown in Table 5.1.

5.2.2 Peptides and enzymes

Unmodified and modified Hst-5 peptides were commercially synthesized (GenScript) with purity $\geq 95\%$ and trifluoroacetic acid salt removal by exchange with hydrochloride. Purified recombinant Sap2 and Sap9 (produced with GPI anchor) were produced in *Pichia pastoris* and were a gift from Dr. Bernard Hube at Friedrich Schiller University in Germany.

Table 5.1 Hst-5 and variants with single leucine or arginine substitutions

Peptide	Sequence																							
	1	2	3	4	5	6	7	8	9	10	11	12	13	14	15	16	17	18	19	20	21	22	23	24
Hst-5	D	S	H	A	K	R	H	H	G	Y	K	R	K	F	H	E	K	H	H	S	H	R	G	Y
K5R	-	-	-	-	R	-	-	-	-	-	-	-	-	-	-	-	-	-	-	-	-	-	-	-
K5L	-	-	-	-	L	-	-	-	-	-	-	-	-	-	-	-	-	-	-	-	-	-	-	-
K11R	-	-	-	-	-	-	-	-	-	-	R	-	-	-	-	-	-	-	-	-	-	-	-	-
K11L	-	-	-	-	-	-	-	-	-	-	L	-	-	-	-	-	-	-	-	-	-	-	-	-
K13R	-	-	-	-	-	-	-	-	-	-	-	-	R	-	-	-	-	-	-	-	-	-	-	-
K13L	-	-	-	-	-	-	-	-	-	-	-	-	L	-	-	-	-	-	-	-	-	-	-	-
K17R	-	-	-	-	-	-	-	-	-	-	-	-	-	-	-	-	R	-	-	-	-	-	-	-
K17L	-	-	-	-	-	-	-	-	-	-	-	-	-	-	-	-	L	-	-	-	-	-	-	-

*Dash indicates residue unchanged from parent Hst-5. Letter R or L indicates that parent residue at that position was modified to either arginine or leucine, respectively.

5.2.3 Proteolytic degradation of Hst-5 and variants by Saps

The degradation of Hst-5 and modified peptides by incubation with purified recombinant Sap2 or Sap9 was examined. Briefly, Hst-5 or variants (final concentration of 150 $\mu\text{g/mL}$) were each mixed with Sap2 or Sap9 (3.13 $\mu\text{g/mL}$ or 6.25 $\mu\text{g/mL}$) in 1 mM NaPB and incubated at 37 $^{\circ}\text{C}$ for 2 hours. A Hst-5 control was prepared with NaPB with no Saps. Tricine sample buffer containing 2% β -mercaptoethanol was added to each and samples were boiled at 100 $^{\circ}\text{C}$ for 10 minutes. The sample buffer added to the control Hst-5 contained Coomassie Blue G-250 in order to visualize the location of the peptides during the electrophoresis process. Degraded and non-degraded peptides were separated by gel

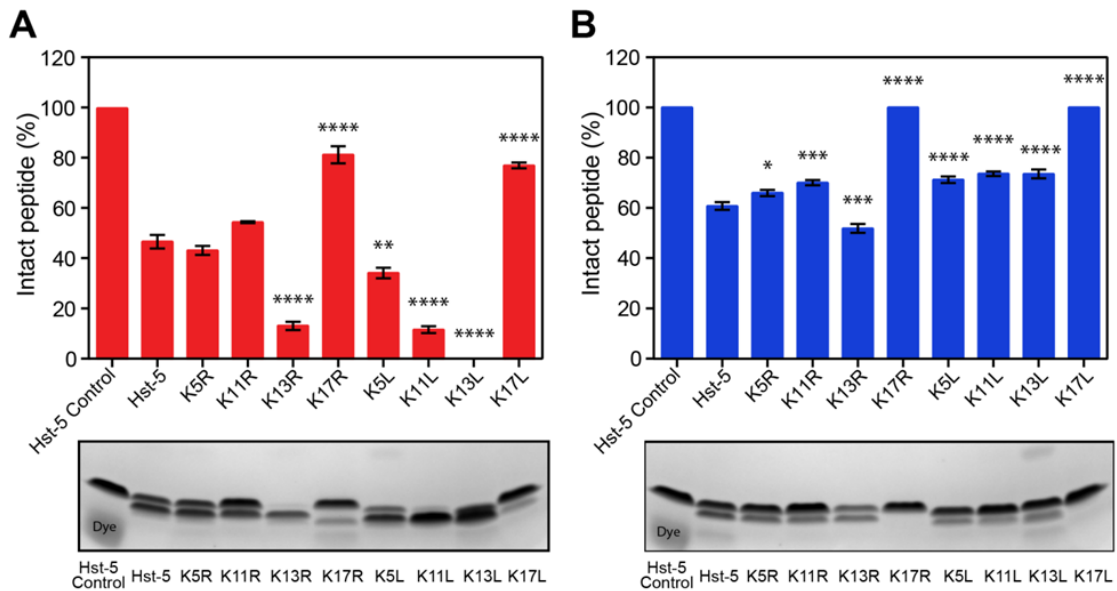


Figure 5.2[†] Degradation of Hst-5 and modified peptides by purified (A) Sap9 and (B) Sap2. Peptides (150 $\mu\text{g/mL}$) were incubated with Sap9 (3.13 $\mu\text{g/mL}$) or Sap2 (6.25 $\mu\text{g/mL}$) for 2 h at 37 $^{\circ}\text{C}$. Following gel electrophoresis, the relative amounts of intact peptide (upper band) and degraded peptide (lower bands) were quantified by densitometry and compared. Error bars represent standard error of the mean ($n = 3$). A one-way ANOVA test and Dunnett's multiple comparison test was performed. Asterisks indicate the level of statistical significance against parent Hst-5 incubated with Sap: * for $p < 0.05$, ** for $p < 0.01$, *** for $p < 0.001$, and **** for $p < 0.0001$. The lower band in the Hst-5 control lanes is due to Coomassie dye.

[†]Figure originally published in *FEBS J.* (2018)

electrophoresis in 10 – 20% Tris-tricine gels (Bio-Rad). Gels were then fixed in a 10% acetic acid/40% methanol/50% water mixture for 30 minutes followed by staining with Bio-Safe Coomassie stain (Bio-Rad) for 1 hour. Gels were washed with water three times and imaged on a ChemiDoc imager (Bio-Rad). Three replicates of the assay were performed. Densitometric analysis was done with Image Lab software (Bio-Rad) to determine the percent intact peptide, where the upper band was considered intact and lower bands considered degraded peptide. A one-way ANOVA tests with $p < 0.05$ and Dunnett's multiple comparison tests with the Hst-5 sample as the control were performed to assess statistical significance.

Densitometric analysis revealed that arginine and leucine substitutions at the K17 site led to an increased resistance to degradation by Sap9 and Sap2, as compared to Hst-5 (Figure 5.2). In fact, no degraded peptide was seen for K17L and K17R Hst-5 variants when incubated with Sap2. Modifications of lysine residues to leucine residues at positions other than K17L (i.e. K5L, K11L, and K13L) led to an increase in degradation by Sap9 as compared to Hst-5 and no intact peptide could be seen for the K13L samples. However, when treated with Sap2, substitution of lysine with leucine residues improved resistance to degradation when compared to Hst-5 for K5R, K11R, and K17R modifications but this effect was not seen for the K13R peptide. The results demonstrate the ability to visualize and quantify peptide degradation by Saps via gel electrophoresis and densitometric analysis as well as the effect that modification of lysine residues has on the resistance to degradation by Sap2 and Sap9. These results establish that single amino acid changes can impart large impacts on the structure and behavior of peptides.

5.2.4 Antifungal activity assay

5.2.4.1 Antifungal activity assay performed with intact peptides

In making modifications to improve resistance to proteolytic degradation, it was of importance to consider the maintenance or improvement of antifungal activity for Hst-5 variants. Thus a antifungal activity assay was performed to determine the antifungal properties of the modified peptides on planktonic *C albicans*.

Briefly, *C. albicans* was inoculated into YPD and grown at 30 °C overnight. The following day it was subcultured and grown until $OD_{600} = 1 - 1.2$. Cells were washed three times with 2 mM NaPB and diluted to either 5×10^5 cells/mL or 5×10^7 cells/mL. Three biological replicated with two technical replicates were performed for each cell density condition. Serial dilutions of Hst-5 and modified peptides were prepared in water, and 20 μ L of each peptide was mixed with 20 μ L of diluted cells and incubated in round-bottom 96-well culture plate at 30 °C for 30 minutes. Final peptide concentrations ranged from 0-50 μ M for experiments using the lower cell density and 0-200 μ M for those using the higher cell density.

Following incubation, 320 μ L of 1 mM NaPB was added to each well and another dilution was performed to dilute the peptide concentration and cell density. A calculation-based estimate of 250 cells were inoculated into respective wells of round-bottom culture plates containing a 1:1 ratio of YPD media and 1 mM NaPB, amounting to a total volume of 200 μ L once diluted cells were added. Sterility and background control wells were included that contained only YPD and NaPB that would assist in determining percent reduction in viability. Plates were incubated at 30 °C overnight while shaking. The

following day the OD₆₀₀ was measured and percent reduction in viability was calculated as follows:

$$\% \text{ reduction in viability} = \left[1 - \frac{(\text{OD}_{\text{with peptide}} - \text{OD}_{\text{background}})}{(\text{OD}_{\text{no peptide}} - \text{OD}_{\text{background}})} \right] \times 100$$

A one-way ANOVA test with $p < 0.05$ and Dunnett's multiple comparison tests with the Hst-5 sample as the control were performed to assess statistical significance.

At the lower *C. albicans* concentration of 2.5×10^5 cells/mL, the modified Hst-5 variants showed only slight observable differences in antifungal activity and all exhibited an increased percent reduction in viability with increasing peptide concentration (Figure 5.3A). The minimum inhibitory concentration for 50% growth (MIC₅₀) value was calculated for all peptides and it can be seen that MIC₅₀ values for variants differ from that of Hst-5 by a maximum of one dilution factor.

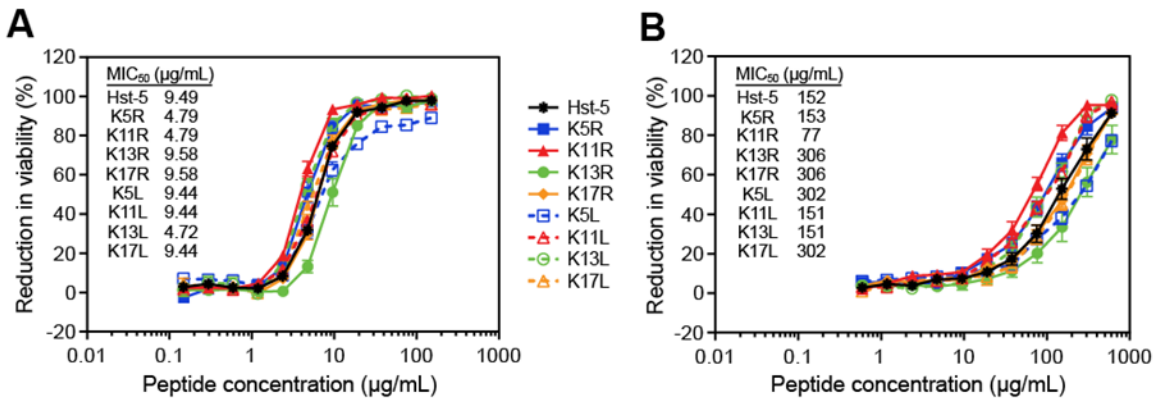


Figure 5.3[†] Antifungal activity of Hst-5 and modified peptides. Peptides were serially diluted and incubated with either (A) 2.5×10^5 cells/mL or (B) 2.5×10^7 cells/mL of *C. albicans* for 30 minutes at 30 °C. Error bars represent standard error of the mean ($n = 6$). MIC₅₀ values for the peptides are shown.

[†]Figure originally published in *FEBS J.* (2018)

At the higher *C. albicans* cell concentration of 2.5×10^7 cells/mL, the Hst-5 variants again follow a trend similar to parent Hst-5 with increasing percent reduction in viability with increasing peptide concentration (Figure 5.3B). The MIC₅₀ values for all peptides increased for this higher cell concentration, which is expected as the peptide concentration was not increased as well. At the lower cell concentration, all growth inhibition curves are fairly similar, however, at the higher cell concentration, the differences in percent reduction in viability between cells treated with the different peptides are increased. From these curves and from the MIC₅₀ values, it is seen that K11R shows enhanced antifungal activity over that of Hst-5, however, it should be noted that MIC₅₀ values for all modified peptides are still within one dilution factor from that of Hst-5. Since the K11 residue resides within the previously-identified active fragment of Hst-5 [121], modifications to this residue will likely modulate antifungal properties of the peptide. It is of interest to note that despite the large enhancement in proteolysis resistance the K17L and K17R modifications imparted on the peptide, neither of these modifications resulted in improved antifungal activity. This may be the result of the short incubation time in the antifungal activity assay which is not yet optimized with Sap proteolysis kinetic properties. Substitution of lysine residues within Hst-5 with leucine or arginine maintains or improves antifungal activity as previously reported [125]. Additionally, in some cases, these modifications improve resistance to proteolytic degradation by Saps.

5.2.4.2 Antifungal activity assay performed with degraded peptides

It was also of importance to look at the antifungal activity of degraded peptide fragments as it is possible to have antifungal activity retained via a smaller active fragment, or that resistance to degradation prolongs the antimicrobial lifetime of an active peptide. In

this experiment, Hst-5 and Hst-5 variants, at a concentration of 150 $\mu\text{g}/\text{mL}$, were first degraded by incubation at 37 °C for 2 hours with purified Sap9 or Sap2, at 6.25 $\mu\text{g}/\text{mL}$ or 18 $\mu\text{g}/\text{mL}$ respectively. This increase in Sap concentration was done in order to amplify differences in antifungal activity caused by degradation, which may otherwise not be seen with low Sap concentrations and only partial degradation. This was followed by heat-inactivation of the Saps at 100 °C for 5 minutes and then using the degraded peptides in the antifungal activity assay as described in 5.2.4.1. A one-way ANOVA tests with $p < 0.05$ and Dunnett's multiple comparison tests with the Hst-5 sample as the control were performed to assess statistical significance.

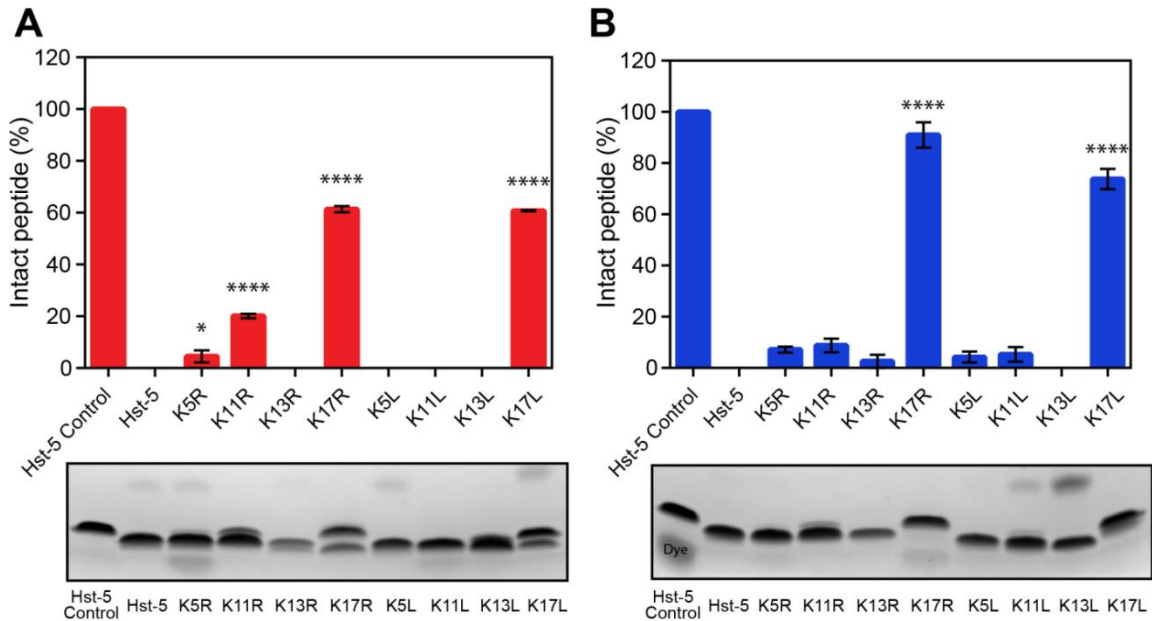


Figure 5.4[†] Degradation of Hst-5 and modified peptides by high concentrations of purified (A) Sap9 and (B) Sap2. Peptides (150 $\mu\text{g}/\text{mL}$) were incubated with Sap9 (6.25 $\mu\text{g}/\text{mL}$) or Sap2 (18 $\mu\text{g}/\text{mL}$) for 2 h at 37 $^{\circ}\text{C}$. Following gel electrophoresis, and the relative amounts of intact peptide (upper band) and degraded peptide (lower bands) were quantified by densitometry and compared. Error bars represent standard error of the mean ($n = 3$). A one-way ANOVA test and Dunnett's multiple comparison test was performed. Asterisks indicate the level of statistical significance against parent Hst-5 incubated with Sap: * for $p < 0.05$ and **** for $p < 0.0001$. The lower band in the Hst-5 control lane in (B) is due to Coomassie dye.

[†] Figure originally published in *FEBS J.* (2018)

It was observed that while incubation with Sap2 cause Hst-5 to lose nearly all of its antifungal activity, incubation with Sap9 only resulted in a loss of approximately 60% when compared to non-degraded Hst-5 (Figure 5.5). The K17R and K17L peptides showed a very minimal loss in antifungal activity, despite being exposed to Saps which is consistent with their apparent high resistance to proteolytic degradation as observed even at these high Sap concentrations (Figure 5.4). Interestingly, the K11R peptide showed some retention of antifungal activity after incubation with Saps and showed significantly higher

resistance to degradation than Hst-5. These results indicate that there are several factors that play a role in determining the antifungal potency of peptides.

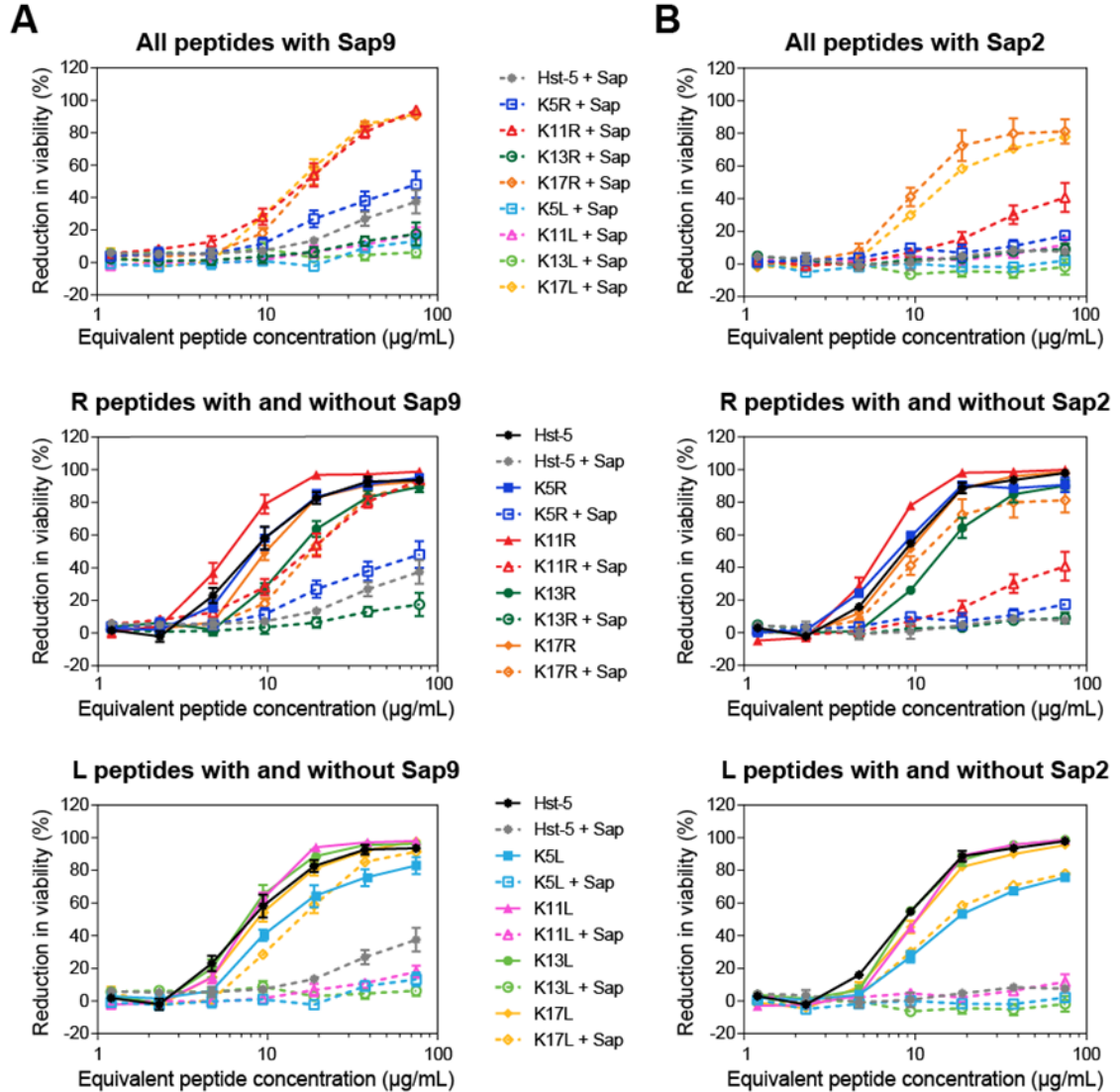


Figure 5.5[†] Antifungal activity of Hst-5 and modified peptides following incubation with Sap9 and Sap2. The peptides (150 µg/mL) were incubated with either (A) Sap9 (6.25 µg/mL) and (B) Sap2 (18 µg/mL) for 2 h at 37 °C. Samples were serially diluted and incubated with 2.5×10^5 cells/mL *C. albicans* for 30 minutes at 30 °C. Error bars represent standard error of the mean ($n = 6$).

[†] Figure originally published in *FEBS J.* (2018)

5.2.6 Peptide degradation by *C. albicans*

The extent to which peptides were degraded by whole *C. albicans* cells was also examined in order to determine whether or not it is accurate and representative to use purified Saps in degradation experiments. *C. albicans* was inoculated overnight and subcultured as previously described in Section 5.2.4.1. Cells were washed three times with 100 mM NaPB and diluted to a concentration of 2×10^9 cells/mL in 100 mM NaPB. The cells were prepared in this high ionic strength solution to prevent internalization of peptides such that the peptides would be available extracellularly to be susceptible to degradation by Saps. Peptides were prepared at a concentration of 300 $\mu\text{g/mL}$ in sterile water. For each peptide, an equal volume of cells and peptides were mixed and the solution was incubated at 37 °C for 2 hours. Three biological replicates were performed for each peptide. Cells were removed by centrifugation and tricine sample buffer was added to the supernatant. Samples were boiled at 100 °C for 10 minutes. Gel electrophoresis, Coomassie staining, and densitometric analysis was performed as described in 5.2.3. A one-way ANOVA tests with $p < 0.05$ and Dunnett's multiple comparison tests with the Hst-5 sample as the control were performed to assess statistical significance.

Consistent with findings from degradation experiments with purified Sap2 and Sap9, the K17L and K17R peptides showed improved resistance to degradation by *C. albicans* cells as compared to Hst-5 (Figure 5.6). Interestingly, the results for K5R and K5L suggest that both Sap2 and Sap9 influence degradation as K5L shows improved resistance and K5R shows no change as compared to Hst-5. These are consistent with the degradation pattern seen for these K5 peptides with Sap2 and Sap9, respectively. While the patterns of peptide degradation following incubation with *C. albicans* reflect results seen

with Sap2 and Sap9 incubation, there may be other Saps contributing to peptide degradation. However, since the degradation patterns resemble those from experiments with purified Saps, it can be assumed that results will be similar regardless of if whole cells or purified Saps are used. To differentiate between effects of Sap2 and Sap9, an experiment with just the culture supernatant would need to be performed.

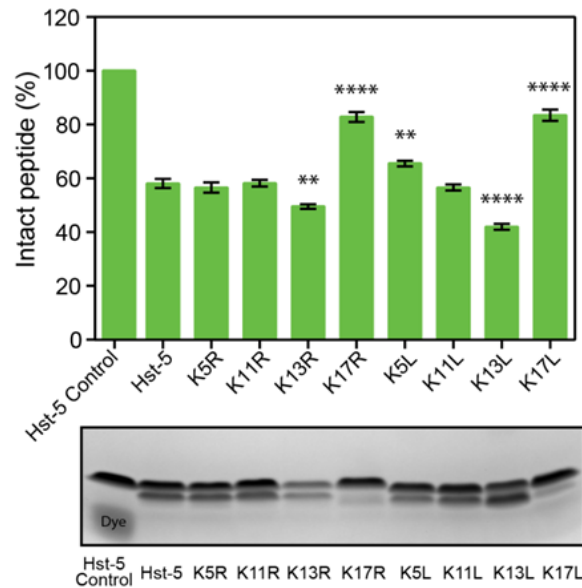


Figure 5.6[†] Degradation of parent Hst-5 and Hst-5 variants by *C. albicans*. Peptides (150 $\mu\text{g/mL}$) were incubated with *C. albicans* (1×10^9 cells/mL) for 2 h at 37 °C. Following gel electrophoresis, the amount of intact peptide (upper band) and degraded peptide (lower bands) were quantified by densitometry and compared. Error bars represent standard error of the mean ($n = 3$). A one-way ANOVA test and Dunnett's multiple comparison test was performed. Asterisks indicate the level of statistical significance against parent Hst-5 incubated with cells: ** for $p < 0.01$ and **** for $p < 0.0001$. The lower band in Hst-5 control lane is due to Coomassie dye.

[†] Figure originally published in *FEBS J.* (2018)

5.2.7 Mass spectrometry analysis

Mass spectrometry (MS) was used to determine peptide cleavage sites and relative amounts of fragments produced following degradation by Saps. Briefly, peptides were incubated with Sap9 or Sap2, desalted, and supplemented with the peptide MRFA as an

internal control for MS. Mass spectra were acquired and molecular weight calculation and fragment prediction was performed. MS/MS spectra were processed to identify peptides and the fragments produced from each, including the relative abundance of each fraction as compared to the MRFA control.

Overall MS results are in agreement with gel electrophoresis degradation analysis in regards to relative abundance of intact peptide for each peptide. For example, following incubation with Sap9 and MS, both K17R and K17L showed the highest signal from intact peptide, which is confirmed by earlier densitometry results (Figure A1). It is important to note that parent Hst-5 was cleaved on the C-terminal side of the K17 residue, but that modification of this lysine to either arginine or leucine prevented this cleavage from occurring. In fact, for Hst-5, the signal for the fragment from residues 1 – 17 was much higher than that of the intact peptide. For Hst-5, cleavage on either side of the lysine at position 13 and between histidine residues at positions 18 and 19 was also observed. Generally, arginine-substituted peptides showed higher relative amounts of intact peptide than their leucine-substituted counterparts. Substitutions also have the ability to shift the cleavage site preference or, as seen for K13R, and to affect the peptide as a whole, as seen by increased amount of intact peptide seen for K11R. This indicates that substitutions can affect the overall cleavage of the peptide and not just at the substitution site.

Incubation with Sap2 resulted in intact peptide being the most observed size for parent Hst-5 (Figure A2). This effect was observed for all peptides and corroborates the differences observed between Sap9 and Sap2 gel electrophoresis results. Whereas with Sap9, K17R and K17L mutations protected this site from cleavage, with Sap2, cleavage was observed on the C-terminal side of the K17 site. MS data suggests that Sap2 greatly

prefers lysine over other residues at cleavage sites, regardless of the charge of amino acid substitutions made. These results confirmed gel electrophoresis results and allowed for the design of new modified Hst-5 peptides.

5.2.8 Additional modification of Hst-5 peptides and results

Based on the results of the first set of modifications, a new set of Hst-5 variants was designed [140]. Since the glutamic acid at residue position 16 is the only negatively charged amino acid in Hst-5, this was selected as one site for modification to either an arginine, to change the charge to be positive, or to leucine, to remove the charge. Modifications to the lysine at position 13 were also explored since it was found that the K13L modification made the peptide highly susceptible to Sap9, despite maintaining antifungal activity. The K17R peptide proved to be highly resistant to degradation and maintained antifungal activity and the K11R enhanced antifungal activity. Therefore, these modifications would be combined in order to observe any synergistic effects. Modifications assessed included K13H, K13E, E16R, E16L, and K11R-K17R and antifungal activity and degradation assays were performed as previously described.

Table 5.2 Hst-5 and variants with one or two residue substitutions

Peptide	Sequence ^a																							
	1	2	3	4	5	6	7	8	9	10	11	12	13	14	15	16	17	18	19	20	21	22	23	24
Hst-5	D	S	H	A	K	R	H	H	G	Y	K	R	K	F	H	E	K	H	H	S	H	R	G	Y
K13H	-	-	-	-	-	-	-	-	-	-	-	H	-	-	-	-	-	-	-	-	-	-	-	-
K13E	-	-	-	-	-	-	-	-	-	-	-	E	-	-	-	-	-	-	-	-	-	-	-	-
E16R	-	-	-	-	-	-	-	-	-	-	-	-	-	-	R	-	-	-	-	-	-	-	-	-
E16L	-	-	-	-	-	-	-	-	-	-	-	-	-	-	L	-	-	-	-	-	-	-	-	-
K11R-K17R	-	-	-	-	-	-	-	-	-	R	-	-	-	-	-	R	-	-	-	-	-	-	-	-

^aDash indicates residue unchanged from parent Hst-5. Letter R or L indicates that parent residue at that position was modified to either arginine or leucine, respectively.

The K11R-K17R peptide was highly resistant to degradation by Sap2 and Sap9 as over 88% remained intact following incubation with Saps. Conversely, E16R and E16L showed increased degradation with both Saps as compared to parent Hst-5 (Figure 5.7A and B). The benefit of arginine substitution is again observed as the E16R peptide shows better resistance than the E16L peptide. The substitutions at K13 showed almost no intact peptide remaining following Sap9 incubation, though they showed a similar percentage of intact peptide remaining as compared to Hst-5 when incubated with Sap2. The identity of the higher molecular weight band observed in the K13H lane is unknown and was disregarded. Degradation results observed after incubation of peptides with whole *C. albicans* cells showed a similar pattern of degradation (Figure 5.7C).

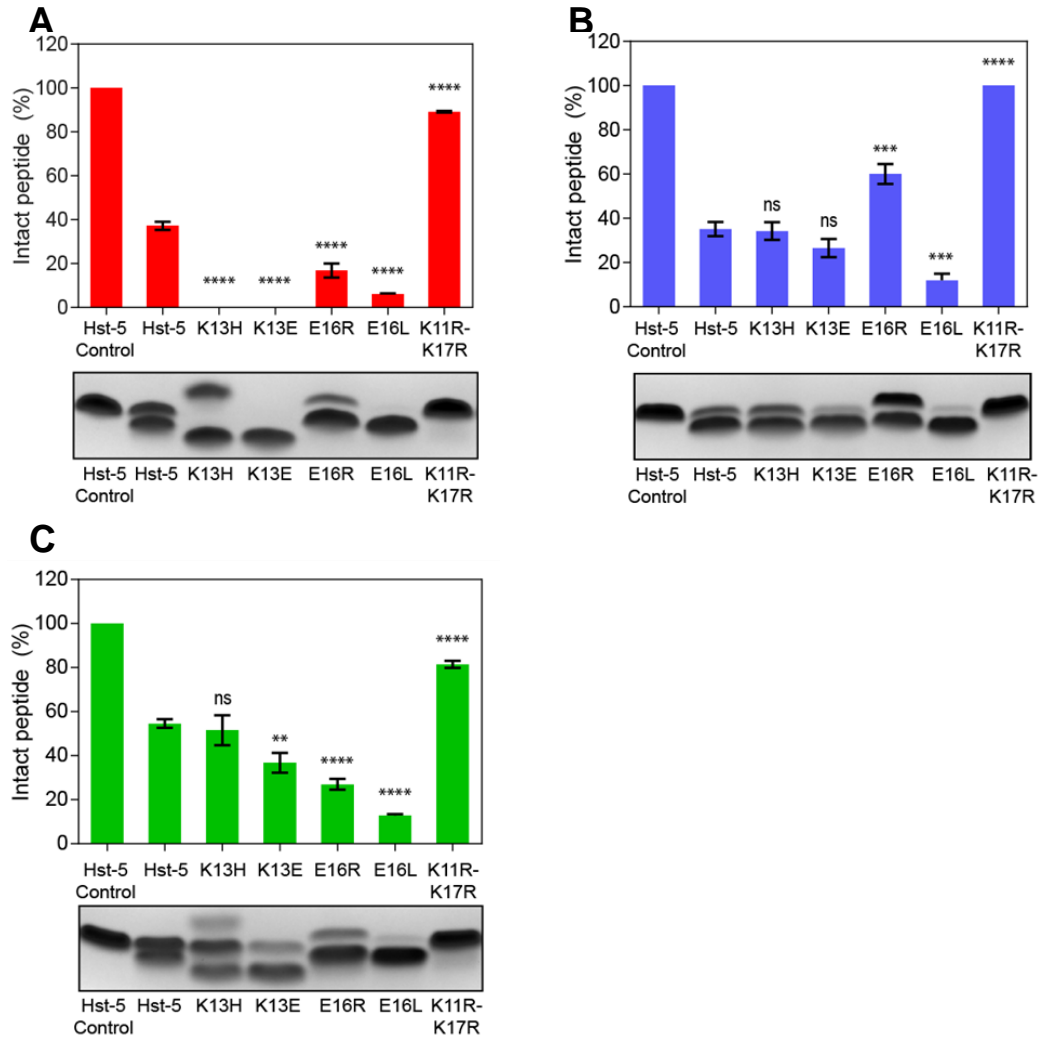


Figure 5.7[§] Extent of proteolysis of parent Hst-5 and Hst-5 variants by purified (A) Sap9 and (B) Sap2. Peptides (50 μ M) were incubated with either Sap9 (3 μ g/mL) or Sap2 (0.05 μ g/mL), respectively for 2 h at 37 $^{\circ}$ C. Following gel electrophoresis, the amount of intact peptide (upper band) and degraded peptide (lower bands) were quantified by densitometry and compared. Error bars indicate standard error of the mean ($n = 6$). A one-way ANOVA test and Dunnett's multiple comparison test was performed. Asterisks indicate significance relative to parent Hst-5: ns for no significance, *** for $p < 0.001$, and **** for $p < 0.0001$. **(C) Extent of degradation for Hst-5 and its variants after exposure to *C. albicans* cells.** Peptides (50 μ M) were incubated with *C. albicans* cells (1×10^9 cells/mL) for 2 hours at 37 $^{\circ}$ C. Following gel electrophoresis, the amount of intact peptide (upper band) and degraded peptide (lower bands) were quantified by densitometry and compared. The source of the additional band in the K13H lane is unknown and not included in the analysis. Error bars indicate standard error of the mean ($n = 6$). A one-way ANOVA test and Dunnett's multiple comparison test was performed. Asterisks indicate the level of statistical significance relative to parent Hst-5: ns for no significance, ** for $p < 0.01$, and **** for $p < 0.0001$.

[§] Data originally published as part of Svetlana Ikonomova's thesis [140].

An antifungal activity assay revealed that both E16R and E16L peptides showed enhanced antifungal activity as compared to parent Hst-5 despite being highly degraded by purified Saps and whole *C. albicans* cells (Figure 5.8). This indicates that some subset of degradation fragments produced for these two peptides are antifungal in nature. Interestingly, the K13E peptide showed decreased antifungal activity, which in conjunction with the E16 peptide results, suggests that a positively-charged residue is preferred over a negatively-charged residue to maintain or enhance antifungal activity. Following degradation by Sap2 or Sap9, degraded peptides were assessed for antifungal activity. Though E16R and E16L peptides were completely degraded by high concentrations of Saps (Figure 5.9A and B), they maintained a high level of antifungal activity (Figure 5.9C). The K11R-K17R peptide showed very high antifungal activity, most likely as a result of its synergistic effect of enhanced activity via the K11R mutation and resistance to degradation via the K17R mutation. These results considered when selecting peptides for experiments on *C. albicans* biofilms as described in Chapter 6.

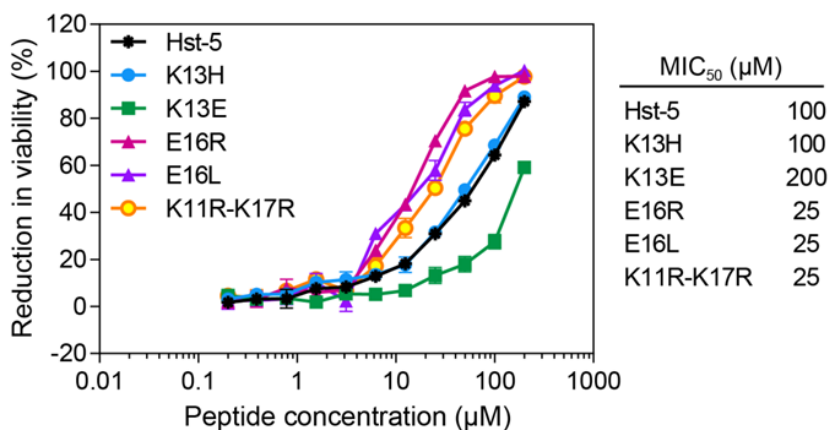


Figure 5.8[§] Antifungal activity of Hst-5 and modified peptides. The peptides (50 µM) were serially diluted and incubated with 2.5×10^7 cells/mL *C. albicans* for 30 minutes at 30 °C. Error bars indicate the standard error of the mean ($n = 6$). MIC₅₀ values for the peptides are shown.

§ Figure originally published as part of Svetlana Ikononova's thesis.

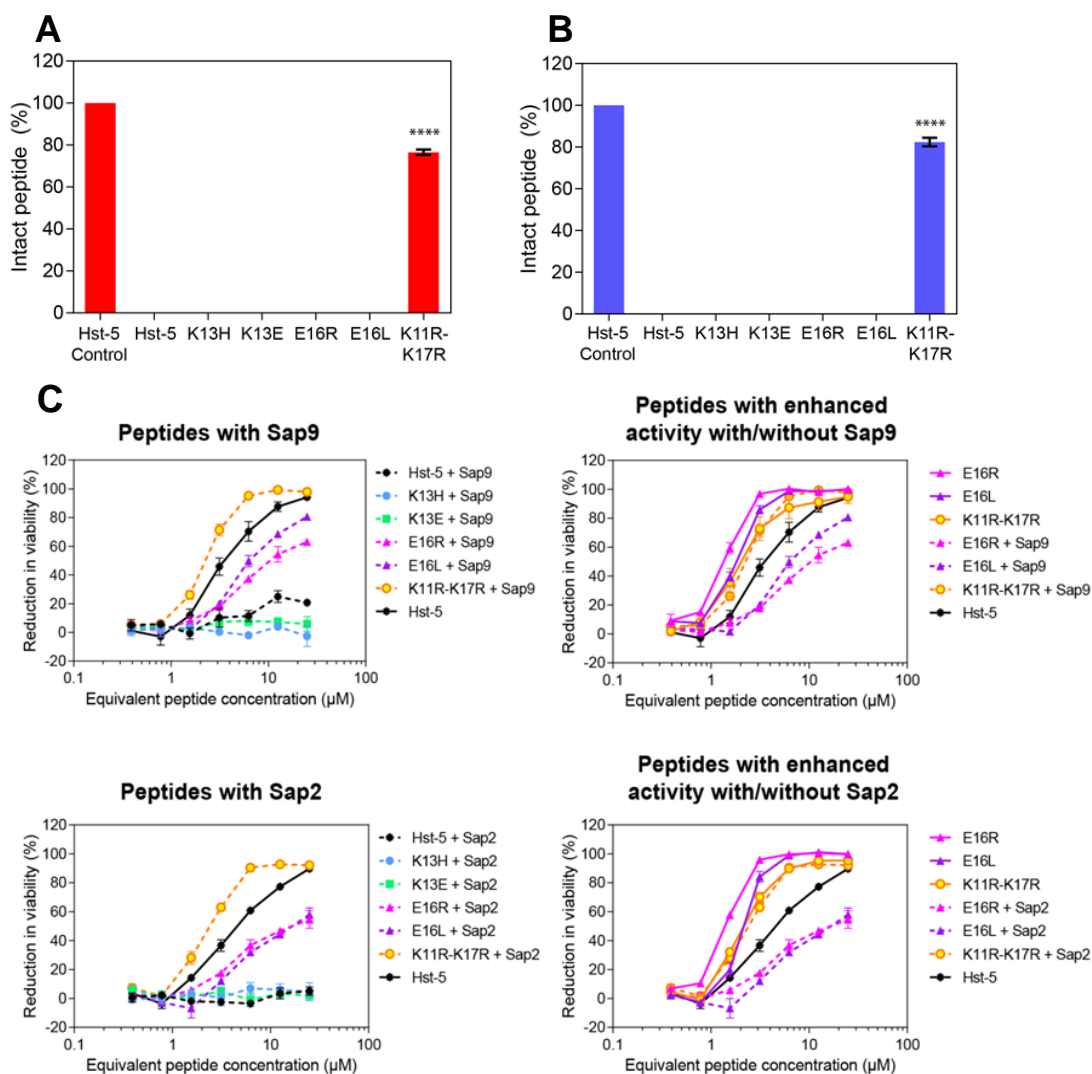


Figure 5.9[§] (A) and (B) Extent of proteolysis of parent Hst-5 and Hst-5 variants by higher concentrations of purified Sap9 and Sap2. Peptides (50 μM) were incubated with Sap9 (6 $\mu\text{g}/\text{mL}$) or Sap2 (0.2 $\mu\text{g}/\text{mL}$), respectively for 2 hours at 37 $^{\circ}\text{C}$. Following gel electrophoresis, the amount of intact peptide (upper band) and degraded peptide (lower bands) were quantified by densitometry and compared. Error bars indicate standard error of the mean ($n = 4$). A one-way ANOVA test and Dunnett's multiple comparison test was performed. Asterisks indicate the level of statistical significance relative to parent Hst-5: **** for $p < 0.0001$. **(C) Antifungal activity of the peptides after incubation with or without Sap9 or Sap2.** Peptides (50 μM) were incubated with Sap9 (6 $\mu\text{g}/\text{mL}$), Sap2 (0.2 $\mu\text{g}/\text{mL}$), or 1 mM NaPB buffer for 2 h at 37 $^{\circ}\text{C}$. Then, peptides were serially diluted and incubated with 2.5×10^5 cells/mL *C. albicans* for 30 min at 30 $^{\circ}$. Error bars indicate the standard error of the mean ($n = 4$).

[§] Figure originally published as part of Svetlana Ikonomova's thesis.

5.3 Materials and Methods

5.3.1 Peptide degradation by *C. albicans* culture supernatant

To confirm the presence and proteolytic activity of fully-secreted active Saps from *C. albicans*, an experiment was designed and performed to determine peptide degradation by *C. albicans* culture supernatant. An overnight culture of *C. albicans* was inoculated in YPD and grown at 30 °C overnight. The following day, a subculture was started and grown to an OD₆₀₀ = 0.8 – 1 and from this, a second subculture of 25 mL was started and grown overnight for 17.5 hours to ensure adequate Sap expression and secretion. This additional subculturing step was performed in order to maintain consistency in the number of cells among biological replicates, which affects total protein expression. Cells were removed by centrifugation and 20 mL of the culture supernatant was transferred to a 10 kDa MWCO column and centrifuged at 20 °C for 20 minutes. Buffer exchange was performed by adding 20 mL of 2 mM NaPB and centrifuging, which was performed three times. The remaining solution was resuspended in 2 mM NaPB to a final volume of 17.5 mL.

Equal volumes of buffer-exchanged culture supernatant and peptide were mixed and incubated at 37 °C for 2 hours. Tricine sample buffer was added and samples were boiled at 100 °C for 10 minutes. Gel electrophoresis, Coomassie staining, and densitometric analysis were performed as described in 5.2.3. Three biological replicates with two technical replicates each were performed. A one-way ANOVA tests with $p < 0.05$ and Dunnett's multiple comparison tests with the Hst-5 sample as the control were performed to assess statistical significance.

5.4 Results

5.4.1 Saps found in *C. albicans* culture supernatant degrade Hst-5 and variants

The densitometric analysis performed on peptides degraded by culture supernatant revealed a pattern of degradation consistent with results from experiments using purified Saps (Figure 5.10). Both K17L and K17R peptides showed improved resistance against degradation, which is in agreement with previous findings. With this assay, the high resistance of these two peptides is highlighted, as there remains 72% intact peptide for K17R and 35% for K17L, compared to 10% or less intact peptide remaining for all other peptides. With the culture supernatant experiment, subtle differences between K17R and K17L can also be seen as there may be other enzymes present in the supernatant that may have a preference for leucine over arginine at cut sites. The supernatant should only contain secreted Saps, and results are consistent with this. For example, the K5R peptide shows more resistance to degradation when incubated with supernatant than when incubated with *C. albicans*, which confirms initial findings that K5R is more resistant to Sap2 than to Sap9. The K11R-K17R peptide also exhibited high resistance to degradation, which was expected due to the resistance imparted by the K17R modification. The K13H and E16R peptides provided some protection against degradation by *C. albicans* supernatant as compared to Hst-5; however, K13H and E16L did not impart any protection against proteolysis. The differences in results from this assay as compared to the assay in which peptides were incubated with *C. albicans* cells demonstrate that both cell wall-anchored Saps and secreted Saps play a role in peptide proteolysis.

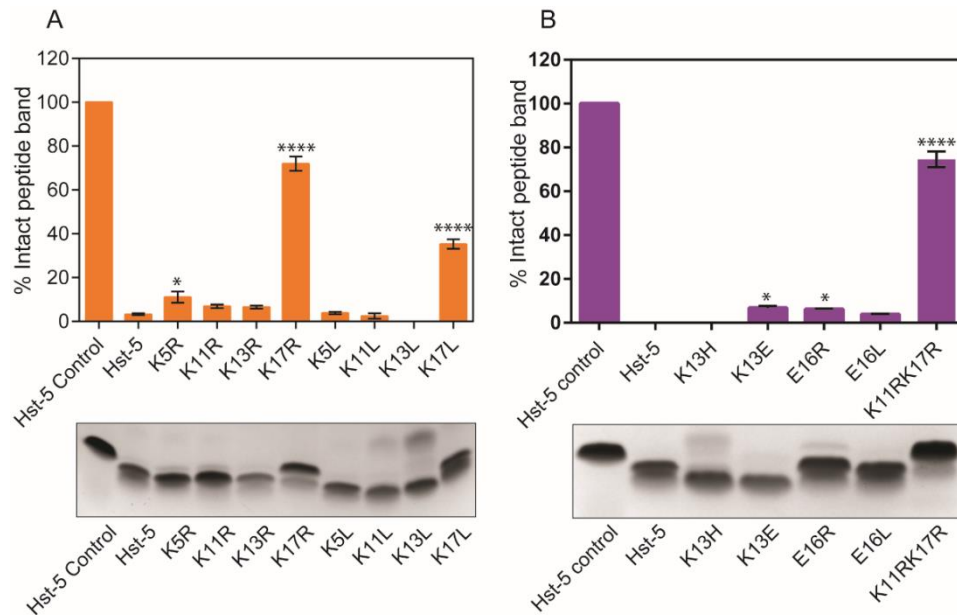


Figure 5.10[†] Degradation of Hst-5 and modified peptides by *C. albicans* culture supernatant. Peptides (150 $\mu\text{g}/\text{mL}$) from the first group of modifications (Table 5.1) (A) or the second set of modifications (Table 5.2) (B) were incubated with culture supernatant for 2 hours at 37 °C. Following gel electrophoresis, the percent intact peptide (upper band) and percent degraded peptide (lower bands) were quantified and compared. Error bars indicate standard error of the mean ($n = 3$). A one-way ANOVA test and Dunnett's multiple comparison test was performed. Asterisks indicate the level of statistical significance relative to parent Hst-5: **** for $p < 0.0001$, * for $p < 0.05$

[†] Figure A originally published in *FEBS J.* (2018)

5.5 Conclusion

These findings demonstrate that specific modifications to the Hst-5 sequence protect from proteolytic degradation by purified Saps, whole *C. albicans* cells, and *C. albicans* culture supernatant. Resistance to degradation correlates with maintained or increased antifungal activity, though some degradation fragments appear to have high antifungal activity. These results contribute to what is known about Sap cleavage site preferences and properties of antimicrobial fragments, which can be used in further modification of Hst-5 or for the design of additional antifungal peptides. To further our

understanding of the antifungal capabilities of the Hst-5 variants, we explored their use in the treatment of *C. albicans* biofilms (Chapter 6).

Chapter 6: Antifungal peptides for treatment of *C. albicans* biofilms

6.1 Introduction

6.1.1 Properties of *C. albicans* biofilms

C. albicans is an opportunistic pathogen that asymptotically inhabits oral, gastrointestinal, and urogenital tracts in the human body. *C. albicans* has the ability to form biofilms on biotic and abiotic surfaces such as implants and catheters. Biofilm colonization of such surfaces is a major contributor to urogenital tract and bloodstream infections, which can be deadly [141]. Hospital-acquired infections of *C. albicans* are on the rise as overuse of antibiotics suppresses normal species of the microbiota and high usage of implants, catheters, and endotracheal tubes allows opportunity for infection [142–144].

The process of *C. albicans* biofilm formation begins by cell wall mediated adherence of yeast cells to a surface between 0 to 11 hours of growth. This is followed by a period during which blastospores proliferate and begin to produce a carbohydrate-rich extracellular matrix (ECM) [103]. During the maturation phase, cells form pseudohyphae and hyphae and are encased by additional ECM [103], although cells are still able to disperse to invade other areas [141]. As *C. albicans* is a dimorphic organism, it exists in biofilms in budding yeast, pseudohyphal, and hyphal forms [142,145] (Figure 6.1). The latter two filamentous forms, while fundamentally different [145], share a genetic regulation factors that contribute to increased virulence. For example, both filamentous forms can exert mechanical force [146], which enables tissue penetration and invasion.

In fact, genes controlling virulence factors, and those controlling hyphal morphogenesis are co-regulated, implying that hyphal formation contributes to the virulence of *C. albicans* [146]. The most prevalent regulator of hyphal morphogenesis is the transcription factor Efg1p which is also responsible for the regulation of genes encoding Saps and adhesins. This expression that coincides with hyphal projection growth allows the cells to have a degradative and adhesive defense system while using the mechanical strength of hyphae to invade tissue, colonize surfaces, or escape epithelial cells following internalization [146].

Additionally, a small portion of clinically isolated strains of *C. albicans* yeast can undergo an epigenetic switch between white and opaque cells that is linked to the mating cycle of the cells [147]. It has been found that over 95% of *C. albicans* clinical isolates are heterozygous for the Mating Type Like (MTL) locus, meaning that they cannot mate unless they undergo homozygosis at the mating locus [141,147]. Interestingly, it has been found that biofilms formed from MTL-heterozygous *C. albicans* are ninefold more viable than those formed by MTL-homozygous cells and are more impermeable [141]. This may suggest that the majority of clinical infections are caused by MTL-heterozygous *C. albicans* as it serves as a protective factor in biofilm survival.

In biofilms, *C. albicans* cells assume different properties from when they are planktonic. They are less susceptible to antimicrobial agents and MICs values were found to increase up to 20,000-fold for *C. albicans* in biofilms as compared to planktonic cells [104]. One of the main factors contributing to the increased antibiotic resistance of *C. albicans* biofilms as compared to planktonic cells is the phase-specific role of efflux pumps and membrane sterols. The *CDR1*, *CDR2*, and *MDR1* genes encode for membrane-

localized efflux pumps that pump drugs out of fungal cells and are characteristic of the multidrug resistant phenotype of *C. albicans* [103,105]. Membrane sterols that contribute to cell wall permeability also contribute to fluconazole resistance. Mukherjee et al. assessed fluconazole resistance of wild-type efflux pump gene knockout strains of *C. albicans* and also assessed the membrane composition of biofilm and planktonic *C. albicans*. Results suggest that efflux pumps impart azole-resistance only during early phases of biofilm formation, and that changes in membrane sterol composition contribute to resistance in mature biofilm development phases [103]. Ramage et al. found that the *CDR1* and *CDR2* mRNA transcript expression was higher for early-phase sessile *C. albicans* in biofilms than for planktonic yeast, implicating their importance in fluconazole-resistance of biofilms in particular [105]. Comparison of temporal changes of membrane ergosterol levels between planktonic and biofilm *C. albicans* established that between 6 to 12 hours of growth the levels decreased 18% and 50%, respectively [103]. This indicates differences in fluconazole-resistance between planktonic and hyphal cells found in biofilms are partly due to membrane composition.

Another factor contributing to the increased resistance of *C. albicans* biofilms to antibiotics is the composition of the extracellular matrix. Al-Fattani et al. describe a method by which *C. albicans* cells were grown under conditions that caused excess production of extracellular matrix material. These cells were found to be more resistant to amphotericin B than those grown in normal, static conditions. Additionally, to simulate conditions that may be present on catheter surfaces, the group performed the same experiment using a mixed culture of *C. albicans* and a slime-producing strain of *Staphylococcus epidermidis* and found the biofilm to be completely resistant to amphotericin B and fluconazole, even

under static conditions [148]. Thus, the use of an alternative therapy, such as antifungal peptides, could prove beneficial to overcome the limitations of current treatments.

6.1.2 Selection of antifungal peptides for the treatment of *C. albicans* biofilms

Previous work from other groups has demonstrated the use of peptides to treat *C. albicans* biofilms. Peptides based on KABT-AMP and uperin 3.6 showed the ability to eradicate biofilms, as decreasing biofilm metabolic activity was observed as peptide

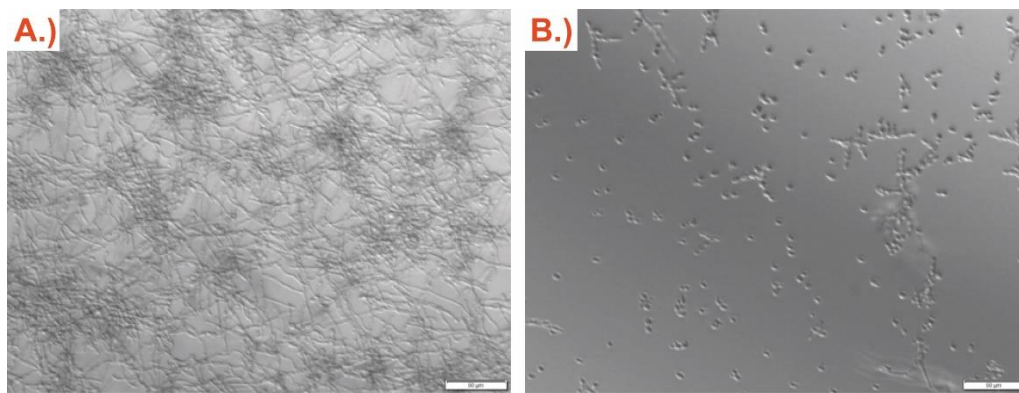


Figure 6.1 Microscopy of treated and untreated *C. albicans* biofilms. (A) Untreated biofilm where primarily hyphal and pseudohyphal *C. albicans* are seen. (B) Biofilm grown in the presence of 0.75 mM E16R peptide that shows primarily yeast form *C. albicans*. Differential interference contrast microscopy images were obtained using an inverted microscope. Scale bars shown are 50 µm in length.

concentrations were increased from 1 – 4 times the MIC₅₀ value for planktonic cells. Unfortunately, these peptides showed significant toxicity on two normal human epithelial cell lines, which puts limitations on their use in therapeutic applications [149]. Karlsson et al. demonstrated the use of β-peptides, constructed with β-amino acid oligomers, against *C. albicans* biofilms. They observed 80% reduction in biofilm metabolic activity when using peptide concentrations that were 1 – 16 times the MIC₅₀ for planktonic cells [150]. Additionally, they demonstrated the ability to incorporate these β-peptides into poly- L- glutamic acid/poly- L-lysine polyelectrolyte multilayer films, which led to a 74% decrease

in biofilm metabolic activity and a decrease in hyphal cell elongation [151]. Other work has demonstrated the use of peptides, including non-amphipathic varieties, that have antifungal properties or that prevent the adhesion of *C. albicans* to surfaces [152–154].

Since Hst-5 is naturally occurring in the saliva, it serves as an ideal template for peptide design for therapeutic purposes. As detailed in previous chapters, specific modifications made to Hst-5 resulted in increased resistance to degradation and maintenance of antifungal activity against planktonic *C. albicans* cells. We chose to assess the ability of parent Hst-5, E16R, K11R-K17R peptides to eradicate *C. albicans* biofilms. The K11R17R peptide was selected for its combined modifications of improved antifungal activity (K11R) and high resistance to degradation by Saps (K17R). The E16R peptide was selected because previous results showed that despite being very susceptible to degradation, it maintained high antifungal activity (Figure 5.9). Hst-5 was used as a control for comparison to determine if modifications also demonstrate enhanced properties when treating *C. albicans* biofilms, which also contain more resistant pseudohyphal and hyphal cells.

6.2 Materials and methods

6.2.1 Planktonic candidacidal assay

This assay was used to assess the antifungal properties of Hst-5, E16R, and K11R-K17R peptides against planktonic *C. albicans* to confirm previous results prior to using the peptides against biofilms (Figure 6.2). *C. albicans* was grown overnight at 30 °C in YPD. Cells were subcultured until $OD_{600} = 1$ to 1.2 and cells. Briefly, cells were washed with 2 mM NaPB by centrifugation and resuspension and resuspended in 1 mL of 2 mM NaPB.

The OD₆₀₀ was measured and a cell suspension of 5×10^7 cells/mL in 2 mM NaPB was prepared. Twofold serial dilutions of peptides were prepared in water 2X final concentration, with the highest 2X concentration being 800 μ M) and 20 μ L peptide was added to the appropriate well of a 96-well round-bottom plate, followed by 20 μ L diluted cells per well. Amphotericin B was used as a control with 4.7 μ M as the highest final concentration in the first well. For each peptide or drug, three biological replicates with two technical replicates each were performed (i.e. 6 total replicates each).

Plates were incubated at 30 °C for 30 minutes and then the reaction was slowed by adding 320 μ L 1 mM NaPB per well. Samples were diluted further in YPD supplemented with NaPB to ~250 cells per well. These diluted samples were loaded into the appropriate wells of a new 96-well round-bottom plate and grown overnight at 30 °C at 350 rpm on a microplate shaker. Cells were resuspended and the absorbance at 600 nm was measured on a microplate reader. The percent reduction in viability was calculated as follows:

$$\% \text{ reduction in viability} = \left[1 - \frac{(OD_{with \text{ peptide}} - OD_{background})}{(OD_{no \text{ peptide}} - OD_{background})} \right] \times 100$$

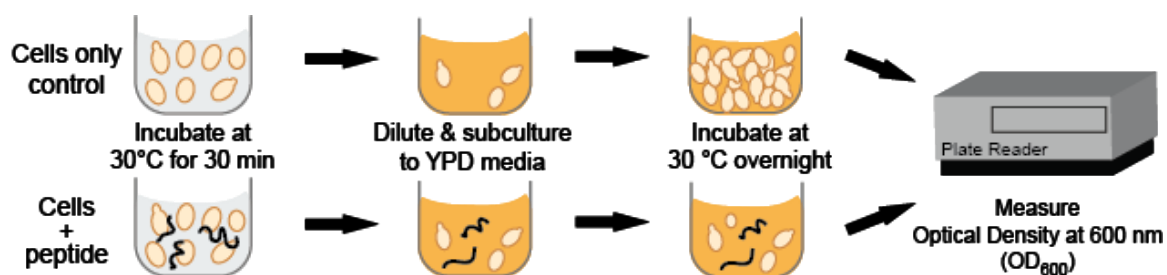


Figure 6.2 Candidacidal assay. *C. albicans* cells are incubated with peptide, then diluted and grown overnight. Cell growth is measured and compared to that of cells without peptide treatment in order to determine the percent reduction in viability that peptide treatment imparts on cells.

6.2.2 Biofilm formation assay

This assay was performed to determine the ability of peptides to prophylactically prevent *C. albicans* biofilm formation. *C. albicans* was grown overnight in YPD at 37 °C. Twofold serial dilutions of peptides were prepared in water at 2X the desired final concentration with the highest 2X concentration being 12 mM. Cells were washed twice with PBS and diluted to a density of 10×10^6 cells/mL in RPMI-1640 medium. RPMI-1640 is a defined media that contains amino acids and mimics the composition of human fluids [155]. To each well of a 96-well high-binding polystyrene ELISA plate, 50 μ L of the appropriate peptide dilution was added followed by 50 μ L of cells. Amphotericin B was used as a positive control for antifungal activity. Again, for each peptide or drug, three biological replicates with two technical replicates each were performed. For each row (i.e. each replicate) a no peptide control and an empty control well were included. Plate edges were sealed with parafilm and plates were incubated at 37 ° for 24 hours. Growth was quantified using a metabolic colorimetric assay. A solution of 0.5 g/L 2,3-bis(2-methoxy-4-nitro-5-sulfo-phenyl)-2H-tetrazolium-5-carboxanilide (XTT) in PBS supplemented with 1 μ L 10 mM menadione in acetone was prepared and protected from light. Biofilms were

washed three times with PBS and 100 μ L of XTT/menadione solution was added to each well, including the empty well control in each row. Films were incubated in the dark at 37 $^{\circ}$ C for 1.5 hours. Plates were centrifuged at $2,000 \times g$ for 5 minutes and 75 μ L of supernatant from each well was transferred to the corresponding well of a new 96-well flat-bottom plate. The absorbance at 490 nm was measured and the percent reduction was calculated as follows:

$$\% \text{ reduction in metabolic activity} = 100 \times \frac{(A_{490}^{490} - A_{490}^{XTT}) - (A_{490} - A_{490}^{XTT})}{(A_{490}^{no \ drug} - A_{490}^{XTT})}$$

6.2.3 Biofilm susceptibility assay

This assay was used to determine if peptides exhibit antifungal activity against preformed biofilms. As described in Section 6.2.2, cell suspensions of *C. albicans* were prepared at a density of 1×10^6 in 1:2 RPMI-1640 medium and 100 μ L was placed into each well of an ELISA plate, with the exception of the final column to serve as an XTT control. Again, three biological replicates and two technical replicates per peptide or drug were used. For each row (i.e. each replicate) a no peptide control and an empty control well were included. Plate edges were sealed with parafilm and incubated at 37 $^{\circ}$ C for 24 hours. Biofilms were washed 3 times with PBS. Twofold serial dilutions of peptides were prepared in 1:2 RPMI-1640 medium at the desired final concentrations with the highest concentration being 12 mM. 100 μ L each was added to the appropriate wells of the ELISA plate and incubated for 24 hours at 37 $^{\circ}$ C. Biofilms were washed the XTT assay was performed as in 6.2.2.

6.2.4 Cytotoxicity analysis of peptides

Peptide solutions were made by resuspending lyophilized peptide in 1 mM NaPB buffer to a final concentration of 200 μ M each. HEK293T cells were cultured in 12-well tissue culture plates to 90%-100% confluency in Dulbecco's modified Eagle's medium (DMEM) with high glucose (ThermoFisher Scientific, Waltham, MA), 10% FBS (ThermoFisher Scientific), and 1% Penicillin-Streptomycin 10,000 U/ml (ThermoFisher Scientific). Cell media was replaced with serum-free media 16 hours prior to peptide incubation. Cells were rinsed with PBS and incubate with 1mL of peptide solution for 30 minutes at 37°C. 1 mM NaPB buffer and ethanol controls were included. 250 μ L of 0.25% Trypsin-EDTA was added to each well and incubated for 5 minutes at 37°C. Each sample was centrifuged at 200 \times g for 5 minutes and supernatant was aspirated. Cells were resuspended in 250 μ L PBS and transferred to flow cytometry tubes. The cell culture, peptide incubation, and preparation of samples for flow cytometry detailed above were performed by Mary Doolin.

Cells were resuspended by pipetting and 1 μ L of 1 mg/mL propidium iodide was added immediately before data acquisition on the flow cytometer (BD FACS Canto II). Data was acquired for each sample for 75 seconds at a high flow rate. Analysis was performed by establishing APC-/APC+ gating between two population peaks, viable and non-viable, on the ethanol control APC-A histogram in FlowJo. This analysis was applied to all groups, resuspended in 250 μ L of PBS, and transferred to the respective flow cytometer tubes. A one-way ANOVA statistical test was performed using GraphPad Prism software to assess statistical significance.

6.2.5 Incorporation of peptides into polyelectrolyte multilayer films

Biofilms colonize surfaces such as catheters and implants inside the body. Therefore, we hypothesize that treating these surfaces with antimicrobial agents that are released in a controlled manner can prevent colonization by *C. albicans* cells. One such method is the incorporation of antifungal peptides into polyelectrolyte multilayer (PEM) films that can be directly assembled on surfaces. PEMs are fabricated by the alternating deposition of polyanions and polycations in a layer-by-layer manner. Previous research demonstrates the incorporation of antifungal peptides into these films and the maintenance of peptide antifungal activity against planktonic *C. albicans* [156] and biofilms [151,157].

To optimize conditions for the engineering of Hst-5 peptide-loaded films, different film fabrication methods were compared. Silicon substrates were cut into 15 mm × 5 mm chips and cleaned with acetone, ethanol, methanol, and water and dried under a filtered air stream. Substrate chips were treated with oxygen plasma to impart charge on the substrate surface. A solution of 50 mM polyethylenimine (PEI, MW = 50,000, Sigma) was prepared in 25 mM NaCl and 5 mM HCl in water. A solution of 50 mM sulfonated polystyrene (SPS, MW = 70,000, Sigma) in 25 mM NaCl in water. PEI and SPS were deposited onto the chip by (1) soaking the chip in the PEI solution for 5 minutes, (2) washing the chip twice by soaking in water for 1 minute per wash, and (3) soaking the chip in the SPS solution for 5 minutes, (4) washing the chip twice by soaking in water for 1 minute per wash. Steps (1) through (4) were repeated until 10 bilayers were formed. The fabrication of these PEI/SPS base layers was performed on a DR3 dipping robot (Riegler & Kirstein GmbH). Preparation of silicon chips and base layer coating was performed by Haleigh Eppler and Dr. Qin Zeng.

Solutions of poly-L-glutamic acid sodium salt (PGA, MW = 50,000, Sigma), poly-L-lysine hydrobromide (PLL, MW = 15,000 – 30,000, Sigma), and Hst-5 were prepared at 1 mg/mL each in 20 mM NaCl in water. Two film preparation conditions were performed with 2 replicates each. For each condition, the film was fabricated by (1) soaking the substrate chip in the first solution for 5 minutes, (2) washing the chip twice by soaking in water for 1 minute per wash, (3) soaking in the second solution for 5 minutes, and (4) washing the chip twice with water as before. For the trilayer method, there was an additional (5) soaking the substrate chip in the third solution, and (6) washing the chip twice with water as before. For each condition, this schema was repeated until 8 bilayers or trilayers were deposited, and thickness measurements were taken after every 2 bilayers or trilayers. Film thickness measurements were taken at 5 points along the center of each chip using an ellipsometer (Gaertner Scientific).

A control condition was performed by alternating deposition of PGA and PLL , which is known to generate films. As modeled after previous antifungal loaded PEMs [151], a trilayer condition was tested by alternating between the PGA solution, the Hst-5 solution, and the PLL solution. The mean thickness and standard error for each condition was calculated after every 2 bilayers or trilayers and from this, the mean base layer thickness was subtracted.

6.3 Results

6.3.1 Modified peptides exhibit enhanced antifungal activity

To assess the antifungal capabilities of the K11R-K17R and E16R peptides, a planktonic Candidacidal assay was performed. The results showed patterns in antifungal

activity for Hst-5, E16R, and K11R-K17R at varying peptide concentrations that confirm earlier results (Figure 6.3). It is of interest to note that at all relevant peptide concentrations, the percent reduction in viability was higher for the modified peptides than for unmodified Hst-5. This could indicate that either modified peptides have enhanced antifungal properties or that their resistance to degradation by Saps allows antifungal fragments to remain active. Small error bars at all concentrations, and particularly for K11R-K17R and E16R peptides imply that these results are reproducible and consistent. A higher error for the Hst-5 peptide is seen at lower peptide concentrations which is due to the large number of cells present, which causes some variability when measuring cell growth by absorbance. These results are consistent with previous planktonic assay results shown in Chapter 5, and highlight the benefits that single residue modifications can impart on the antifungal capabilities of peptides such as Hst-5.

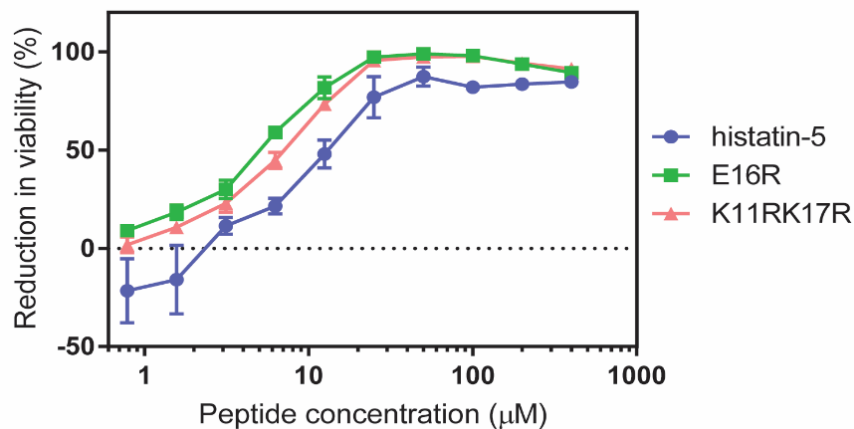


Figure 6.3 Planktonic *Candidacidal* assay. Planktonic *C. albicans* cells were grown in the presence of histatin-5, E16R or K11R-K17R peptide. An XTT assay was performed to determine cell metabolic activity of the cells and the percent reduction in metabolic activity, as compared to untreated cells, was calculated. Error bars represent standard of the mean with $n = 6$.

6.3.2 Histatin-5 and modified peptides inhibit biofilm formation

To determine the capabilities of Hst-5 and modified peptides in the preventing growth of biofilms, a biofilm formation assay was performed. The results for the biofilm formation assay indicate that Hst-5, E16R, and K11R-K17R exhibit antifungal properties and can prevent the formation of biofilms (Figure 6.4). Once again, at relevant concentrations, E16R and K11R-K17R performed better than Hst-5 in terms of reduction of metabolic activity, indicating that the modifications impart beneficial effects on the antifungal activity of the peptides. Again, error bars are small, indicating that results are consistent and reproducible. It is important to note that the peptide concentrations needed to show reduction in metabolic activity for cells where biofilm formation is being induced is in the millimolar range, whereas concentrations in the micromolar range were enough to show antifungal activity against planktonic *C. albicans*. This reiterates the higher resistance of *C. albicans* biofilms to antifungal agents as compared to their planktonic counterparts and emphasizes the need for improving therapy. Though these concentrations may appear high, only a high local concentration at the surface is needed for preventing biofilm growth. Additional mammalian cell cytotoxicity studies using millimolar concentrations of peptide will be performed in the future and the immunogenicity of the peptides will be tested. The

results from this assay are a good indication that biofilm formation can be prophylactically prevented with the use of Hst-5 or modified peptides.

6.3.3 Histatin-5 and modified peptides show antifungal activity against preformed biofilms

While preventing biofilm formation is ideal, another mode of therapeutic use of antifungal peptides is to treat preformed biofilms (Figure 6.5). Here, when peptides were incubated with preexisting *C. albicans* biofilms, there was a marked reduction in metabolic activity. In this case, the modified peptides showed enhanced antifungal activity against *C.*

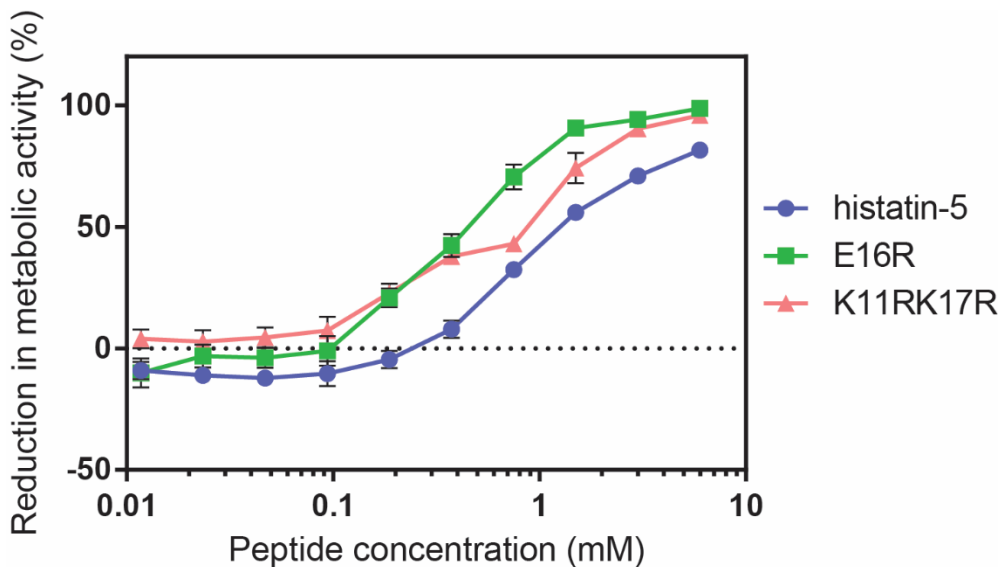


Figure 6.4 Biofilm formation assay. *C. albicans* biofilms were grown for 24 hours in the presence of histatin-5, E16R, or K11R-K17R peptide. An XTT assay was performed to determine metabolic activity of the cells. The percent reduction in metabolic activity, as compared to untreated cells, was calculated. Error bars represent standard of the mean with n = 6.

albicans over Hst-5, except at the highest concentrations where Hst-5 performed equally or better than E16R and K11R-K17R. It is of interest to note that while K11R-K17R and E16R both show very small error bars, that Hst-5 shows large error bars, and that this is

specific to this assay. One possible explanation could be how the degradation kinetics of Hst-5 compared to those of K11R-K17R. From preliminary kinetic analysis (data not shown) it seems that E16R degrades much more quickly than Hst-5, and as speculated before, we believe that one of the degradation fragments of E16R has antifungal capabilities. Thus, E16R likely degrades quickly and in a consistent manner. In comparison, Hst-5 degrades more slowly and as degradation is dependent on Saps from *C. albicans* cells, there will likely be more variability which contributes to the high error seen. K11R-K17R is not readily degradable by Saps, which means that it will perform in a consistent manner, as suggested by the small error bars. The results of this assay demonstrate the therapeutic potential for Hst-5 and modified peptides to be used to treat preexisting biofilms that have formed on surfaces.

In microscopy images taken of treated *C. albicans* biofilms vs. untreated biofilms, we observed a distinct lack of hyphal cell formation in treated samples (Figure 6.1). There were still a few yeast form cells in treated samples, which indicate that there were still potentially live cells present, and that few, if any, were pseudohyphal or hyphal in nature. This observation may be of interest as it may indicate that Hst-5 and its variants in part function by preventing hyphal growth, and since hyphal cells are more resistant to antifungals, demonstrating this capability would be compelling to the treatment of fungal disease. In Chapter 7, we discuss the potential for using this information to elucidate the mechanism of Hst-5 in biofilm prevention.

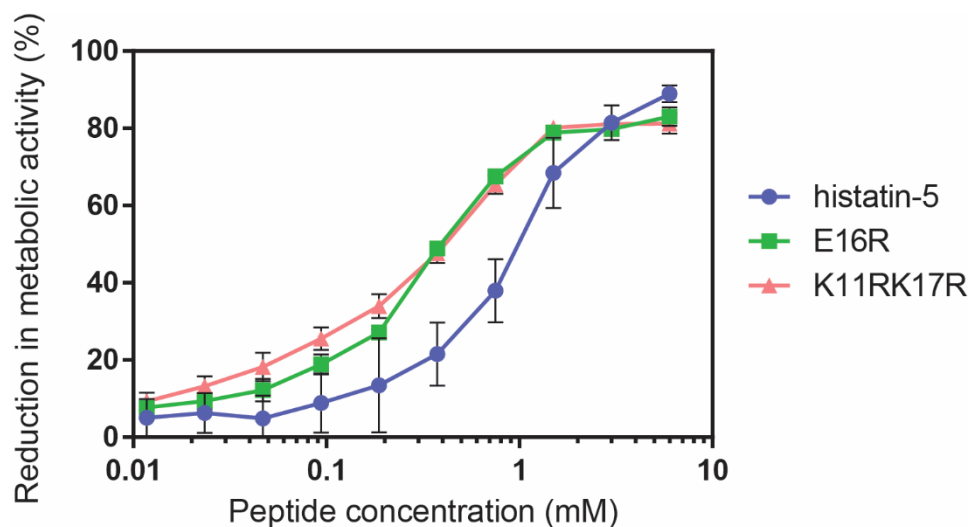


Figure 6.5 Biofilm susceptibility assay. *C. albicans* biofilms were grown for 24 hours and then incubated with histatin-5, E16R, or K11R-K17R peptide for 24 hours. An XTT assay was performed to determine metabolic activity of the cells. The percent reduction in metabolic activity, as compared to untreated cells, was calculated. Error bars represent standard of the mean with n = 6.

6.3.4 Peptides are not cytotoxic to mammalian cells

To ensure that modified peptides did not cause significant mammalian cell cytotoxicity, incubation of peptides with HEK293T cells was performed and the percent of non-viable cells was quantified using propidium iodide staining and flow cytometry. Propidium iodide can only enter cells when the cellular membrane is destabilized, indicating a damaged, non-viable cell. The percent PI-positive cells for each modified

Table 6.1 Cytotoxicity analysis of Hst-5 and variants

Peptide	% PI-positive cells \pm SEM
1 mM NaPB control	5.106 \pm 1.385
Hst-5	7.215 \pm 1.025
E16R	10.74 \pm 3.625
E16L	5.252 \pm 0.7552
K11R-K17R	4.626 \pm 0.8321
K13E	6.328 \pm 1.3
K13H	4.687 \pm 1.083

peptide was compared to that of a 1mM NaPB buffer control with a one-way ANOVA tests with $p < 0.05$ and Dunnett's multiple comparison tests with the Hst-5 sample as the control were performed to assess statistical significance. No significant differences were observed (Table 6.1), indicating that peptides are no more cytotoxic than buffer alone. Additionally, the percent PI-positive cells for each modified peptide was compared to that of Hst-5 and no significant differences were observed. These results demonstrate that peptides are not cytotoxic to mammalian cells and that the peptide modifications do not cause changes in cytotoxicity from the parent Hst-5. Additional testing with millimolar peptide concentrations will be performed to ensure that concentrations used in biofilm assays are not toxic to mammalian cells.

6.3.5 Peptides can be incorporated into PEMs

Preliminary results indicate the ability to incorporate Hst-5 into PGA/PLL polyelectrolyte multilayer films. The growth of the PEMs fabricated in the trilayer method show a generally positive growth as the number of deposited trilayers increases, with an increase of 408 Å from the initial base layer thickness (Figure 6.6). The PGA/PLL control also showed film growth, but at a lower level than the Hst-5 incorporated trilayers, which is expected. It should be noted that large error bars seen are likely an artifact of inadequate base layer homogeneity which led to differences in film thickness at different locations on each chip, which are particularly apparent when more layers are deposited. The deposition of base layers will be optimized to promote homogeneous film growth.

Optimizing concentrations of PGA, PLL, and Hst-5 will allow for more consistent growth with an increasing number of trilayers. Additionally, ensuring base layers are properly and homogeneously built onto the chip surface will allow for more consistent polyelectrolyte deposition and less variability in measurements. With these initial results confirming that peptide can be incorporated into films, more studies should be performed to characterize these films and their ability to prevent biofilm formation. These studies are outlined in Chapter 7.

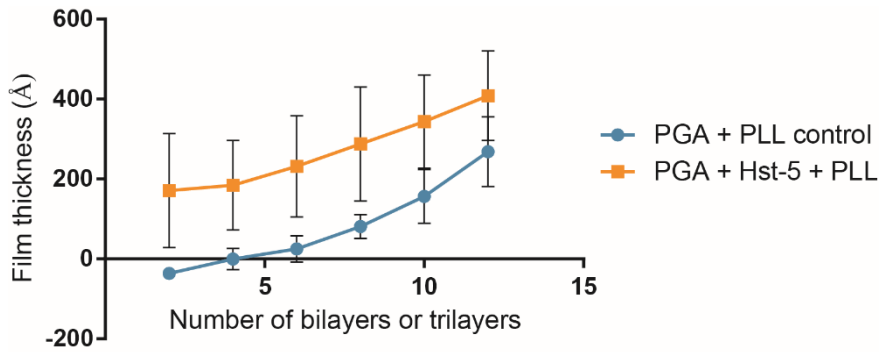


Figure 6.6. Thickness of fabricated polyelectrolyte multilayer films. Films were fabricated as described in Section 6.2.5 by alternating deposition of poly-L-glutamic acid, poly-L-lysine, and histatin-5. Film thickness was measured at 5 points per sample after every 2 bilayers or trilayers on an ellipsometer and averaged. Error bars show standard error of the mean with $n = 2$.

6.4 Conclusion

Hst-5 and the variants E16R and K11R-K17R can be used to prevent formation of *C. albicans* biofilms and to eradicate preformed biofilms. The modified peptides exhibit enhanced antifungal activity as compared to parent Hst-5 in the treatment of both planktonic cells and biofilms. Hst-5 and modified peptides are not toxic to mammalian cells, which makes the suitable agents for therapeutic purposes. Hst-5 and its variants are attractive candidates for treating fungal disease in humans as Hst-5 is natively produced and present in the oral cavity. The non-foreign nature lends itself to greater tolerance and some predictability of properties and immunogenicity of modified variants.

The incorporation of these antimicrobial peptides into PEMs will allow the coating of implantable surfaces to prevent *C. albicans* growth and fungal disease. Peptide loaded films can be used to coat a variety of surfaces such as prostheses and catheters, which will confer a high local surface concentration of peptide. This can effectively prevent biofilm formation on implantable devices as the peptide release rate can be adjusted. As the risk of *C. albicans* infection is higher immediately after implantation, such a coating would release peptide initially and eventually degrade when the risk of biofilm growth decreases over time. In Chapter 7, we discuss studies that will facilitate the use of peptide loaded PEMs against *C. albicans* biofilms in *in vivo* studies.

**PART III: SUMMARY AND
RECOMMENDATIONS FOR FUTURE WORK**

Chapter 7: Summary and recommendations for future work

7.1 Summary

The work presented in this dissertation contributes new methodology, novel insights, and potential therapeutic agents to the protein and peptide engineering field.

With our intrabody engineering work, we demonstrated the ability to isolate highly soluble scFvs from a naïve library using Tat inner-membrane display and screening. We found that screening of naïve libraries using this method requires optimization as the isolated scFvs exhibited nonspecific binding behavior. In our efforts to increase assay stringency to improve the properties of isolated scFvs, we found that inclusion of a soluble competitor during the screening process altered the overall properties of isolates. Upon further characterization, those scFvs isolated from screening in which a soluble competitor was included exhibited more saturable binding curves and greater discrimination between binding signal of different library members. This reduces the number of false positives and nonsaturable binding seen in concentration dependent ELISAs. Additionally, we found that choice of blocking agent as a diluent when incubating lysates affects the binding of scFvs at higher concentrations, which is an important consideration during isolate characterization.

We also implemented modifications to the library cloning process that shorten the time it takes to generate new libraries from enriched sublibraries or isolated antibodies. Whole plasmid PCR eliminates the need to perform plasmid purification and restriction enzyme digest digestion to prepare vector backbone. We also demonstrated the ability to perform whole plasmid PCR on plasmid DNA directly from lysed spheroplasts.

Additionally, we were able to transform *E. coli* with plasmid from spheroplast lysate, which eliminates the need to amplify plasmids, though additional work needs to be performed to determine if libraries generated in this manner are comparable in diversity to those generated using cloning methods. The implementation of these protocol modifications will save valuable time when repeatedly panning and constructing libraries, which will allow for a shorter timescale to discovery of high binding antibodies. These findings and method improvements will help to shape a general protocol for intrabody engineering that promotes antigen specificity and cytoplasmic solubility.

In our work with antifungal peptides, we demonstrated that specific modifications to Hst-5 made modified peptides more resistant to degradation by Saps found on *C. albicans* cells and in the culture supernatant. We also established the use of three of these peptides, Hst-5, E16R, and K11R-K17R, for the prevention of *C. albicans* biofilm formation and eradication of preformed biofilms. It was seen that the antifungal activity of the modified peptides was enhanced as compared to Hst-5. Results also indicate that K11R-K17R and E16R behave in a more predictable and consistent manner as compared to parent Hst-5, likely due to differences in the kinetics of peptide degradation by *C. albicans* secreted Saps and the properties of their respective fragments. The results from this work contribute to the knowledge of current antimicrobial peptides and can be used in the engineering of additional peptides.

Based on our work, we have several recommendations for future studies to build upon our findings and continue moving towards therapeutic application of intrabodies and antifungal peptides.

7.2 Improving library screening for the isolation of intrabodies

7.2.1 Improving library quality

7.2.1.1 Use of an immunized library

Our first suggestion is to explore the use of an immunized library as a starting point for affinity maturation using the Tat inner-membrane display method. To obtain an immunized library, the target antigen is introduced into an animal (e.g. a llama) whereby the antibodies are generated in response to this antigen. Antibodies are isolated by extracting mRNA from lymphocytes from the animal and then genes encoding antibody fragments can then be cloned into the selected display vector. Immunization is advantageous because of the intrinsic clonal expansion and affinity maturation that occurs when an immunogen is introduced into the animal's body. This results in a library that is made of many members that already have at least a low level of binding to the antigen. Using Tat inner-membrane display to further affinity mature an immunized library is valuable for intrabody engineering applications as it will deplete the library of poorly soluble members.

7.2.1.2 Use of a commercial anti-survivin antibody

Commercially available monoclonal antibodies targeted towards survivin for research purposes are available. One option to improve the quality of the library is to use such an existing antibody as a template for the library. This would ensure that the parent antibody has some specificity for survivin, which will be further engineered. In this approach, it would be necessary to receive the gene sequence from the commercial antibody manufacturer and determine the heavy chain and light chain regions in order to

generate an scFv or other antibody fragment from the full length IgG. The isolated fragment would then be mutagenized to generate a library to display and screen against survivin. Binding affinity and specificity for survivin would be characterized.

7.2.1.3 Modifications to the antibody fragment frameworks to improve solubility

The highly reducing cytoplasm of mammalian cells prevent the formation of stabilizing disulfide bonds normally needed for antibodies and antibody fragments to fold and function correctly. It has been shown that an scFv framework that has been modified to eliminate cysteines that form disulfide bonds allows for isolation of scFvs that are well folded and stable [158]. We suggest extending this framework modification to VHHs, as they are already more stable than scFvs and show great potential for use as intrabodies.

In VHHs, there are two conserved cysteines at residue positions 22 and 92 in the framework FR1 and F3 regions, respectively, that are prone to forming disulfide bonds. Site-directed mutagenesis can be performed to substitute the framework cysteine residues at positions 22 and 92 with alanine residues. Alanine residues are typically used for cysteine substitution are small and are not likely to cause major structural changes. This would prevent the formation of this disulfide bond and decrease the likelihood that a promising VHH would show low solubility upon further characterization. We would expect that a VHH library based on a framework that is non-reliant on stabilizing disulfide bonds will produce VHHs with greater cytoplasmic solubility earlier in rounds of directed evolution than a library based on a traditional VHH framework.

An alternative method to improving the solubility of antibody fragments, including both VHHs and scFvs, is to pack the core of the folded proteins with hydrophobic residues.

The inclusion of more hydrophobic residues on the interior and more hydrophilic residues on the exterior of the folded protein may confer additional thermal stability and solubility to the antibodies. This method would rely on an analysis of existing antibody fragment framework structures. Such an approach would entail engineering the solubility first, and then following this with library construction, display, and screening to engineer binding affinity and specificity.

7.2.2 Increasing assay stringency

As we demonstrated in our work, modifications to the screening assay can change the binding behavior of isolated antibodies and allow better discrimination between isolates. Therefore, we suggest continuing along this route to systematically modify the panning and screening protocols and compare outcomes. One suggestions for improvement is the inclusion of soluble parent antibody in various steps of the protocol so that library antibodies have to bind more strongly to the antigen than the parent scFv in order to remain bound and be recovered. Specifically related to the survivin antigen, we recommend improving the purification of scFv-F4 for use as a soluble competitor. We also recommend assessing the extent to which adding additional negative panning steps affects the presence of false positives in the library secondary screening process. Elimination of false positives early on will save time and resources that would not need to be spent on further characterization of such antibodies.

7.2.3 Modifications to survivin target

The commercially available recombinant human survivin used in our work had an N-terminal calmodulin tag which was nearly as large as monomeric survivin itself. As such,

it is quite possible that libraries were being screened for binding to epitopes on the calmodulin tag rather than on the survivin protein. We suggest the use of a recombinant survivin protein with either no tag or a smaller tag to prevent antibodies from binding to non-target domains.

Orienting survivin in unidirectionally during surface coating for binding assays may promote isolation of antibodies that bind to specific domains. One potential method for achieving this is to express survivin as a fusion to the biotin carboxyl carrier protein (BCCP) or its minimal substrate, AviTag. These can be biotinylated *in vivo* [159], purified, and immobilized onto streptavidin-coated plates in a method similar to that developed by Ikonomova et al. for immobilization of scFvs [160]. This method would orient the survivin molecules once the biotin-streptavidin non-covalent bond is formed as the terminus bearing BCCP will be bound to the surface. Other methods for orienting survivin can also be explored.

7.3 Understanding histatin-5 cell entry mechanisms and potential as a candidacidal therapy

7.3.1 Oriented CD

As detailed in Chapter 5, Hst-5 does not cause pore formation when it enters *C. albicans* and enters the cell through a combination of energy dependent and energy independent mechanisms. While it is known that Hst-5 is unstructured in aqueous solution and helical in hydrophobic solutions, more information about the structure of Hst-5 near the cell surface is warranted. We suggest performing oriented circular dichroism (OCD) to gather information about the secondary structure of Hst-5 and variants near synthetic

oriented lipid multibilayers [161]. This method relies on the assumption that the dipole moment of the transition of amide bond is polarized either parallel or perpendicular to the helical axis [162]. The orientation of the helical peptide with respect to the lipid multilayer is conveyed through the OCD spectra produced. Understanding the direction at which Hst-5 approaches the membrane will contribute to our knowledge of its entry mechanism and provide additional amino acid targets for modification.

7.3.2 Formation of peptide-loaded PEMs to coat implantable surfaces

We demonstrated the success of Hst-5 and modified peptides in treating *C. albicans* biofilms. While our results for incorporation of Hst-5 into PGA/PLL PEMs are preliminary, once it is demonstrated that the films can be fabricated, we suggest the following set of experiments. Peptide-loaded films should be characterized for thickness and peptide incorporation. Thickness measurements can be performed during layer-by-layer formation as described in Chapter 6.2.5 and peptide incorporation can be confirmed by taking absorbance measurements of PEMs fabricated with fluorescently-labeled peptide. The stability of the films in RPMI-1640 media should also be assessed as their use in these growth conditions is necessary. Most importantly, the antifungal activity of the films should be assessed by inducing biofilm formation in the presence of peptide-loaded films and then quantifying cell viability with an XTT metabolic or PI stain. Growth of biofilms on coated substrates will be compared to their growth on the surrounding surface and on untreated samples via the metabolic assay and visual comparison using bright field microscopy. Additional details for designing and performing these assays is described by Karlsson et al. [151]. Establishing the maintenance of antifungal activity will serve as a foundation for *in vivo* studies involving PEM-coated implantable surfaces. The information

gained from these studies will continue the advancement of applying Hst-5 and its variants toward therapeutic purposes.

7.3.3 Assessment of Hst-5 and modified peptides ability to prevent hyphal formation

As described in Chapter 6, there was lack of hyphal cell formation in treated samples of the biofilm formation assay, though a few yeast form cells were still seen. It is of interest to determine whether or not Hst-5 and its variants prevent *C. albicans* biofilm formation by preventing hyphal cell growth that contributes to the network-structure of biofilms. The dense network formed by hyphal cells, which later become encapsulated by extracellular matrix, is one of the contributing factors to the increased resistance of *C. albicans* in this form. It could be speculated that preventing these connections would inhibit the ability of the cells to form such a network, thus reducing their resistance to treatment. Therefore, developing an assay to assess mRNA transcripts in response to peptide treatment at varying time points would help to elucidate whether or not peptide in part function by preventing hyphal growth.

Appendix

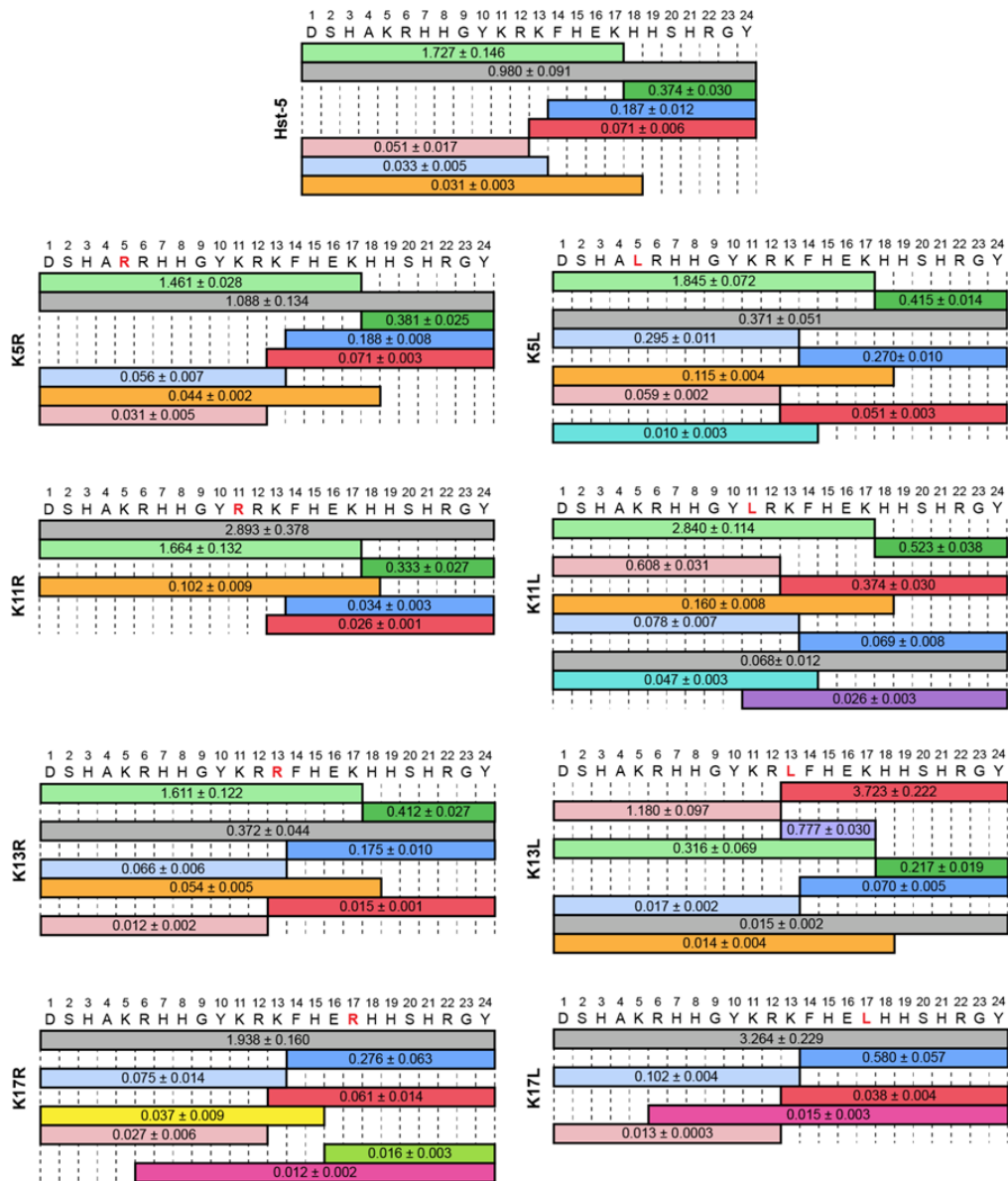


Figure A1† Relative mass spectrometry signal intensity of intact peptide (gray) and peptide fragments produced by incubation of parent Hst-5 and Hst-5 variants (modified residue in red) with 3.13 $\mu\text{g/mL}$ Sap9. The values on each fragment indicate the signal for the fragment relative to the signal for an internal standard. Fragments with signals greater than 0.01 relative to the standard are shown. The relative signal is the mean with standard error ($n = 3$).

†Figure and caption originally published in *FEBS J.* (2018)

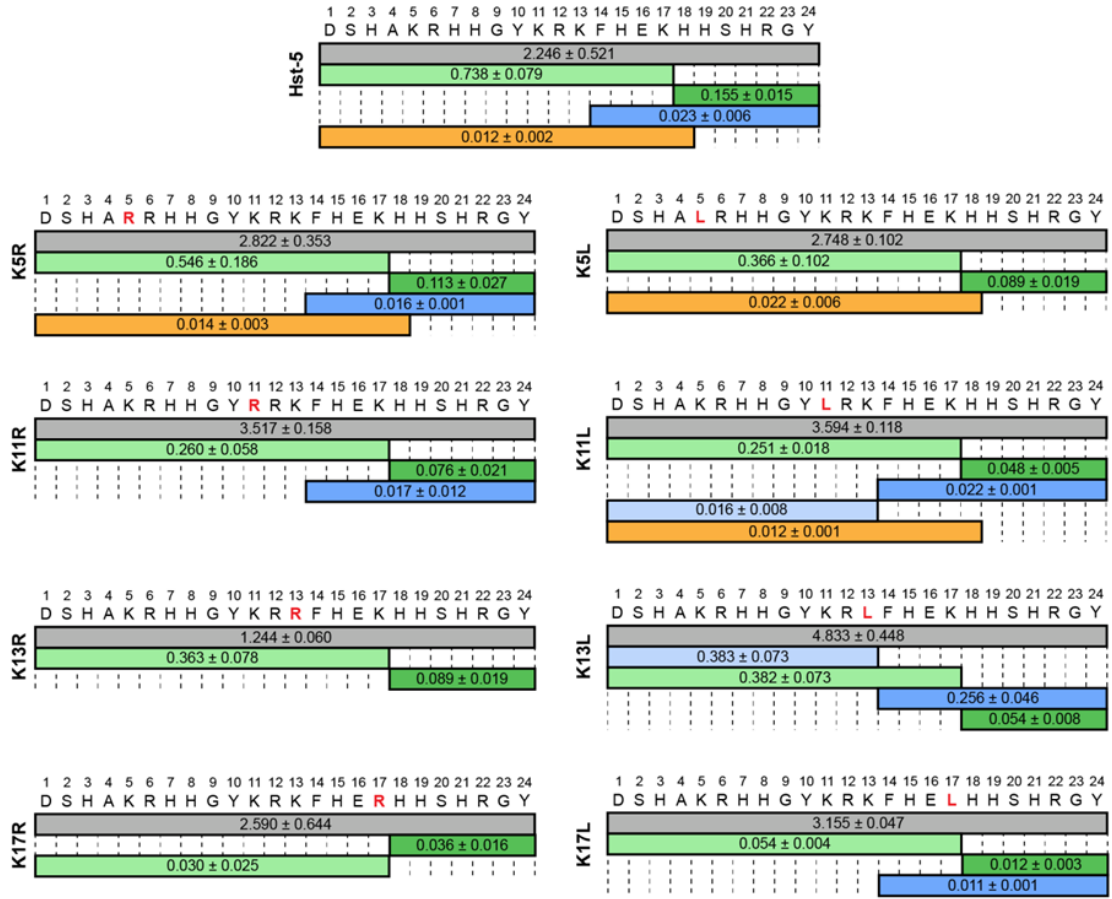


Figure A2† Relative mass spectrometry signal intensity of intact peptide (gray) and peptide fragments produced by incubation of parent Hst-5 and Hst-5 variants (modified residue in red) with 6.25 μg/mL Sap2. The values on each fragment indicate the signal for the fragment relative to the signal for an internal standard. Fragments with signals greater than 0.01 relative to the standard are shown. The relative signal is the mean with standard error (n = 3).

†Figure and caption originally published in *FEBS J.* (2018)

Publications and Presentations

Accepted publications

Moghaddam-Taaheri P and Karlsson AJ. "Protein labeling in live cells for immunological applications." *Bioconjugate Chemistry*. doi: 10.1021/acs.bioconjchem.7b00722. (2018).

Ikonomova SP, **Moghaddam-Taaheri P**, Wang Y, Jabra-Rizk MA and Karlsson AJ. "Engineering improved variants of the antifungal peptide histatin 5 with reduced susceptibility to *Candida albicans* secreted aspartic proteases and enhanced antimicrobial potency." *FEBS J*. doi: 10.1111/febs.14327 (2017).

Moghaddam-Taaheri P, Ikonomova SP, Gong Z, Wiesnieski J, and Karlsson AJ. "Bacterial inner-membrane display for screening a library of antibody fragments." *J Vis. Exp.* (116), e54583, doi:10.3791/54583 (2016).

Publications under preparation

Moghaddam-Taaheri P, Ikonomova SP, Eppler H, and Karlsson AJ. "Histatin 5 variants inhibiting *Candida albicans* biofilm formation." In preparation.

Ikonomova SP, **Moghaddam-Taaheri P**, Doolin M, Wang Y, and Karlsson AJ. "Histatin 5 variants with improved resistance to degradation by *Candida albicans* secreted aspartic proteases." In preparation.

Presentations (presenting author underlined)

Moghaddam-Taaheri P, Ikonomiva S and Karlsson AJ. "Antifungal peptide variants with reduced degradation by fungal proteases and improved antifungal activity against planktonic and biofilm cells." AIChE Annual Meeting, Pittsburgh, PA, October 2018. In preparation. (Poster)

Dearing R, Yao Q, **Moghaddam-Taaheri P**, Karlsson A and Asa-Awuku A. "Identification of toxic mold genes in aerosolized *Stachybotrys*." International Aerosol Conference, St. Louis, MO, September 2018. In preparation. (Poster)

Moghaddam-Taaheri P and Karlsson AJ. "Bacterial inner membrane display for isolating intracellular antibodies that bind survivin." International Conference on Biomolecular Engineering, Austin, TX, January 2015. (Oral Presentation)

References

- [1] R.J. Kazlauskas, U.T. Bornscheuer (2009) Finding better protein engineering strategies, *Nat. Chem. Biol.* 5, 526–529. doi:10.1038/nchembio0809-526.
- [2] G. Güven, R. Prodanovic, U. Schwaneberg (2010) Protein engineering - an option for enzymatic biofuel cell design, *Electroanalysis.* 22, 765–775. doi:10.1002/elan.200980017.
- [3] O. Kirk, T.V. Borchert, C.C. Fuglsang (2002) Industrial enzyme applications, *Curr. Opin. Biotechnol.* 13, 345–351. doi:10.1016/S0958-1669(02)00328-2.
- [4] P.J. Carter (2011) Introduction to current and future protein therapeutics: A protein engineering perspective, *Exp. Cell Res.* 317, 1261–1269. doi:10.1016/j.yexcr.2011.02.013.
- [5] J. Maynard, G. Georgiou (2000) Antibody Engineering, *Annu. Rev. Biomed. Eng.* 2, 339-376.
- [6] P.J. Carter (2006) Potent antibody therapeutics by design, *Nat. Rev. Immunol.* 6, 343–357. doi:10.1038/nri1837.
- [7] A.L. Nelson, E. Dhimolea, J.M. Reichert (2010) Development trends for human monoclonal antibody therapeutics, *Nat. Rev. Drug Discov.* 9, 767–774. doi:10.1038/nrd3229.
- [8] G. Walsh (2010) Biopharmaceutical benchmarks 2010, *Nat. Biotechnol.* 28, 910-917. doi: 10.1038/nbt0910-917
- [9] G.S. Martin (2003) Cell signaling and cancer, *Cancer Cell.* 4, 167–174. doi:10.1016/S1535-6108(03)00216-2.
- [10] H.S. Bell, K.M. Ryan (2005) Intracellular signalling and cancer: complex pathways lead to multiple targets, *Eur. J. Cancer.* 41, 206–215. doi:10.1016/j.ejca.2004.10.022.
- [11] M. Mahlapuu, J. Håkansson, L. Ringstad, C. Björn (2016) Antimicrobial peptides: an emerging category of therapeutic agents, *Front. Cell. Infect. Microbiol.* 6, 194. doi:10.3389/fcimb.2016.00194.
- [12] M. Zasloff (2002) Antimicrobial peptides of multicellular organisms, *Nature.* 415, 389–395. doi:10.1038/415389a.
- [13] Antibiotic Resistance Threats in the United States, 2013, U.S. Department of Health and Human Services Centers for Disease Control and Prevention, 2013.

- [14] About Antimicrobial Resistance | Antibiotic/Antimicrobial Resistance | CDC, (2018). <https://www.cdc.gov/drugresistance/about.html> (accessed July 2, 2018).
- [15] S. Lutz (2010) Beyond directed evolution—semi-rational protein engineering and design, *Curr. Opin. Biotechnol.* 21, 734–743. doi:10.1016/j.copbio.2010.08.011.
- [16] P.A. Romero, F.H. Arnold (2009) Exploring protein fitness landscapes by directed evolution, *Nat. Rev. Mol. Cell Biol.* 10, 866–876. doi:10.1038/nrm2805.
- [17] K.T. O’Neil, R.H. Hoess (1995) Phage display: protein engineering by directed evolution, *Curr. Opin. Struct. Biol.* 5, 443–449. doi:10.1016/0959-440X(95)80027-1.
- [18] E.T. Boder, K.D. Wittrup (2000) Yeast surface display for directed evolution of protein expression, affinity, and stability, *Methods Enzymol.*, 328, 430-444. doi:10.1016/S0076-6879(00)28410-3.
- [19] S.A. Gai, K.D. Wittrup (2007) Yeast surface display for protein engineering and characterization, *Curr. Opin. Struct. Biol.* 17, 467–473. doi:10.1016/j.sbi.2007.08.012.
- [20] D. Colby, B. Kellog, C. Graff, Y. Yeung, J. Swers, D. Wittrup (2004) Engineering antibody affinity by yeast surface display, *Methods Enzymol.*, 388, 348-358. doi: 10.1016/S0076-6879(04)88027-3
- [21] D. Gueorguieva, S. Li, N. Walsh, A. Mukherji, J. Tanha, S. Pandey (2006) Identification of single-domain, Bax-specific intrabodies that confer resistance to mammalian cells against oxidative-stress-induced apoptosis, *The FASEB Journal.* 20, 2636–2638.
- [22] S. Zielonka, et al. (2014) Shark Attack; High affinity binding proteins derived from shark vNAR domains by stepwise in vitro affinity maturation, *J. Biotech.* 191, 236–245.
- [23] E. Boder, K. Midelfort, K. Wittrup (2000) Directed evolution of antibody fragments with monovalent femtomolar antigen-binding affinity, *Proc. Natl. Acad. Sci.* 97, 10701–10705.
- [24] M. Levisson, R. Spruijt, I. Winkel, S. Kengen, J. van der Oost (2014) Phage display of engineered binding proteins, *Methods Mol. Biol.* 1129, 211–229. doi: 10.1007/978-1-62703-977-2_19.
- [25] J.J. VanAntwerp, K.D. Wittrup (2008) Fine affinity discrimination by yeast surface display and flow cytometry, *Biotechnol. Prog.* 16, 31–37. doi:10.1021/bp990133s.
- [26] G. Chao, W.L. Lau, B.J. Hackel, S.L. Sazinsky, S.M. Lippow, K.D. Wittrup (2006) Isolating and engineering human antibodies using yeast surface display, *Nat. Protoc.* 1, 755–768. doi:10.1038/nprot.2006.94.

- [27] M.C. Kieke, E.V. Shusta, E.T. Boder, L. Teyton, K.D. Wittrup, D.M. Kranz (1999) Selection of functional T cell receptor mutants from a yeast surface-display library, *Proc. Natl. Acad. Sci.* 96, 5651–5656. doi:10.1073/pnas.96.10.5651.
- [28] D. Steiner, P. Forrer, M.T. Stumpp, A. Plückthun (2006) Signal sequences directing cotranslational translocation expand the range of proteins amenable to phage display, *Nat. Biotechnol.* 24, 823–831. doi:10.1038/nbt1218.
- [29] A.J. Karlsson, H.-K. Lim, H. Xu, M.A. Rocco, M.A. Bratkowski, A. Ke, M.P. DeLisa (2012) Engineering antibody fitness and function using membrane-anchored display of correctly folded proteins, *J. Mol. Biol.* 416, 94–107. doi:10.1016/j.jmb.2011.12.021.
- [30] S. Marshall, G. Lazar, A. Chirino, J. Desjarlis (2003) Rational design and engineering of therapeutic proteins, *Drug Discov.Today.* 8, 212-221.
- [31] Y. Chen, C.T. Mant, S.W. Farmer, R.E.W. Hancock, M.L. Vasil, R.S. Hodges (2005) Rational design of α -helical antimicrobial peptides with enhanced activities and ppecificity/therapeutic index, *J. Biol. Chem.* 280, 12316–12329. doi:10.1074/jbc.M413406200.
- [32] C. Loose, K. Jensen, I. Rigoutsos, G. Stephanopoulos (2006) A linguistic model for the rational design of antimicrobial peptides, *Nature.* 443, 867–869. doi:10.1038/nature05233.
- [33] S. Tangri, B.R. Mothe, J. Eisenbraun, J. Sidney, S. Southwood, K. Briggs, J. Zinckgraf, P. Bilsel, M. Newman, R. Chesnut, C. LiCalsi, A. Sette (2005) Rationally engineered therapeutic proteins with reduced immunogenicity, *J. Immunol.* 174, 3187–3196. doi:10.4049/jimmunol.174.6.3187.
- [34] A. Sircar, E. Kim, J. Gray (2009) RosettaAntibody: antibody variable region homology modeling server, *Nucleic Acids Res.* 37, W474-9. doi: 10.1093/nar/gkp387
- [35] S. Lyskov, J.J. Gray (2008) The RosettaDock server for local protein-protein docking, *Nucleic Acids Res.* 36, W233–W238. doi:10.1093/nar/gkn216.
- [36] United States Cancer Statistics: 1999-2013 Incidence and Mortality Web-based Report, CDC. (2016).
- [37] R. Weinberg (2007)The Biology of Cancer, Garland Science.
- [38] R. Olie, et al. (2000) A novel antisense oligonucleotide targeting survivin expression induces apoptosis and sensitizes lung cancer cells to chemotherapy, *Cancer Research.* 60, 2805–2809.
- [39] K. Tanaka, et al. (2000) Expression of survivin and its relationship to loss of apoptosis in breast carcinomas, *AARC.* 6, 127–134.

- [40] H. Kawasaki, et al. (1998) Inhibition of apoptosis by survivin predicts shorter survival rates in colorectal cancer, *Cancer Research*. 58, 5071–5074.
- [41] M. Zhang, D. Latham, M. Delaney, A. Chakravarti (2005) Survivin mediates resistance to antiandrogen therapy in prostate cancer, *Oncogene*. 24, 2474–2482.
- [42] C. Jeon, M. Kim, C. Kwak, H. Kim, J. Ku (2013) Prognostic role of survivin in bladder cancer: a systematic review and meta-analysis, *PLoS ONE*. 8, e76719. 10.1371/journal.pone.0076719
- [43] C. Cheung, et al. (2013) Survivin – biology and potential as a therapeutic target in oncology, *OncoTargets and therapy*. 6, 1453–1462.
- [44] A. Sarela, R. Macadam, S. Farmery, A. Markham, P. Guillou (2000) Expression of the antiapoptosis gene, Survivin, predicts death from recurrent colorectal carcinoma, *Gut*. 46, 645–650.
- [45] H. Kawasaki, et al. (2001) Expression of survivin correlates with apoptosis, proliferation, and angiogenesis during human colorectal tumorigenesis, *Cancer*. 91, 2026–2032.
- [46] C. Adida, et al. (1998) Developmentally regulated expression of the novel cancer anti-apoptosis gene survivin in human and mouse differentiation, *The Amer. J. Pathology*. 152, 43–49.
- [47] M. Coumar, F. Tsai, J. Kanwar, S. Sarvagalla, C. Cheung (2013) Treat cancers by targeting survivin: just a dream or future reality?, *Cancer Treat. Rev.*, 39, 802–811.
- [48] M. Johnson, E. Howerth (2004) A bifunctional inhibitor of apoptosis protein, *Vet. Pathol.*, 41, 599–607.
- [49] G. Ambrosini, C. Adida, D. Altieri (1997) A novel anti-apoptosis gene, survivin, expressed in cancer and lymphoma, *Nat Med*. 3, 917–921.
- [50] S. Chettiar, et al. (2013) Design, synthesis and biological studies of Survivin dimerization modulators that prolong mitotic cycle, *Bioorg. & Med. Chem. Letters*. 23, 5429–5433.
- [51] D.C. Altieri (2003) Survivin, versatile modulation of cell division and apoptosis in cancer, *Oncogene*. 22, 8581–8589. doi:10.1038/sj.onc.1207113.
- [52] A.M. Aljaberi, J.R. Webster, S.P. Wheatley (2015) Mitotic activity of survivin is regulated by acetylation at K129, *Cell Cycle*. 14, 1738–1747. doi:10.1080/15384101.2015.1033597.
- [53] M.A. Verdecia, H. Huang, E. Dutil, D.A. Kaiser, T. Hunter, J.P. Noel (2000) Structure of the human anti-apoptotic protein survivin reveals a dimeric arrangement, *Nat. Struct. Biol.* 7, 7.

- [54] F. Li, G. Ambrosini, E.Y. Chu, J. Plescia, S. Tognin, P.C. Marchisio, D.C. Altieri (1998) Control of apoptosis and mitotic spindle checkpoint by survivin, *Nature*. 396, 580–584. doi:10.1038/25141.
- [55] L. Chantalat, et al. (2000) Crystal structure of human survivin reveals a bow tie shaped dimer with two unusual α -helical extensions, *Mol. Cell*. 6, 183–189. doi:10.1016/S1097-2765(00)00019-8.
- [56] T. Dohi, K. Okada, F. Xia, C.E. Wilford, T. Samuel, K. Welsh, H. Marusawa, H. Zou, R. Armstrong, S. Matsuzawa, G.S. Salvesen, J.C. Reed, D.C. Altieri (2004) An IAP-IAP complex inhibits apoptosis, *J. Biol. Chem.* 279, 34087–34090. doi:10.1074/jbc.C400236200.
- [57] D. Hu, S. Liu, L. Shi, C. Li, L. Wu, Z. Fan (2010) Cleavage of survivin by granzyme M triggers degradation of the survivin-X-linked inhibitor of apoptosis orotein (XIAP) complex to free caspase activity leading to cytolysis of target tumor Cells, *J. Biol. Chem.* 285, 18326–18335. doi:10.1074/jbc.M109.083170.
- [58] R. Moriai, N. Tsuji, M. Moriai, D. Kobayashi, N. Watanabe (2009) Survivin plays as a resistant factor against tamoxifen-induced apoptosis in human breast cancer cells, *Breast Cancer Res. Treat.* 117, 261–271. doi:10.1007/s10549-008-0164-5.
- [59] N.E. Weisser, J.C. Hall (2009) Applications of single-chain variable fragment antibodies in therapeutics and diagnostics, *Biotechnol. Adv.* 27, 502–520. doi:10.1016/j.biotechadv.2009.04.004.
- [60] A. Messer, J. McLear (2006), The therapeutic potential of intrabodies in neurologic disorders, *BioDrugs*. 20, 327–333.
- [61] A. Wörn, A. Auf der Maur, D. Escher, A. Honegger, A. Barberis, A. Plückthun (2000) Correlation between in vitro stability and in vivo performance of anti-GCN4 intrabodies as cytoplasmic inhibitors, *J. Biol. Chem.* 275, 2795–2803. doi:10.1074/jbc.275.4.2795.
- [62] R.C. Cumming, N.L. Andon, P.A. Haynes, M. Park, W.H. Fischer, D. Schubert (2004) Protein disulfide bond formation in the cytoplasm during oxidative stress, *J. Biol. Chem.* 279, 21749–21758. doi:10.1074/jbc.M312267200.
- [63] S.N. Joshi, D.C. Butler, A. Messer (2012) Fusion to a highly charged proteasomal retargeting sequence increases soluble cytoplasmic expression and efficacy of diverse anti-synuclein intrabodies, *MAbs*. 4, 686–693. doi:10.4161/mabs.21696.
- [64] M.P. DeLisa, D. Tullman, G. Georgiou (2003) Folding quality control in the export of proteins by the bacterial twin-arginine translocation pathway, *Proc. Natl. Acad. Sci.* 100, 6115–6120. doi:10.1073/pnas.0937838100.

- [65] A.C. Fisher, W. Kim, M.P. Delisa (2006) Genetic selection for protein solubility enabled by the folding quality control feature of the twin-arginine translocation pathway, *Protein Sci.* 15, 449–458. doi:10.1110/ps.051902606.
- [66] P. Martineau, P. Jones, G. Winter (1998) Expression of an antibody fragment at high levels in the bacterial cytoplasm, *J. Mol. Biol.* 280,117–127. doi:10.1006/jmbi.1998.1840.
- [67] E.G. Bogsch, F. Sargent, N.R. Stanley, B.C. Berks, C. Robinson, T. Palmer (1998) An essential component of a novel bacterial protein export system with homologues in plastids and mitochondria, *J. Biol. Chem.* 273, 18003–18006. doi:10.1074/jbc.273.29.18003.
- [68] C. Tayapiwatana, R. Chotpadiwetkul, W. Kasinrerak (2006) A novel approach using streptavidin magnetic bead-sorted in vivo biotinylated survivin for monoclonal antibody production, *J. Immunol. Methods.* 317, 1–11. doi:10.1016/j.jim.2006.07.024.
- [69] R. Rauchenberger, E. Borges, E. Thomassen-Wolf, E. Rom, R. Adar, Y. Yaniv, M. Malka, I. Chumakov, S. Kotzer, D. Resnitzky, A. Knappik, S. Reiffert, J. Prassler, K. Jury, D. Waldherr, S. Bauer, T. Kretzschmar, A. Yayon, C. Rothe (2003) Human combinatorial Fab library yielding specific and functional antibodies against the human fibroblast growth factor receptor 3, *J. Biol. Chem.* 278, 38194–38205. doi:10.1074/jbc.M303164200.
- [70] H.J. de Haard, N. van Neer, A. Reurs, S.E. Hufton, R.C. Roovers, P. Henderikx, A.P. de Bruïne, J.-W. Arends, H.R. Hoogenboom (1999) A large non-immunized human Fab fragment phage library that permits rapid isolation and kinetic analysis of high affinity antibodies, *J. Biol. Chem.* 274, 18218–18230. doi:10.1074/jbc.274.26.18218.
- [71] K.Y. Yau, M.A. Groves, S. Li, C. Sheedy, H. Lee, J. Tanha, C.R. MacKenzie, L. Jermutus, J.C. Hall (2003) Selection of hapten-specific single-domain antibodies from a non-immunized llama ribosome display library, *J. Immunol. Methods.* 281, 161–175. doi:10.1016/j.jim.2003.07.011.
- [72] A. M. Levin, G. A. Weiss (2006) Optimizing the affinity and specificity of proteins with molecular display, *Mol. Biosyst.* 2, 49–57. doi:10.1039/B511782H.
- [73] I. Liu, M. Liu, K. Shergill (2006) The effect of spheroplast formation on the transformation efficiency in escherichia coli DH5 α , *J. Exp. Microbiol. Immun.* 9, 81-85.
- [74] W.-K. Min, S.-G. Kim, J.-H. Seo (2015) Affinity maturation of single-chain variable fragment specific for aflatoxin B1 using yeast surface display, *Food Chem.* 188, 604–611. doi:10.1016/j.foodchem.2015.04.117.

- [75] T.S. Chen, H. Palacios, A.E. Keating (2013) Structure-based redesign of the binding specificity of anti-apoptotic Bcl-xL, *J. Mol. Biol.* 425, 171–185. doi:10.1016/j.jmb.2012.11.009.
- [76] C.F. Barbas, J.D. Bain, D.M. Hoekstra, R.A. Lerner (1992) Semisynthetic combinatorial antibody libraries: a chemical solution to the diversity problem., *Proc. Natl. Acad. Sci.* 89, 4457–4461. doi:10.1073/pnas.89.10.4457.
- [77] M.J. Feldhaus, R.W. Siegel, L.K. Opresko, J.R. Coleman, J.M.W. Feldhaus, Y.A. Yeung, J.R. Cochran, P. Heinzelman, D. Colby, J. Swers, C. Graff, H.S. Wiley, K.D. Wittrup (2003) Flow-cytometric isolation of human antibodies from a nonimmune *Saccharomyces cerevisiae* surface display library, *Nat. Biotechnol.* 21, 163–170. doi:10.1038/nbt785.
- [78] G.M. Cherf, J.R. Cochran (2015) Applications of yeast surface display for protein engineering, *Methods Mol. Bio.* 1319, 155–175. doi:10.1007/978-1-4939-2748-7_8.
- [79] J.A.V. Deventer, K.D. Wittrup (2014) Yeast surface display for antibody isolation: library construction, library screening, and affinity maturation, *Methods Mol. Bio.* 1131, 151–181. doi:10.1007/978-1-62703-992-5_10.
- [80] A. Angelini, T.F. Chen, S. de Picciotto, N.J. Yang, A. Tzeng, M.S. Santos, J.A.V. Deventer, M.W. Traxlmayr, K.D. Wittrup (2015) Protein engineering and selection using yeast surface display, *Methods Mol. Bio.* 1319, 3–36. doi:10.1007/978-1-4939-2748-7_1.
- [81] C. McMahon, A.S. Baier, R. Pascolutti, M. Wegrecki, S. Zheng, J.X. Ong, S.C. Erlandson, D. Hilger, S.G.F. Rasmussen, A.M. Ring, A. Manglik, A.C. Kruse (2018) Yeast surface display platform for rapid discovery of conformationally selective nanobodies, *Nat. Struct. Mol. Biol.* 25, 289–296. doi:10.1038/s41594-018-0028-6.
- [82] J. Hanes, C. Schaffitzel, A. Knappik, A. Plückthun (2000) Picomolar affinity antibodies from a fully synthetic naive library selected and evolved by ribosome display, *Nat. Biotechnol.* 18, 1287–1292. doi:10.1038/82407.
- [83] B. Wang, C.-H. Lee, E.L. Johnson, C.A. Kluwe, J.C. Cunningham, H. Tanno, R.M. Crooks, G. Georgiou, A.D. Ellington (2016) Discovery of high affinity anti-ricin antibodies by B cell receptor sequencing and by yeast display of combinatorial VH:VL libraries from immunized animals, *MAbs.* 8, 1035–1044. doi:10.1080/19420862.2016.1190059.
- [84] X. Yu, L. Qu, D.D. Bigner, V. Chandramohan (2017) Selection of novel affinity-matured human chondroitin sulfate proteoglycan 4 antibody fragments by yeast display, *Protein Eng. Des. Sel.* 30, 639–647. doi:10.1093/protein/gzx038.

- [85] M.M. Harmsen, H.J. De Haard (2007) Properties, production, and applications of camelid single-domain antibody fragments, *Appl. Microbiol. Biotechnol.* 77, 13–22. doi:10.1007/s00253-007-1142-2.
- [86] A.L. Marschall, S. Dübel, T. Böldicke (2015) Specific in vivo knockdown of protein function by intrabodies, *MAbs.* 7, 1010–1035. doi:10.1080/19420862.2015.1076601.
- [87] U. Rothbauer, K. Zolghadr, S. Tillib, D. Nowak, L. Schermelleh, A. Gahl, N. Backmann, K. Conrath, S. Muyldermans, M.C. Cardoso, H. Leonhardt (2006) Targeting and tracing antigens in live cells with fluorescent nanobodies, *Nat. Methods.* 3, 887–889. doi:10.1038/nmeth953.
- [88] R.H.J. van der Linden, L.G.J. Frenken, B. de Geus, M.M. Harmsen, R.C. Ruuls, W. Stok, L. de Ron, S. Wilson, P. Davis, C.T. Verrips (1999) Comparison of physical chemical properties of llama VHH antibody fragments and mouse monoclonal antibodies, *Biochim. Biophys. Acta BBA - Protein Struct. Mol. Enzymol.* 1431, 37–46. doi:10.1016/S0167-4838(99)00030-8.
- [89] J. Tanha, G. Dubuc, T. Hirama, S.A. Narang, C.R. MacKenzie (2002) Selection by phage display of llama conventional VH fragments with heavy chain antibody VHH properties, *J. Immunol. Methods.* 263, 97–109. doi:10.1016/S0022-1759(02)00027-3.
- [90] M.A. Ghahroudi, A. Desmyter, L. Wyns, R. Hamers, S. Muyldermans (1997) Selection and identification of single domain antibody fragments from camel heavy-chain antibodies, *FEBS Lett.* 414, 521–526. doi:10.1016/S0014-5793(97)01062-4.
- [91] R. van der Linden, B. de Geus, W. Stok, W. Bos, D. van Wassenaar, T. Verrips, L. Frenken (2000) Induction of immune responses and molecular cloning of the heavy chain antibody repertoire of Lama glama, *J. Immunol. Methods.* 240, 185–195. doi:10.1016/S0022-1759(00)00188-5.
- [92] P. Verheesen, M. ten Haaft, N. Lindner, C. Verrips, J.J. de Haard (2003) Beneficial properties of single-domain antibody fragments for application in immunoaffinity purification and immuno-perfusion chromatography, *Biochim. Biophys. Acta BBA - Gen. Subj.* 1624, 21–28. doi:10.1016/j.bbagen.2003.09.006.
- [93] E.R. Goldman, G.P. Anderson, J.L. Liu, J.B. Delehanty, L.J. Sherwood, L.E. Osborn, L.B. Cummins, A. Hayhurst (2006) Facile generation of heat-stable antiviral and antitoxin single domain antibodies from a semisynthetic llama library, *Anal. Chem.* 78, 8245–8255. doi:10.1021/ac0610053.
- [94] Y. Sun, B. Ban, A. Bradbury, G.A.S. Ansari, D.A. Blake (2016) Combining yeast display and competitive FACS to select rare hapten-specific clones from recombinant antibody libraries, *Anal. Chem.* 88, 9181–9189. doi:10.1021/acs.analchem.6b02334.

- [95] E.T. Boder, K.D. Wittrup (1997) Yeast surface display for screening combinatorial polypeptide libraries, *Nat. Biotechnol.* 15, 553–557. doi:10.1038/nbt0697-553.
- [96] A. Pugsley (1993) The Complete General Secretory Pathway in Gram-Negative Bacteriat, *Microbiol. Rev.* 57, 59.
- [97] M.P. Rapoza, R.E. Webster (1993) The filamentous bacteriophage assembly proteins require the bacterial SecA protein for correct localization to the membrane., *J. Bacteriol.* 175, 1856–1859. doi:10.1128/jb.175.6.1856-1859.1993.
- [98] E. Mössner, H. Koch, A. Plückthun (2001) Fast selection of antibodies without antigen purification: adaptation of the protein fragment complementation assay to select antigen-antibody pairs¹ Edited by I. A. Wilson, *J. Mol. Biol.* 308, 115–122. doi:10.1006/jmbi.2001.4575.
- [99] J. Lloyd-Price, G. Abu-Ali, C. Huttenhower (2016) The healthy human microbiome, *Genome Med.* 8, 51. doi:10.1186/s13073-016-0307-y.
- [100] M.A. Pfaller, D.J. Diekema (2007) Epidemiology of invasive candidiasis: a persistent public health problem, *Clin. Microbiol. Rev.* 20, 133–163. doi:10.1128/CMR.00029-06.
- [101] P.G. Pappas, C.A. Kauffman, D.R. Andes, C.J. Clancy, K.A. Marr, L. Ostrosky-Zeichner, A.C. Reboli, M.G. Schuster, J.A. Vazquez, T.J. Walsh, T.E. Zaoutis, J.D. Sobel (2016) Clinical Practice Guideline for the Management of Candidiasis: 2016 Update by the Infectious Diseases Society of America, *Clin. Infect. Dis. Off. Publ. Infect. Dis. Soc. Am.* 62, e1–e50. doi:10.1093/cid/civ933.
- [102] M.B. Lohse, M. Gulati, A.D. Johnson, C.J. Nobile (2017) Development and regulation of single- and multi-species *Candida albicans* biofilms, *Nat. Rev. Microbiol.* 16, 19–31. doi:10.1038/nrmicro.2017.107.
- [103] P.K. Mukherjee, J. Chandra, D.M. Kuhn, M.A. Ghannoum (2003) Mechanism of fluconazole resistance in *Candida albicans* biofilms: phase-specific role of efflux pumps and membrane sterols, *Infect. Immun.* 71, 4333–4340. doi:10.1128/IAI.71.8.4333-4340.2003.
- [104] S.P. Hawser, L.J. Douglas (1995) Resistance of *Candida albicans* biofilms to antifungal agents in vitro, *Antimicrob. Agents Chemother.* 39, 2128–2131. doi:10.1128/AAC.39.9.2128.
- [105] G. Ramage, S. Bachmann, T.F. Patterson, B.L. Wickes, J.L. López-Ribot (2002) Investigation of multidrug efflux pumps in relation to fluconazole resistance in *Candida albicans* biofilms, *J. Antimicrob. Chemother.* 49, 973–980. doi:10.1093/jac/dkf049.
- [106] M.A. Jabra-Rizk, W.A. Falkler, T.F. Meiller (2004) Fungal biofilms and drug resistance, *Emerg. Infect. Dis.*, 10, 14-19. doi:10.3201/eid1001.030119.

- [107] K.C. Gray, D.S. Palacios, I. Dailey, M.M. Endo, B.E. Uno, B.C. Wilcock, M.D. Burke (2012) Amphotericin primarily kills yeast by simply binding ergosterol, *Proc. Natl. Acad. Sci.* 109, 2234–2239. doi:10.1073/pnas.1117280109.
- [108] M.A. Ghannoum, L.B. Rice (1999) Antifungal agents: mode of action, mechanisms of resistance, and correlation of these mechanisms with bacterial resistance, *Clin. Microbiol. Rev.* 12, 501–517.
- [109] T. Xu, S.M. Levitz, R.D. Diamond, F.G. Oppenheim (1991) Anticandidal activity of major human salivary histatins., *Infect. Immun.* 59, 2549–2554.
- [110] P.A. Raj, E. Marcus, D.K. Sukumaran (1997) Structure of human salivary histatin 5 in aqueous and nonaqueous solutions, *Biopolymers.* 45, 51–67. doi:10.1002/(SICI)1097-0282(199801)45:1<51::AID-BIP5>3.0.CO;2-Y.
- [111] O. Salvatori, S. Puri, S. Tati, M. Edgerton (2016) Innate immunity and saliva in *Candida albicans*–mediated oral diseases, *J. Dent. Res.* 95, 365–371. doi:10.1177/0022034515625222.
- [112] A.N. Amerongen, E.C.I. Veerman (2002) Saliva – the defender of the oral cavity, *Oral Dis.* 8, 12–22. doi:10.1034/j.1601-0825.2002.1o816.x.
- [113] F.G. Oppenheim, T. Xu, F.M. McMillian, S.M. Levitz, R.D. Diamond, G.D. Offner, R.F. Troxler (1988) Histatins, a novel family of histidine-rich proteins in human parotid secretion. Isolation, characterization, primary structure, and fungistatic effects on *Candida albicans*., *J. Biol. Chem.* 263, 7472–7477.
- [114] T.F. Meiller, B. Hube, L. Schild, M.E. Shirtliff, M.A. Scheper, R. Winkler, A. Ton, M.A. Jabra-Rizk (2009) A novel immune evasion strategy of *Candida albicans*: proteolytic cleavage of a salivary antimicrobial peptide, *PLoS ONE.* 4. doi:10.1371/journal.pone.0005039.
- [115] S. Puri, M. Edgerton (2014) How does it kill?: understanding the candidacidal mechanism of salivary histatin 5, *Eukaryot. Cell.* 13, 958–964. doi:10.1128/EC.00095-14.
- [116] M. Edgerton, S.E. Koshlukova, T.E. Lo, B.G. Chrzan, R.M. Straubinger, P.A. Raj (1998) Candidacidal activity of salivary histatins: identification of a histatin 5-binding protein on *Candida albicans*, *J. Biol. Chem.* 273, 20438–20447. doi:10.1074/jbc.273.32.20438.
- [117] C.R. Pusateri, E.A. Monaco, M. Edgerton (2009) Sensitivity of *Candida albicans* biofilm cells grown on denture acrylic to antifungal proteins and chlorhexidine, *Arch. Oral Biol.* 54, 588–594. doi:10.1016/j.archoralbio.2009.01.016.
- [118] S.A. Khan, P.L. Fidel, A.A. Thunayyan, S. Varlotta, T.F. Meiller, M.A. Jabra-Rizk (2013) Impaired histatin-5 levels and salivary antimicrobial activity against *C.*

- albicans* in HIV infected individuals, *J. AIDS Clin. Res.* 4. doi:10.4172/2155-6113.1000193.
- [119] S.R. Torres, A. Garzino-Demo, T.F. Meiller, V. Meeks, M.A. Jabra-Rizk (2009) Salivary histatin-5 and oral fungal colonisation in HIV+ individuals, *Mycoses.* 52, 11–15. doi:10.1111/j.1439-0507.2008.01602.x.
- [120] A.B. Mochon, H. Liu (2008) The antimicrobial peptide histatin-5 causes a spatially restricted disruption on the *Candida albicans* surface, allowing rapid entry of the peptide into the cytoplasm, *PLoS Pathog.* 4, e1000190. doi:10.1371/journal.ppat.1000190.
- [121] D.M. Rothstein, P. Spacciapoli, L.T. Tran, T. Xu, F.D. Roberts, M. Dalla Serra, D.K. Buxton, F.G. Oppenheim, P. Friden (2001) Anticandida activity is retained in p-113, a 12-amino-acid fragment of histatin 5, *Antimicrob. Agents Chemother.* 45, 1367–1373. doi:10.1128/AAC.45.5.1367-1373.2001.
- [122] H. Situ, S.V. Balasubramanian, L.A. Bobek (2000) Role of alpha-helical conformation of histatin-5 in candidacidal activity examined by proline variants., *Biochim. Biophys. Acta.* 1475, 377–382. doi:10.1016/S0304-4165(00)00096-9.
- [123] J. Driscoll, C. Duan, Y. Zuo, T. Xu, R. Troxler, F.G. Oppenheim (1996) Candidacidal activity of human salivary histatin recombinant variants produced by site-directed mutagenesis, *Gene.* 177, 29–34. doi:10.1016/0378-1119(96)00265-X.
- [124] P.A. Raj, M. Edgerton, M.J. Levine (1990) Salivary histatin 5: dependence of sequence, chain length, and helical conformation for candidacidal activity, *J. Biol. Chem.* 265, 3898–3905.
- [125] E.J. Helmerhorst, W. Van't Hof, E.C. Veerman, I. Simoons-Smit, A.V. Nieuw Amerongen (1997) Synthetic histatin analogues with broad-spectrum antimicrobial activity, *Biochem. J.* 326, 39–45.
- [126] E.J. Helmerhorst, W. van't Hof, P. Breeuwer, E.C.I. Veerman, T. Abee, R.F. Troxler, A.V.N. Amerongen, F.G. Oppenheim (2001) Characterization of histatin 5 with respect to amphipathicity, hydrophobicity, and effects on cell and mitochondrial membrane integrity excludes a candidacidal mechanism of pore formation, *J. Biol. Chem.* 276, 5643–5649. doi:10.1074/jbc.M008229200.
- [127] A.L.A. Ruissen, J. Groenink, E.J. Helmerhorst, E. Walgreen-Weterings, W. van't Hof, E.C.I. Veerman, A.V.N. Amerongen (2001) Effects of histatin 5 and derived peptides on *Candida albicans*, *Biochem. J.* 356, 361–368. doi:10.1042/bj3560361.
- [128] X.S. Li, J.N. Sun, K. Okamoto-Shibayama, M. Edgerton (2006) *Candida albicans* cell wall Ssa proteins bind and facilitate import of salivary histatin 5 required for toxicity, *J. Biol. Chem.* 281, 22453–22463. doi:10.1074/jbc.M604064200.

- [129] E.J. Helmerhorst, P. Breeuwer, W. van 't Hof, E. Walgreen-Weterings, L.C.J.M. Oomen, E.C.I. Veerman, A.V.N. Amerongen, T. Abee (1999) The cellular target of histatin 5 on *Candida albicans* is the energized mitochondrion, *J. Biol. Chem.* 274, 7286–7291. doi:10.1074/jbc.274.11.7286.
- [130] O. Bochenska, M. Rapala-Kozik, N. Wolak, W. Aoki, M. Ueda, A. Kozik (2016) The action of ten secreted aspartic proteases of pathogenic yeast *Candida albicans* on major human salivary antimicrobial peptide, histatin 5, *Acta Biochim. Pol.* 63, 403–410. doi:10.18388/abp.2016_1318.
- [131] A. da Silva Dantas, K.K. Lee, I. Raziunaite, K. Schaefer, J. Wagener, B. Yadav, N.A. Gow (2016) Cell biology of *Candida albicans*–host interactions, *Curr. Opin. Microbiol.* 34, 111–118. doi:10.1016/j.mib.2016.08.006.
- [132] A. Albrecht, A. Felk, I. Pichova, J.R. Naglik, M. Schaller, P. de Groot, D. MacCallum, F.C. Odds, W. Schäfer, F. Klis, M. Monod, B. Hube (2006) Glycosylphosphatidylinositol-anchored proteases of *Candida albicans* target proteins necessary for both cellular processes and host-pathogen interactions, *J. Biol. Chem.* 281, 688–694. doi:10.1074/jbc.M509297200.
- [133] J.R. Naglik, S.J. Challacombe, B. Hube (2003) *Candida albicans* secreted aspartyl proteinases in virulence and pathogenesis, *Microbiol. Mol. Biol. Rev.* 67, 400–428. doi:10.1128/MMBR.67.3.400-428.2003.
- [134] W. Aoki, N. Kitahara, N. Miura, H. Morisaka, Y. Yamamoto, K. Kuroda, M. Ueda (2011) Comprehensive characterization of secreted aspartic proteases encoded by a virulence gene family in *Candida albicans*, *J. Biochem. (Tokyo)*. 150, 431–438. doi:10.1093/jb/mvr073.
- [135] L. Schild, A. Heyken, P.W.J. de Groot, E. Hiller, M. Mock, C. de Koster, U. Horn, S. Rupp, B. Hube (2011) Proteolytic cleavage of covalently linked cell wall proteins by *Candida albicans* sap9 and sap10, *Eukaryot. Cell.* 10, 98–109. doi:10.1128/EC.00210-10.
- [136] M.B. Zepelin, S. Beggah, K. Boggian, D. Sanglard, M. Monod (2002) The expression of the secreted aspartyl proteinases Sap4 to Sap6 from *Candida albicans* in murine macrophages, *Mol. Microbiol.* 28, 543–554. doi:10.1046/j.1365-2958.1998.00815.x.
- [137] J.R. Naglik, D. Moyes, J. Makwana, P. Kanzaria, E. Tsihlaki, G. Weindl, A.R. Tappuni, C.A. Rodgers, A.J. Woodman, S.J. Challacombe, M. Schaller, B. Hube (2008) Quantitative expression of the *Candida albicans* secreted aspartyl proteinase gene family in human oral and vaginal candidiasis, *Microbiol. Read. Engl.* 154, 3266–3280. doi:10.1099/mic.0.2008/022293-0.
- [138] O. Bochenska, M. Rapala-Kozik, N. Wolak, W. Kamysz, D. Grzywacz, W. Aoki, M. Ueda, A. Kozik (2015) Inactivation of human kininogen-derived antimicrobial

peptides by secreted aspartic proteases produced by the pathogenic yeast *Candida albicans*, *Biol. Chem.* 396. doi:10.1515/hsz-2015-0167.

- [139] G. Koelsch, J. Tang, J.A. Loy, M. Monod, K. Jackson, S.I. Foundling, X. Lin (2000) Enzymic characteristics of secreted aspartic proteases of *Candida albicans*, *Biochim. Biophys. Acta BBA - Protein Struct. Mol. Enzymol.* 1480, 117–131. doi:10.1016/S0167-4838(00)00068-6.
- [140] S. Ikonomova, Protein engineering approaches to improving diagnosis and treatment of *Candida albicans* infections, PhD Dissertation, University of Maryland, 2017.
- [141] L. Mathé, P. Van Dijck (2013) Recent insights into *Candida albicans* biofilm resistance mechanisms, *Curr. Genet.* 59, 251–264. doi:10.1007/s00294-013-0400-3.
- [142] G. Baillie, L.J. Douglas (1999) *Candida* biofilms and their susceptibility to antifungal agents, in: R. Doyle (Ed.), *Methods Enzymol.*, 310, 644–656.
- [143] L.J. Douglas (2003) *Candida* biofilms and their role in infection, *Trends Microbiol.* 11, 30–36. doi:10.1016/S0966-842X(02)00002-1.
- [144] S.P. Hawser, L.J. Douglas (1994) Biofilm formation by *Candida* species on the surface of catheter materials in vitro, *Infect. Immun.* 62, 915-921.
- [145] P. Sudbery, N. Gow, J. Berman (2004) The distinct morphogenic states of *Candida albicans*, *Trends Microbiol.* 12, 317–324. doi:10.1016/j.tim.2004.05.008.
- [146] C.A. Kumamoto, M.D. Vinces (2005) Contributions of hyphae and hypha-co-regulated genes to *Candida albicans* virulence, *Cell. Microbiol.*, 7,1546–1554. doi:10.1111/j.1462-5822.2005.00616.x.
- [147] M.B. Lohse, A.D. Johnson (2009) White–opaque switching in *Candida albicans*, *Curr. Opin. Microbiol.* 12, 650–654. doi:10.1016/j.mib.2009.09.010.
- [148] M.A. Al-Fattani, L.J. Douglas (2006) Biofilm matrix of *Candida albicans* and *Candida tropicalis*: chemical composition and role in drug resistance, *J. Med. Microbiol.* 55, 999–1008. doi:10.1099/jmm.0.46569-0.
- [149] K.Y. Lum, S.T. Tay, C.F. Le, V.S. Lee, N.H. Sabri, R.D. Velayuthan, H. Hassan, S.D. Sekaran (2015) Activity of novel synthetic peptides against *Candida albicans*, *Sci. Rep.* 5, 9657. doi:10.1038/srep09657.
- [150] A.J. Karlsson, W.C. Pomerantz, K.J. Neilsen, S.H. Gellman, S.P. Palecek (2009) Effect of sequence and structural properties on 14-Helical β -Peptide activity against *Candida albicans* planktonic cells and biofilms, *ACS Chem. Biol.* 4, 567–579. doi:10.1021/cb900093r.

- [151] A.J. Karlsson, R.M. Flessner, S.H. Gellman, D.M. Lynn, S.P. Palecek (2010) Polyelectrolyte multilayers fabricated from antifungal β -peptides: design of surfaces that exhibit antifungal activity against *Candida albicans*, *Biomacromolecules*. 11, 2321–2328. doi:10.1021/bm100424s.
- [152] L.L. Burrows, M. Stark, C. Chan, E. Glukhov, S. Sinnadurai, C.M. Deber (2006) Activity of novel non-amphipathic cationic antimicrobial peptides against *Candida* species, *J. Antimicrob. Chemother.* 57, 899–907. doi:10.1093/jac/dkl056.
- [153] P.-W. Tsai, C.-Y. Yang, H.-T. Chang, C.-Y. Lan (2011) Human antimicrobial peptide Il-37 inhibits adhesion of *Candida albicans* by interacting with yeast cell-wall carbohydrates, *PLoS ONE*. 6, e17755. doi:10.1371/journal.pone.0017755.
- [154] M.J.S. Mendes Giannini, T. Bernardi, L. Scorzoni, A.M. Fusco-Almeida, J.C.O. Sardi (2013) *Candida* species: current epidemiology, pathogenicity, biofilm formation, natural antifungal products and new therapeutic options, *J. Med. Microbiol.* 62, 10–24. doi:10.1099/jmm.0.045054-0.
- [155] M.M. Weerasekera, G.K. Wijesinghe, T.A. Jayarathna, C.P. Gunasekara, N. Fernando, N. Kottegoda, L.P. Samaranayake (2016) Culture media profoundly affect *Candida albicans* and *Candida tropicalis* growth, adhesion and biofilm development, *Mem. Inst. Oswaldo Cruz.* 111, 697–702. doi:10.1590/0074-02760160294.
- [156] N. Raman, M.-R. Lee, S.P. Palecek, D.M. Lynn (2014) Polymer multilayers loaded with antifungal β -peptides kill planktonic *Candida albicans* and reduce formation of fungal biofilms on the surfaces of flexible catheter tubes, *J. Controlled Release.* 191, 54–62. doi:10.1016/j.jconrel.2014.05.026.
- [157] O. Etienne, C. Gasnier, C. Taddei, J.-C. Voegel, D. Aunis, P. Schaaf, M.-H. Metz-Boutigue, A.-L. Bolcato-Bellemin, C. Egles (2005) Antifungal coating by biofunctionalized polyelectrolyte multilayered films, *Biomaterials.* 26, 6704–6712. doi:10.1016/j.biomaterials.2005.04.068.
- [158] K. Proba, A. Wörn, A. Honegger, A. Plückthun (1998) Antibody scFv fragments without disulfide bonds, made by molecular evolution, *J. Mol. Biol.* 275, 245–253. doi:10.1006/jmbi.1997.1457.
- [159] P. Moghaddam-Taaheri, A.J. Karlsson (2018) Protein labeling in live cells for immunological applications, *Bioconjug. Chem.* 29, 680–685. doi:10.1021/acs.bioconjchem.7b00722.
- [160] S.P. Ikonomova, Z. He, A.J. Karlsson (2016) A simple and robust approach to immobilization of antibody fragments, *J. Immunol. Methods.* 435, 7–16. doi:10.1016/j.jim.2016.04.012.

- [161] J. Cruz, M. Mihailescu, G. Wiedman, K. Herman, P.C. Searson, W.C. Wimley, K. Hristova (2013) A membrane-translocating peptide penetrates into bilayers without significant bilayer perturbations, *Biophys. J.* 104, 2419–2428. doi:10.1016/j.bpj.2013.04.043.
- [162] J. Bürck, P. Wadhvani, S. Fanghänel, A.S. Ulrich (2016) Oriented circular dichroism: a method to characterize membrane-active peptides in oriented lipid bilayers, *Acc. Chem. Res.* 49, 184–192. doi:10.1021/acs.accounts.5b00346.